Norges miljø- og
biovitenskapelige
universitet

Master's Thesis 2021/22   60 ECTS
Department of Chemistry, Biotechnology and Food Science (KBM)

Examining the anti-inflammatory effects of β-hydroxybutyrate injections on LPS treated mice

Undersøkelse av anti-inflammatoriske egenskaper til β-hydroxybutyrate injeksjoner på LPS-behandlet mus

Nikolai Ellingstad From
Biochemistry, Biotechnology

Acknowledgements

Abstract

Background:

Elevated levels of ketones, especially β-Hydroxybutyrate (BHB), have been proposed to impact several essential mechanisms in the immune system. This is mainly suggested through the anti-inflammatory properties observed in studies on elevated BHB concentrations in mice and cell cultures. Inflammation is considered the essential mechanism of the innate immune response, a response against harmful pathogens and well as essential for damaged tissue repair and regeneration. While beneficial in the short term, excessive inflammation can lead to a state of chronic inflammation, linked to several important diseases. Some of these diseases are cardiovascular diseases, cancer, autoimmune diseases, and several neurodegenerative diseases. With BHB implicated in several mechanisms central to the inflammation process, three suggested interactions are highly important for this project.

1) BHB inhibiting NLRP3 inflammasome activation through interactions with potassium efflux channels and reactive oxygen species (ROS). This negatively impacts the maturation of pro-inflammatory cytokines IL-1β and IL-18.

2) BHB as an HDAC inhibitor that can upregulate expression of molecules protecting against oxidative stress or directly impact the NF-κB subunits through phosphorylation.

3) BHB acting as a GPR109a agonist, a mechanism proven to reduce colon inflammation.

Aim: The goal of the project is to examine if four bolus injections of different BHB-containing solutions can reduce the severity of acute systemic inflammation in mice treated with LPS.

Methods: 26 transgenic mice were sorted into four groups, all given a different amount of BHB. Group 1, the control, was only given a saline solution with 0 mM BHB. Group 2 was given 5 mmol/kg BHB solution (Low). Group 3 was given 10 mmol/kg BHB solution (Medium), and group 4 was given 15 mmol/kg BHB (High). The severity of the inflammation caused by LPS was measured through *in vivo* imaging of NF-κB activity and cytokine profiling from plasma samples.

Results: While a substantial NF-κB activity was observed through *in vivo* imaging, no dose-dependent relationship between BHB and NF-κB activity was found. Male mice on average were found to exhibit a higher NF-κB activity compared to the female mice. Data from cytokine

profiling showed a greater IFN-γ concentration in plasma samples from the male mice compared to those from females. A weak but significant dose-dependent effect of BHB on IL-10 and IL-6 were found.

Conclusion: We did not observe a reduction in NF-κB activity in any of the groups given BHB. With BHB theorized to inhibit NLRP3i activation, it was expected to see a dose-dependent reduction of IL-1β and IL-18. Instead, a dose-dependent increase in IL-6 and IL-10 was observed.

Abbreviations

ATP:	Adenosine triphosphate
BDH1:	Beta-hydroxybutyrate dehydrogenase
BHB:	β-Hydroxybutyrate
CLR:	C-type lectin receptor
DAMPs:	Damage-associated molecular pattern
EDTA:	Ethylenediamine tetraacetic acid
ELISA:	Enzyme-linked immunosorbent assay
FFAs:	Free fatty acids
FOXO3:	Forkhead box O3
GEF:	Guanine nucleotide exchange factor
GDP:	Guanine diphosphate
GPCR:	G Protein coupled receptor
GTP:	Guanine triphosphate
HAT:	Histone acetyl transferase
HCAR2:	Hydroxycarboxylic acid receptor 2 / GPR109a
HDAC:	Histone deacetylases
HMGB1:	Chromatin-associated protein high-mobility group box 1
HSP:	Heat shock protein
IC50:	The half maximal inhibitory concentration
IFN-γ:	Interferon gamma
IL-1R:	Interleukin-1 receptor
IL-1RA:	Interleukin-1 receptor agonist
IL-1β/10/18:	Interleukin 1β/10/18
IP:	Intraperitoneal
IRAK:	IL-1R-associated kinase
IV:	Intravenously
KD:	Ketogenic diet
LD50:	Lethal dose 50%
LPS:	Lipopolysaccharide
MCTs:	Monocarboxylate transporters
Mn-SOD:	Mitochondrial superoxide dismutase

MT2:	Metallothionein 2
mtDNA:	Mitochondrial DNA
mtROS:	Mitochondrial ROS
MyD88:	Myeloid differentiation primary response gene 88
NADPH:	Nicotinamide adenine dinucleotide phosphate
NF-κB:	Nuclear Factor Kappa-Light-Chain enhancer of activated B-cells
NLR:	NOD-like receptor
NLRP3:	NOD-like receptor P3
NLRP3i:	NLRP3 inflammasome
NOX2:	NADPH oxidase 2
PAMPs:	Pathogen-associated molecular pattern
PGN:	Peptidoglycans
PRRs:	Pattern recognition receptors
RIP1:	Receptor interacting protein kinase 1
RLR:	RIG-like receptor
ROS:	Reactive oxygen species
STAP:	Signal transducing adapter proteins
TAK1:	Transforming-growth-factor-beta-activated kinase
TCA:	Tricarboxylic acid cycle
TLRs:	Toll-like receptors
TNFR:	Tumor necrosis factor receptor
TNF-α:	Tumor necrosis factor alpha
TRADD:	Tumor necrosis factor receptor type1-associated death domain protein
TRAF:	Tumor-necrosis-factor-receptor-associated factor

Figures and tables

Table of contents

1 Introduction and theory

The immune system is a highly regulated complex system necessary for individuals to protect themselves from harm. However, when dysregulated, it can cause more harm than good. Dysregulation of inflammation has been linked to several diseases and is widely considered the most significant underlying death factor in today's modern world (Furman et al., 2019). Plenty of studies have linked the dysregulation of inflammation to obesity, resulting in the common understanding that consuming less fat and living a healthier lifestyle reduces the risk of inflammation-related diseases. However, there is one diet that instead of trying to avoid fatty food, instead focuses on it. The so-called Keto-diet (KD) is a diet focused on obtaining most of your caloric intake through fat and heavily restricting the consumption of carbohydrates. The ketogenic diet has gained a lot of popularity in the last decade primarily due to evidence showing its short-term benefits to weight loss, among other advantages such as a decrease in blood pressure, glycosylated hemoglobin and triglyceride levels, as well as higher levels of high-density lipoprotein (Batch et al., 2020). With β-hydroxybutyrate (BHB) being the most common ketone observed during KD, the hypothesis is that BHB is the main driver behind these observations. While short-term advantages have been observed, long-term effects are less studied. Currently, there is a lack of research suggesting long-term health benefits of KD. Therefore, several health organizations recommend that individuals with liver, pancreas, thyroid, or gallbladder conditions avoid strict diets such as KD, which can cause extra stress on the body.

By injecting BHB into mice, the effects of BHB can be studied in a vacuum without relying on KD or starvation. This way, any potential effects BHB has on inflammation will be observed without KD and starvation being a factor. To measure and quantify the effect BHB exerts on inflammation, reporter mice with luciferase under the control of NF-κB will be used. NF-κB is a protein of vital importance in regulating the transcription of several cytokines and proteins necessary for inflammation.

1.1 What is inflammation?

While the immune system differentiates between self and not self, it also differentiates between non-dangerous and dangerous (Matzinger, 1994). This differentiation allows symbiotic

relationships with commensal bacteria while detecting potentially harmful pathogens. To sense all the dangerous invading agents, the innate immune system relies on a large family of pattern recognition receptors, abbreviated PRRs. These receptors recognize structures highly conserved in pathogens called pathogen-associated-molecular patterns (PAMPs) or molecules called danger-associated molecular patterns (DAMPs). Examples of PAMPs are the conserved structures such as cytosine-phosphate-guanine motifs, heat shock proteins (HSP), peptidoglycans (PGN), and lipopolysaccharides (LPS) (Kany et al., 2019). DAMPs are intracellular or nucleic acids typically not found outside the cell. Examples are degraded extracellular matrixes like biglycan, heparan, uric acid, and adenosine triphosphate (ATP) from the cytosol (Roh & Sohn, 2018).

As PRRs are a vast family of receptors, they are usually categorized into four smaller subfamilies: Toll-like receptors (**TLR**) located on the cell surface or within endosomes. Two intracellular subfamilies of cytosolic sensors; NOD-like receptors (**NLR**) & RIG-like receptors (**RLR**), and lastly, C-type lectin receptors (**CLR**), helicases that primarily sense viruses (Luigi Franchi et al., 2009). These are implicated in inflammatory pathways and intracellular signaling, resulting in the activation of kappa-light-chain-enhancer of activated B cells (NF-κB), a regulator for transcription of many critical inflammatory genes. These genes lead to the induction of pro-inflammatory mediators, including cytokines such as Interleukin-1/2/6/8/12 (IL-1/2/6/8/12), tumor necrosis factor-alpha (TNF-α) and type 1 interferons (INFs), chemokines such as Interleukin-18 and several inflammatory mediators in different innate immune cells (Lawrence, 2009). These inflammatory mediators can then potentiate the inflammation reaction through autocrine, paracrine and in some cases endocrine actions (J.-M. Zhang & J. An, 2007).

In response to infection or injury, resident cells in the tissue secrete vasoactive amines leading to vasodilation and increased vascular permeability. Vasodilation is the process in which the smooth muscle in the wall of the arteries or veins relaxes, opening the blood vessels and increasing blood flow to the area. Vasoactive amines such as histamine, prostaglandins, and leukotrienes cause contraction of endothelium cells. Contraction of endothelium cells leads to increased vascular permeability, letting plasma flow into the interstitial space. Large proteins in the bloodstream can then leak out to and water follows due to the oncotic pressure. Specific cytokines and inflammatory mediators stimulate the expression of adhesion molecules on vascular endothelial cells allowing leukocytes to attach to the endothelial cells and then migrate to the site of inflammation, where they degranulate and phagocytize the pathogens. While these

processes only happen at the inflammation site, some released cytokines such as IL-1 and IL-6 can affect the hypothalamus leading to a system-wide increase of body temperature (fever), while TNF-α can interfere with the regulation of energy balance suppressing appetite (de Kloet et al., 2011).

The inflammation process usually ends with the release of anti-inflammatory mediators and/or the end of proinflammatory mediators when the problem is alleviated. These acute inflammations usually last hours until days. A chronic condition can occur when the inflammation response is constantly activated, resulting in inflammation that can last months until years (Roma et al., 2021). Failure to eliminate the causing agent, reoccurring acute inflammations, normal components of the body getting recognized as foreign antigens, or defects in cells responsible for mediating inflammation are the most common reasons for chronic inflammation (Pahwa R, 2022).
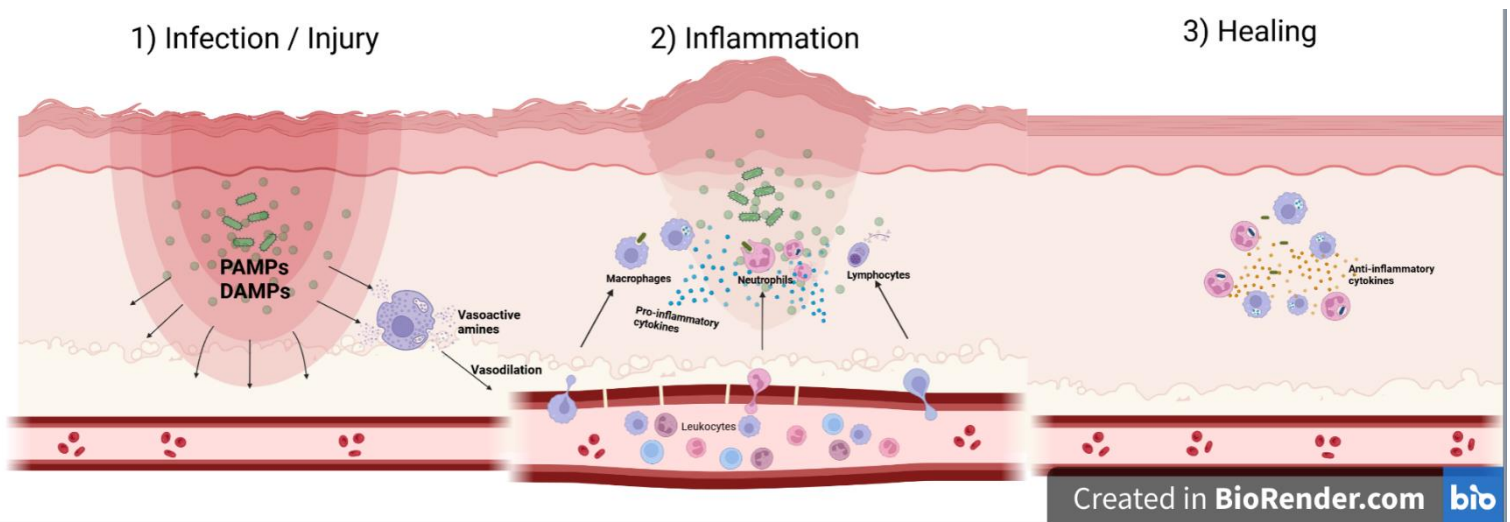
Figure 1.1 - Inflammation simplified in three stages:

First an injury or infection leads to resident cells secrete vasoactive amines leading to vasodilation and increased vascular permeability. Plasma flows into the injured/infected area and inflammation occurs. Leukocytes enter the site of inflammation and try to clear the area of pathogens through phagocytosis. Secreted pro-inflammatory cytokines help recruit more immune cells to the inflammation site. Once the causing agent is dealt with and the damaged tissue is removed, anti-inflammatory cytokines help down regulating the response inflammation response allowing the body to focus on healing.

Once the inflammation goes from acute to chronic, a shift in cells at the inflammation site happens. The composition of white blood cells shifts over to mononuclear leukocytes, such as macrophages and lymphocytes, instead of the short-lived neutrophils (Roma et al., 2021). This

persistent inflammation response will damage nearby healthy tissue over time. Today it is commonly recognized that chronic inflammatory diseases are the most significant cause of death (Furman et al., 2019). In that context, research into understanding all the mechanisms and interactions involved is important.

1.1.1 Chronic inflammation and diseases

Plenty of research on the relationship between inflammation and diseases, risk factors and treatments has been done. Most focusing on lifestyle and diets. Some of the most common risk factors that promote low-grade chronic inflammation are as follows: age, obesity, stress & sleep disorders, as well as low sex hormones.

An increase in the concentration of circulating pro-inflammatory markers are associated with chronic inflammations and many of the diseases it may cause. As individual ages, such an increase in the concentration of circulating pro-inflammatory markers is observed, even in healthy individuals. The exact mechanism of why aging causes an increase in circulating pro-inflammatory molecules is yet to be fully understood. A combination of oxidative damage, declining sex hormone levels after menopause/andropause and an increase of adipose tissue is suggested as the primary drivers (Singh & Newman, 2011). To this day the causality between these markers and diseases are discussed. A question frequently asked is whether the increase in pro-inflammatory molecules is due to stressors or simply due to dysregulation of the immune system that comes with age.

The accumulation of adipose tissue (body fat), either through aging or through an unhealthy lifestyle, has been linked to chronic inflammation. Obesity, the accumulation of excessive fat due to an imbalance between energy intake and expenditure, is a core characteristic of metabolic syndrome (Ellulu et al., 2017). Metabolic syndrome is a cluster of risk factors specific to cardiovascular disease. Adipose tissue synthesizes and secrete pro- and anti-inflammatory molecules, such as the adipokines; leptin, adiponectin & resistin as well as chemokines & cytokines (Fantuzzi, 2005). Adipokines are proteins produced by adipocytes (fat cells).

Leptin, a small protein mainly produced by the adipocytes, has been linked to massive obesity in humans with mutations in the genes coding for leptin or the leptin receptors (Clément et al., 1998). The suggested reason is leptin's central role in controlling appetite (Maffei et al., 1996). This causes a compounding problem with excessive adipose tissue resulting in more secretion

of leptin, leading to a further increase in adipose tissue. As well as being implicated in the regulation of hunger, leptins have also been shown to exhibit effects on inflammatory responses. *In vitro* as well as animal experiments have shown that leptin stimulates modulation of T cell-derived cytokines, upregulating the secretion of several pro-inflammatory cytokines (Fantuzzi & Faggioni, 2000).

Adiponectin is the adipokine that circulates at the highest concentrations and is best known for its role in insulin sensitivity but also inhibits certain inflammatory processes (Bełtowski, 2003). In contrast to leptin, adiponectin levels are not shown to increase in obese subjects, rather there is a tendency to observe lower levels of adiponectin in subjects with excess adipose tissue compared to leaner ones (Chandran et al., 2003). While it is suggested that TNF-α secreted by adipocytes is what downregulates synthesis of adiponectin, adiponectin has also been shown to downregulate synthesis and activation of TNF-α (Masaki et al., 2004). As well as its interactions with TNF-α, adiponectin has also been shown to stimulate the production of the anti-inflammatory cytokine IL-10 & IL-1RA in humans (Wolf et al., 2004). IL-1RA is a protein that binds to the IL-1 Receptor, negatively regulating IL-1 signaling, an important pathway in inflammation. With excess fat strongly implicated in the dysregulation of the immune system, it makes sense that a change in diet or exercise is the focus when discussing methods to prevent chronic inflammation.

Another common risk factor is stress, an umbrella term that includes everything from feeling distressed to physical events leading to physiological responses such as activation of the autonomic nervous system. While being more difficult to quantify and examine compared to age and obesity, several studies have shown evidence of a connection between mental stress and elevated levels of circulating pro-inflammatory cytokines such as IL-6, TNF-α, and IL-1β (Marsland et al., 2017). Sleep disorder and its effect on inflammation is another risk factor hard to quantify as different studies use and value different markers. Some studies have shown both increases in circulating pro-inflammatory markers as well as no significant difference when reducing participants sleep by 50% (Irwin et al., 2016; Irwin et al., 2015). Yet there is a consensus among researchers that sleep deprivation is linked to elevated levels of systemic inflammation.

In most studies that focus on inflammation, a gender effect is observed. This difference is mainly ascribed to a difference in sex hormones. Testosterone is the main sex hormone for males, while females have both estrogen and progesterone. While they all help regulate the immune system, they impact different mechanisms with regard to inflammation. Estrogen is a

potent anti-inflammatory hormone, proven to enhance the expression of IκB-α (Xing et al., 2012), a protein with the function to inhibit NF-κB transcription, which is a central regulator of pro-inflammatory genes. Testosterone, while less potent, has been shown to inhibit adipose tissue from expressing adipokines and cytokines such as TNF-α, IL-6 and IL-1 (Bianchi, 2019).

1.1.2 How is inflammation linked to diseases?

It is quite clear that risk factors that all impact the immune system can lead to a higher risk of an unbalanced state, with a chance of causing chronic inflammation. Chronic inflammation is linked to a wide variety of diseases, such as cardiovascular diseases, diabetes, Alzheimer's disease, cancer among many more. Taking a look at World Health Organization's overview of the top 10 causes of death from 2019, diseases heavily linked to chronic inflammation are the leading causes (W.H.O., 2020).

Cardiovascular diseases (CVDs) are often categorized as a state of chronic inflammation of the blood vessels associated with elevated levels of pro-inflammatory markers such as IFN-γ, IL-1β, IL-6, and TNF-α (Tian et al., 2014). These pro-inflammatory cytokines can cause atherosclerosis, the hardening of the arteries due to the build-up of plaques, an abnormal tissue on a body part or organ (Amin et al., 2020).

Cytokines take a role in regulating, proliferation, cell migration, cell differentiation, cell death and immune cell activation. For instance, TNF-α has been shown to stimulate anti-apoptotic genes allowing cells to avoid apoptosis-inducing tumor cell survival. Tumorigenesis, the initial formation of a tumor within the body, has a higher probability of occurring with elevated levels of TNF-α as it triggers production of genotoxic molecules leading to DNA damage. IL-6 is another cytokine involved in tumorigenesis through its growth- and antiapoptotic-promoting factors (Kabel, 2014). IL-1β has been shown to be expressed in an increased concentration in patients with breast cancer and is considered an important biomarker to predict the risk of the patient developing breast cancer bone metastasis (Sirotkovic-Skerlev et al., 2012) (Tulotta & Ottewell, 2018).

While aging is considered one of the greatest risk factors of these neurodegenerative disorders, studies focusing on chronic neuroinflammation, have found clear links between several neurodegenerative disorders, such as Alzheimer's disease and Parkinson disease and the

accumulation of several pro-inflammatory cytokines in cerebrospinal fluid (Herrero et al., 2015; Mogi et al., 1994).

1.2   NF-κB

Nuclear factor kappa-light-chain-enhancer of activated B-cells (NF-κB) is a family of transcriptional regulatory protein complexes that regulate a large array of crucial genes involved in the immune system and cell defense. The family consists of five subunits; p50, p52, p65/RelA, RelB, and c-Rel that occur in various homo- and hetero-dimers with the most common NF-κB being a hetero-dimer of p50 and p65 (Grimm & Baeuerle, 1993). In non-stimulated cells, NF-κB dimers are found latent in the cytoplasm, sequestered by interactions with different inhibitory proteins depending on the subunits making up the dimer. The most studied inhibitory proteins are the inhibitor-of-nuclear-factor-kappa-B-family (IκB-family), most notably the IκB-α protein and precursor proteins of the subunits p50 and p52 (p105 and p100). These precursor proteins contain a C-terminal resembling that of IκB proteins, giving them NF-κB inhibitory properties (Sun, 2011).

1.2.1   NF-κB pathways

Activation of the NF-κB is commonly split into two signal pathways, the canonical, and the non-canonical (alternative) pathway. While both pathways lead to a NF-κB dimer free from its inhibitory protein through phosphorylation of the inhibitory protein, there are some important differences.

The canonical pathway relies on a scaffolding protein called NF-κB essential modulator (NEMO) and two kinase subunits IκK-α and IκK-β, binding together to make an IκK-complex. Upon stimuli from ligands and various cytokine receptors, transduction signals activate the IκK-complex, leading to the phosphorylation of the inhibitory protein IκB-α. The formation of a ubiquitin chain on the inhibitory protein marks it for proteasomal degradation, ultimately leading to the dissociation of NF-κB from IκB-α (Schröfelbauer et al., 2012; Sun & Ley, 2008). These liberated NF-κB units translocate from the cytoplasm into the nucleus. In the nucleus, NF-κB binds to DNA and turns on transcriptional factors that induce specific gene expression. Notable immune receptors involved in the canonical NF-κB pathway are: Pattern Recognition

receptors (PRRs) such as Toll-like receptors (TLRs) & NOD-like receptors (NLR), B-cell receptors, T-cell receptors (TCR) and Tumor Necrosis Factor receptors (TNFR) (Zhang & Sun, 2015).
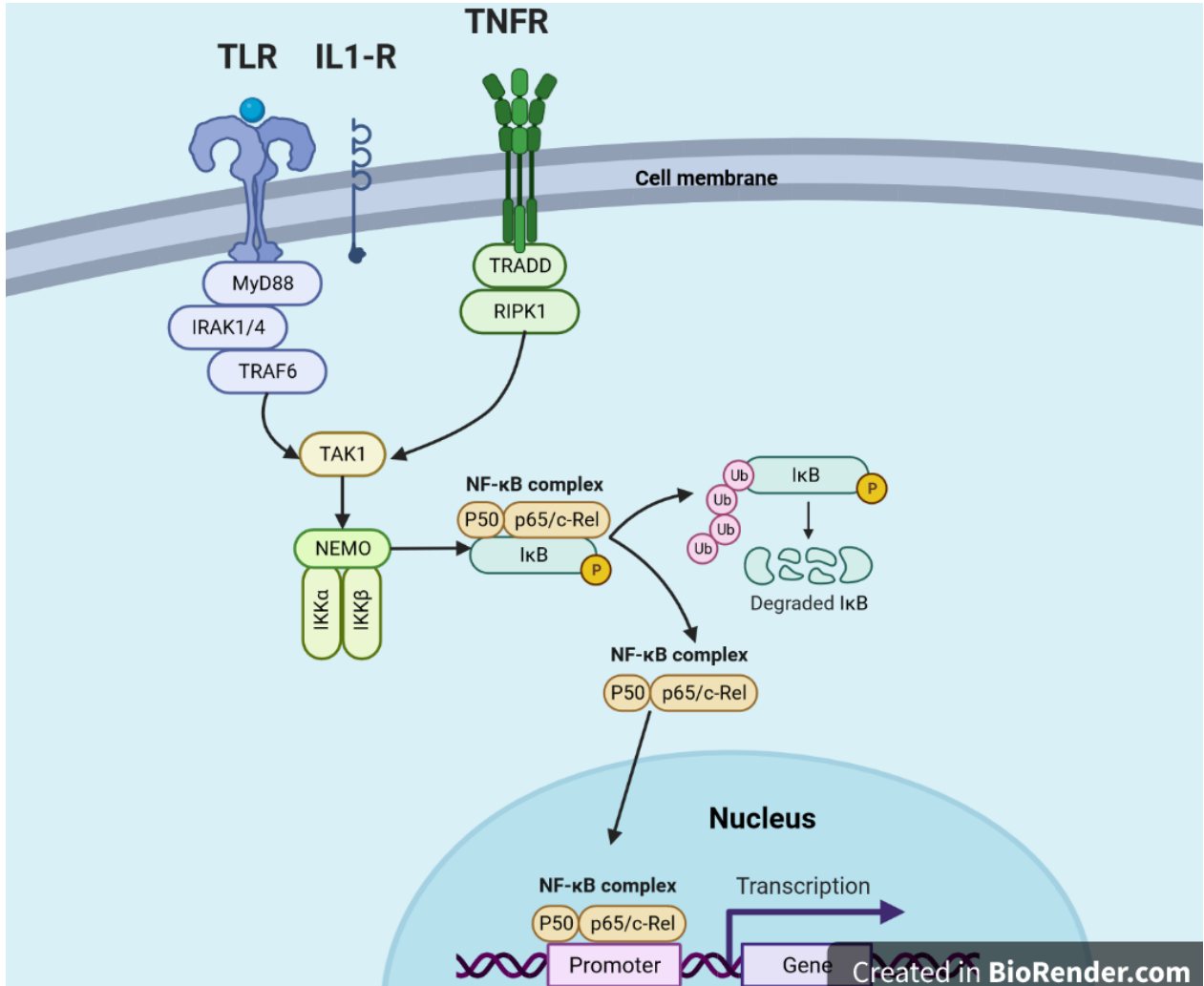
Figure 1.2 - The canonical NF-κB pathway:

Illustration of how binding of a ligand to TLR/IL1-R/TNFR, transduction signalling leads to the activation of the IκK-complex consisting of NEMO and IκK-α and IκK-β. The active IκK-complex then phosphorylate the inhibitory protein IκB, resulting in a ubiquitin chain that marks the inhibitory protein for proteasomal degradation. The degradation of IκB liberate NF-κB. Liberated NF-κB then translocate into the nucleus where it binds to DNA and induce specific gene transcription.

In contrast to the canonical pathway, the non-canonical only responds to very specific stimuli and does not rely on an IκK-complex. Instead, this pathway relies on NF-κB-inducing-Kinase (NIK) activating IκK-α leading phosphorylation of the p100's IκB-like C-terminals (Xiao et al., 2001). This ubiquitination leads to partial proteolysis, resulting in a p52/RelB NF-κB dimer free to translocate into the nucleus.

While the non-canonical pathway has been implicated in immune regulation, and some inflammatory diseases such as autoimmunity (Sun, 2017), this experiment use lipopolysaccharide (LPS) to induce acute inflammation in mice. A bacterial toxin found on the outer membrane of most gram-negative bacteria, and a known TLR4 agonist, leading to the activation of the canonical NF-κB pathway (Nunes-Alves, 2014). Hence going forward, the focus will be on the canonical pathway.

1.2.2 NF-κB agonist

As mentioned, a wide variety of stimuli activate the canonical NF-κB pathway. While not all the pathways are the same, generally binding of a ligand to one of these receptors starts a signal transduction. The signal transduction leads to activation of the IκK-complex, and the degradation of the inhibitor protein IκB resulting in the translocation of NF-κB into the nucleus and transcription of NF-κB target genes. The main difference between the different receptors is which agonist starts the signal transduction pathway and what signal transducing adaptor proteins (STAPs) that are recruited.

For ligands such as LPS, IL-1β, and IL-18 binding to their respective receptor, activation of the IκK-complex occurs through the TLR pathway (O'Neill & Bowie, 2007). A central adaptor protein involved in this pathway is Myeloid differentiation primary response gene 88 (MyD88). MyD88 is a universal adaptor protein used by almost all the TLR receptors and some specific cytokine receptors (O'Neill & Bowie, 2007). Once MyD88 is recruited, intracellular signal transduction involving IL-1R-associated kinase 4 (IRAK4), IL-1R-associated kinase 1 (IRAK1) and tumor-necrosis-factor-receptor-associated factor 6 (TRAF6) results in activated IκK-complex with the help of Transforming-growth-factor-beta-activated kinase (TAK1) (Figure 1.2) (Hayden & Ghosh, 2014; O'Neill & Bowie, 2007).

When ligands such as TNF-α bind to TNFR, the signal transduction pathway relies on adaptor protein tumor necrosis factor receptor type 1-associated death domain protein (TRADD) to interact with receptor-interacting protein kinase 1 (RIP1). With the help of TAK1, the IκK-complex can then be activated. This pathway can also stimulate cell death through apoptosis or necroptosis (Hayden & Ghosh, 2014; Pistorio et al., 2022).

1.2.3 NF-κB regulated gene expression

Once NF-κB translocate to the nucleus, it can activate the transcription of a wide array of genes. The transcription of these genes results in small proteins central to inflammation. These small secreted proteins are released by many different cells upon stimuli, with the predominant producers being T-cells and macrophages (J. M. Zhang & J. An, 2007). NF-κB plays a vital role by inducing a vital transcription factor of M1 macrophages, the most classically activated macrophage known for producing high levels of pro-inflammatory cytokines such as IL-1, IL-6, IL-12, IL-18, TNF-α as well as several chemokines (Wang et al., 2014).

NF-κB regulated gene expression also includes cell cycle regulators and anti-apoptotic factors, as well as increased cell proliferation, morphogenesis, and cell differentiation (T. Liu et al., 2017). However, we will focus on the interaction between NF-κB, NLRP3 inflammasome (NLRP3i) leading to the maturation of pro-IL-1β and pro-IL-18

1.3 Inflammasome NLRP3

Inflammasomes are a group of intracellular multi-protein complex that assembles in response to either PAMPs or DAMPs in several cells, with the main characterization of activating inflammatory cysteine-dependent aspartate-directed protease (caspase) (Kumar et al., 2011). These inflammatory caspases promote the maturation of the cytokines IL-1β and IL-18, as well as induce a type of cell death known as pyroptosis (Broz & Dixit, 2016).

NLRP3 inflammasome (NLRP3i) consists of a ligand-sensing receptor from the NLR family called NLRP3, an adapter protein called apoptosis-associated speck-like protein containing a CARD (ASC), and pro-caspase 1 (Broz & Dixit, 2016). As with any pro-inflammatory processes, its activation must be strictly regulated, and NLRP3i is no exception. Generally, NLRP3i activation requires two steps, often referred to as priming (step 1) and protein-complex assembly (step 2) (Paik et al., 2021). The priming occurs when pathogens are being recognized by PRRs such as TLRs, TNFs or specific cytokine receptors and have two main functions. The first function is to upregulate the transcription of pro-interleukins and ligand-sensing receptor NLRP3 through the NF-κB pathway. The second function of priming is the induction of posttranslational modifications of the NLRP3 to a stable inactive state (Swanson et al., 2019).

Protein complex assembly (step 2) occurs following a wide variety of unrelated stimuli from PAMPs, DAMPs, pore-forming toxins, ATP, pathogen-associated RNA, particulate matter, or bacterial toxins (Kelley et al., 2019; Paik et al., 2021). Upon stimuli, the inflammasome receptors oligomerize and recruit pro-caspase 1 through ASC. This stimulates the pro-caspase 1, resulting in its conversion to active caspase 1, responsible for cleaving pro-IL-1β and pro-IL-18 resulting in active mature IL-1β and IL-18 able to be secreted from the cell (Schroder & Tschopp, 2010).

The only unifying factor of these activators is that they all induce cellular stress, which NLRP3 senses (Paik et al., 2021). While not precisely understood, several non-mutually exclusive activators and upstream signals have been suggested. The most common ones are ionic flux, reactive oxygen species (ROS), and mitochondrial dysfunction (Kelley et al., 2019; Swanson et al., 2019). Potassium-ion (K^+) efflux and ROS are two activators of particular interest as BHB has been shown to interact with these (Figure 1.4).

1.3.1   Potassium efflux

While there is an abundance of data on NLRP3 activators, there is also plenty of contradicting data on the suggested activators. When it comes to K^+ efflux, it is commonly seen as the most robust event involved in activating NLRP3i. This is due to studies showing that K^+ efflux can activate the inflammasome by itself and that higher extracellular concentrations of K^+ can inhibit the activation of NLRP3i (Muñoz-Planillo et al., 2013; Perregaux & Gabel, 1994).

The idea that K^+ efflux was necessary for NLRP3i activation was however contradicted, when it was shown that mutant NLRP3 mouse macrophages were able to activate the inflammasome following LPS stimulation without the occurrence of K^+ efflux. The suggestion was a pathway involving Na^+ influx instead (Muñoz-Planillo et al., 2013). Further examining mice cells, Muñoz-Planillo and colleagues proved that reducing extracellular Na^+ resulted in a dose-dependent inhibitory effect of the NLRP3i activation induced by a K^+-free medium. Thus, they concluded that Na^+ influx can impact NLRP3i activation independently of K^+ efflux but that Na^+ influx is not necessary for the activation of NLRP3i (Muñoz-Planillo et al., 2013).

1.3.2 ROS

Reactive oxygen species (ROS) are oxygen-containing molecules generated during oxidative mitochondrial metabolisms but can also be greatly increased as a cellular response to environmental stressors (Pizzino et al., 2017; Ray et al., 2012). Even though cells have a cellular antioxidant capacity, a state known as oxidative stress can occur either through an increase in ROS or when the cell cannot detoxify these reactive products. While ROS are important for redox homeostasis, proper cardiovascular function, and the immune system, prolonged oxidative stress can cause cellular damage and play a role in the onset or progression of several diseases (Roma et al., 2017; Taniyama & Griendling, 2003).

1.3.3 Cytosolic ROS

Due to contradicting evidence in research on the importance of ROS in NLRP3i activation, its importance is somewhat controversial. ROS was considered a common upstream event of NLRP3i activation. With the idea that most NLRP3 stimuli result in the induction of ROS, and research showing caspase-1 activation being ROS dependent (Cruz et al., 2007; Dostert et al., 2008; L. Franchi et al., 2009). A study inhibiting NADPH oxidase in mice and human cells, the enzyme assumed to be the primary source of ROS production, they found that NLRP3i activation was unimpacted. Thus questioning the importance of cytosolic ROS in NLRP3i activation (van Bruggen et al., 2010).

More recent studies link inflammasome activation in the brain, kidney, heart, and testis to ROS-mediated pathways (Minutoli et al., 2016). These findings were supported by a head injury mice model examining the regulation of NLRP3i activation by NADPH. NOX2 knockout mice were used, and a reduction in NLRP3 in the cerebral cortex was observed. With no observable changes found in the umbilical vein endothelium, they then concluded that cytosolic ROS might have a tissue-specific role when it comes to activating NLRP3i (Ma et al., 2017).

1.3.4 Mitochondrial ROS

ROS is also a by-product of mitochondrial respiration. Mitochondrial ROS (mtROS) was first implicated in NLRP3i activation when a study utilizing blockade of critical cellular processes

led to the accumulation of mtROS producing damaged mitochondria and activation of the NLRP3i (Zhou et al., 2011). By treating mice macrophages with mitochondrial-targeted antioxidants, LPS, and ATP, dose-dependent inhibition of caspase-1 activation and IL-1β secretion were observed (Nakahira et al., 2011).

A link between released mitochondrial DNA (mtDNA) and NLRP3i activation was observed when research investigating inflammasome activity in *Chlamydia pneumoniae* (CP) infected mice. They found that oxidized mtDNA was able to bind to NLRP3 and activate the inflammasome (Shimada et al., 2012). Strengthening the idea that mtROS might play an important role in NLRP3i activation, as previous studies showed a mtROS dependent release of mtDNA into the cytosol (Nakahira et al., 2011).

However, there are also studies showing no link between mtROS and NLRP3i activation. Muñoz-Planillo and colleagues found no change in priming or activation of NLRP3i when using ROS scavengers to inhibit cellular redox states (Muñoz-Planillo et al., 2013).

1.4 Ketogenic diet

The ketogenic diet was a diet introduced early nineteen hundred to help treat epilepsy. A few years prior, a study on the effect of intermittent starvation on epilepsy had been done and reported less severe seizures during the treatment. Interestingly it was observed that increased levels of circulating acetone and β-hydroxybutyric acid appeared both in starving subjects and subjects on a diet with a low amount of carbohydrates and high amounts of fat. A new diet based on this information was suggested. This diet, named ketogenic diet was tried and showed great success in helping individuals control their seizures (Wheless, 2008). As data on ketogenic diet increased, some studies reported behavior and cognitive improvement in subjects treated with ketogenic diet (Angeloni et al., 2020). In recent years more interest in studies aimed at understanding and mapping these effects has increased.

In most projects observing the effects of ketogenic diet, overall energy intake from carbohydrates is limited to under 5% (usually 2-4%), while fat accounts for 90% of the energy, with the remaining from proteins (Rusek et al., 2019; Ułamek-Kozioł et al., 2019). As the body does not receive enough carbohydrates from the diet, more fatty acids are released into circulation from adipose tissue and metabolized to ketones in the liver through a process called ketogenesis. This increased production of ketone provides an alternative energy source that

most organs can utilize. Notable organs able to utilize ketones are the brain, heart, and muscles. Ketogenesis is considered a very important survival mechanism that allows the body to switch to stored fat as an energy source during periods of starvation.

As an effect of either starvation or a ketogenic diet, insulin levels drop, glucagon secretion increases, and together with other metabolic hormones, triglycerides in fat cells break down into fatty acids through lipolysis. These fatty acids enter circulation and are brought to the mitochondria of liver cells by transferase CPT-1. In the mitochondria of the liver cells, the fatty acids are broken down into acetyl-CoA through mitochondrial β-oxidation.

Since the liver cells lack essential enzymes to utilize ketones, some of the acetyl-CoA is oxidized in the tricarboxylic acid cycle (TCA) to produce ATP. The amount of fatty acid-derived acetyl-CoA produced through β-oxidation exceeds what the liver can use, and the excess acetyl-CoA is condensed to Acetoacetyl-CoA with the help of an enzyme called Thiolase. Acetoacetyl-CoA is further converted to 3-hydroxy-3-methylglutaryl CoA (HMG-CoA) with the help of HMG-CoA synthase, an enzyme stimulated by the glucagon and downregulated by insulin (Cantrell CB, 2022). HMG-CoA is then converted to the first ketone; acetoacetate, with the help of HMG-CoA lyase. Acetoacetate is mainly converted to β-hydroxybutyrate (BHB) with the help of β-hydroxybutyrate dehydrogenase (BDH1). Some acetoacetate goes through decarboxylation and produce acetone (Evans et al., 2017) (Dhillion KK, 2022) (Fletcher et al., 2019).

Once the circulating ketones, BHB and to a lesser extent acetoacetate, reach ketone favoring extrahepatic tissue such as the brain, skeletal muscle, and the heart, BHB is first converted back to acetoacetate by BDH1. Then acetoacetate gets converted to Acetyl-CoA with the help of succinyl-CoA:3-ketoacyl-CoA transferase (SCOT). The acetyl-CoA can then be oxidized by the TCA cycle to produce energy (22 ATP per ketone molecule) (Evans et al., 2017). The steps of ketogenesis and utilization of BHB in organs are visually represented in Figure 1.3 below.
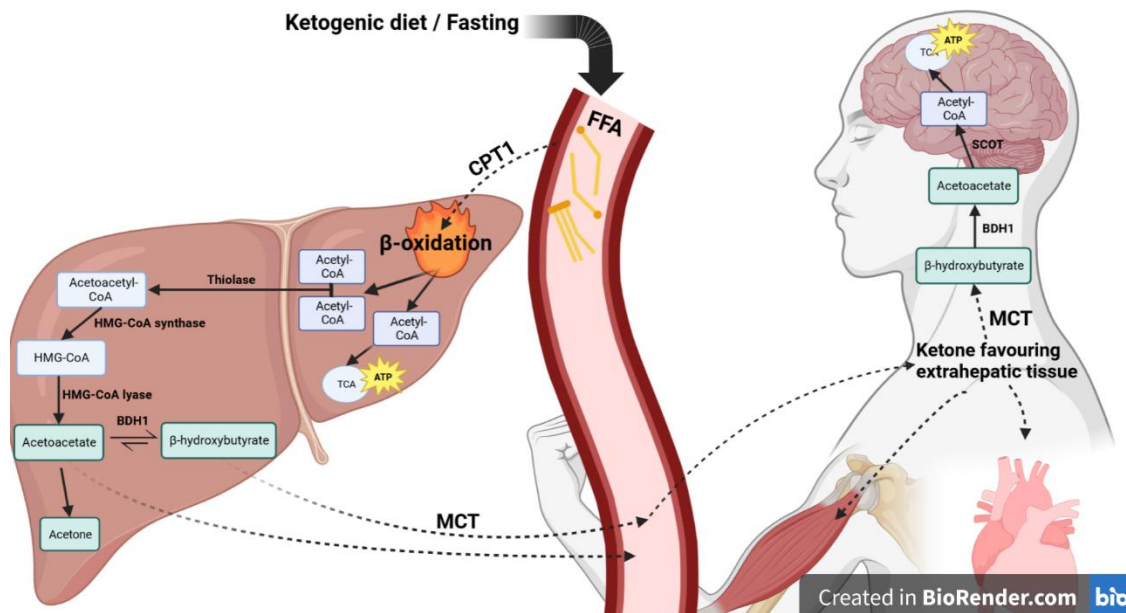
Figure 1.3 – Ketogenesis:

Illustration of ketogenesis in the liver, the transport of BHB to ketone favouring extrahepatic tissue and the process where BHB is converted back into Acetyl-CoA for energy through the TCA.

While the synthesis of ketones is considered well-known, the exact details of how BHB and acetoacetate enter circulation and is transported into different cells are less understood. Some research suggests that monocarboxylate transporter (MCTs) might be the key to how BHB is exported from the liver and transported into target cells. MCTs are plasma membrane transporters that catalyze proton-linked transport of molecules with a carboxylate group across membranes, such as BHB. For transport out of the hepatocyte, MCT Slc16a6 is suggested to be vital in the process (Hugo et al., 2012), while MCT1 and MCT2 have been shown to carry BHB into the brain across the blood-brain barrier (Pellerin et al., 2005)

1.5   β-hydroxybutyrate, more than just an energy molecule

In addition to working as fuel, the ketone BHB has also been shown to exhibit cellular signaling functions. Currently, there are several indirect and direct mechanisms BHB has been suggested to be involved in. Some examples are epigenetic regulation through HDAC inhibition, regulation of ion channels, and G-protein receptor interactions, all with implications in inflammation (J. C. Newman & E. Verdin, 2017).

1.5.1 BHB as an HDAC inhibitor

Histone deacetylases (HDACs) and histone acetyltransferase (HATs) are two counteracting families of enzymes involved in the deacetylation and acetylation of histones and some non-histone proteins. HATs typically stimulate transcriptional activation by acetylation of lysine residues of histone tails, creating a more relaxed chromatin-like structure. This relaxed chromatin-like structure increases the accessibility of target gene promoters. HDACs do the opposite. As the name indicates, it represses transcriptional activation by removing the acetyl groups from the same lysine residues, resulting in a more compact chromatin structure which typically will repress transcription (Elmallah & Micheau, 2019). This balance between HATs and HDAC is a critical epigenetic regulator that regulates gene expression through "opening" or "closing" the chromatin structure.

In vitro experiments on human embryonic kidney cells and *in vivo* experiments on mice showed BHB increasing histone acetylation in a dose-dependent matter. In human embryonic kidney cells, HDAC1, HDAC3, HDAC4 were 50% inhibited (IC50) by BHB concentrations previously observed in humans (> 5,3 mM), while IC50 for HDAC6 was significantly higher at 48,4 mM (Shimazu et al., 2013). Several tissue samples from different organs in mice with increased circulating BHB showed a significant increase in acetylation. Further mRNA analysis showed an increased protein expression of mitochondrial superoxide dismutase (Mn-SOD), Forkhead box O3 (FOXO3), and catalase, in line with the increased histone acetylation observed at the Foxo3a and MT2 promoters (Shimazu et al., 2013). Mn-SOD, FOXO3. and catalase are proven to protect against oxidative stress and reactive oxygen species by having an antiapoptotic role (Stefanetti et al., 2018). Mn-SOD primary function is to clear mtROS, while FOXO3 takes a vital part in substrate metabolism, and catalase catalyzes the decomposition of hydrogen peroxides.

As previously mentioned, HDACs/HATs can also deacetylate/acetylate non-histone proteins. Two such non-histone protein of interest are the NF-κB subunit p65 (RelA) and NF-κB subunit p50, which together make up the "classic NF-κB", the most studied NF-κB dimer. With several acetylation points discovered on p65, the interaction between HAT p300 and HDAC 3 at some of these acetylation points have shown to regulate both DNA and IκB-α binding (Calao et al., 2008). Inhibition of either enzyme impacts the balance, with HDAC 3 inhibitors leading to more acetylated p65 and enhanced NF-κB activity through increased DNA binding and less IκB-α

binding. While HDAC3 inhibition by BHB has been examined and proven, a direct link between p65 acetylation and BHB is yet to be observed.

1.5.2   BHB as GPR109a agonist

G-protein-coupled cell surface receptors (GPCR) are one of three major cell surface categories we find in all eukaryotes. GPCR consists of trimeric G-proteins that detect molecules outside the cell and activate cellular responses. Upon activation by an agonist, GPCR stabilizes and conforms, allowing it to act like a guanine nucleotide exchange factor (GEF). The GPCR interacts with G-proteins and induces a significant conformational change in the G-protein due to GDP being exchanged with GTP. The α-subunit dissociates from the β-γ-complex, and previously hidden areas get exposed, allowing the subunits to separately mediate downstream signals activities (Weis & Kobilka, 2018).

Hydroxycarboxylic acid receptor 2 (HCAR2), also known as GPR109a. is a G-protein-coupled cell surface receptor expressed various cell types. In adipocytes, immune cells, and colonic epithelial cells, GPR109a has been found to mediate anti-inflammatory effects (Graff et al., 2016). While first being identified as a nicotinic acid receptor, it has been shown to also be activated by BHB (Taggart et al., 2005; Tunaru et al., 2003).

A connection between inflammation or colon cancer and GPR109a was suggested after colon cells in humans with colon cancer and mice model of colon cancer showed a reduction in GPR109a expression (Thangaraju et al., 2009). Later, activation of GPR109a was suggested to result in colonic macrophages and dendritic cells inducing differentiation of regular T-cells and T cells producing the anti-inflammatory cytokine IL-10. Furthermore, niacr1 knockout mice (niacr1 being the gene coding for GPR109a) were confirmed to be more susceptible to the development of colonic inflammation and colon cancer, strongly linking GPR109a to inflammation and inflammation-derived conditions such as cancer (Singh et al., 2014).

1.5.3 BHB regulating potassium channels.

When a series of *in vitro* experiments on cell cultures proved BHB's ability to inhibit NLRP3i from activating, the suggested mechanisms were the inhibition of the potassium efflux through interactions with the potassium ion channel (Guo et al., 2015). Additional experiments to exclude this being a side effect of other known BHB properties, such as HDAC inhibition or binding to G-protein coupled receptors were conducted. Trichostatin A was used as an HDAC inhibitor but did not impact the NLRP3i activation in LPS-primed macrophages. Neither was any impact found when using niacin, a known GPR109a agonist, on LPS-primed macrophages (Youm et al., 2015).

The hypothesis that BHB inhibited NLRP3i activation through inhibition of potassium efflux was further strengthened when it was shown to prevent intracellular potassium decline. LPS-primed cell cultures treated with known agonists for the potassium efflux channel showed less reduction in intracellular potassium levels when BHB was introduced (Youm et al., 2015).

1.6 Interactions between NF-κB, NLRP3i and BHB

With a better understanding of NF-κB, NLRP3i, and BHB, interactions between them become more apparent. When bacterial toxins such as LPS bind to TLRs and signal through the TLR pathway, NF-κB gets activated, and NF-κB dependent gene transcription occurs. The NF-κB dependent transcription of Pro-IL-1β, Pro-IL-18, and NLRP3 is often referred to as priming, the first step in activating the NLRP3 inflammasome.

K^+ efflux and ROS are some triggers resulting in the second step of NLRP3i activation (protein-complex assembly), where NLRP3i components oligomerize, resulting in the activation of pro-caspase1 and cleavage of pro-IL-1β and pro-IL-18 to mature IL-1β and IL-18. With BHB's potential to inhibit K^+ efflux and upregulate anti-oxidative genes, it is theorized that injections of BHB could inhibit NLRP3i activation by downregulating these triggers.
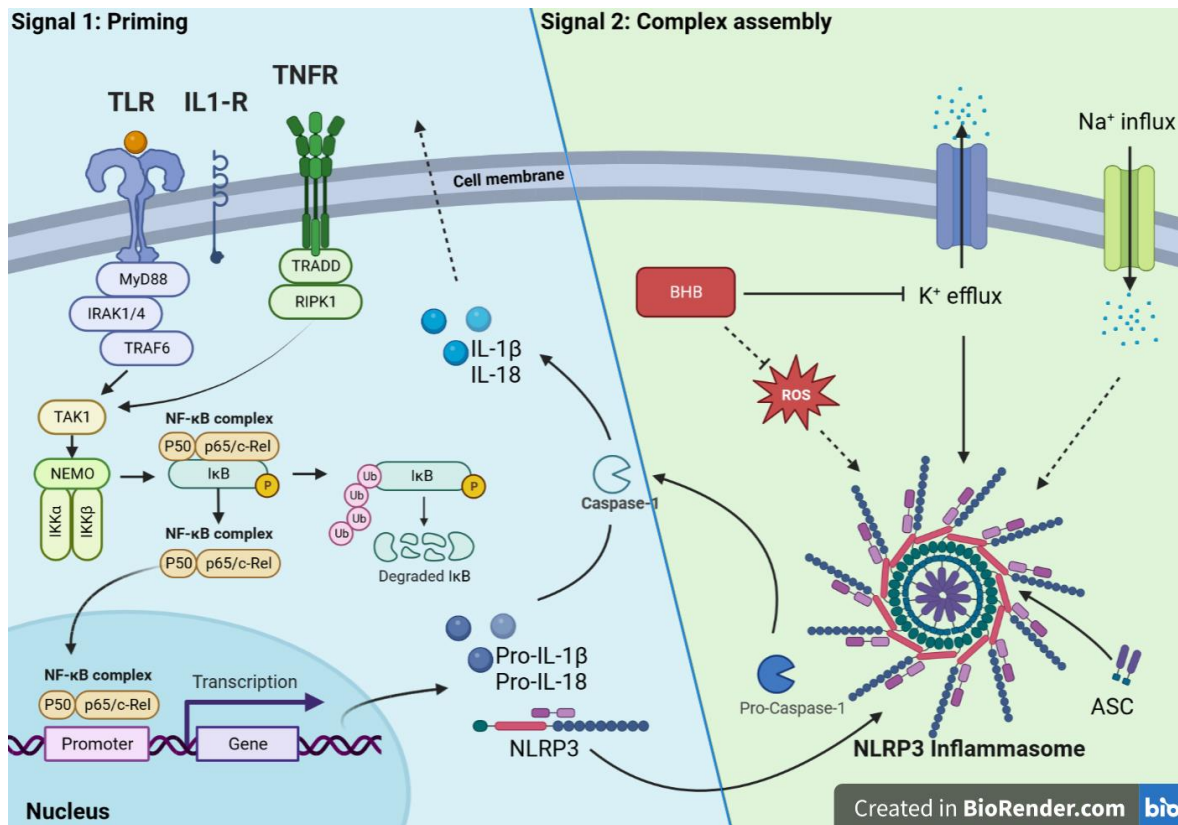
Figure 1.4– Visual representation of the interactions between NF-κB, NLRP3i, and BHB:

Visual illustration of how NF-kB activation is vital in the priming of NLRP3i (Step 1) and how activation of NLRP3i through K^+ efflux and ROS is impacted by BHB (Step 2). The NLRP3i-dependent maturation of Pro-Caspase1 to Caspase 1 is important to maturate Pro-IL-1β and Pro-IL-18. By inhibiting K^+ efflux or reducing oxidative stress caused by ROS, BHB downregulates the two commonly suggested mechanisms involved in the complex assembly of NLRP3i. This results in less secretion of the two pro-inflammatory cytokines IL-1β and IL-18

Additionally, by inhibiting NLRP3i activation, reduced maturation of IL-1β and IL-18 is theorized to downregulate NF-κB activation through a positive feedback loop involving IL-1R and IL-18R. Two cytokine receptors known to activate NF-κB through the TLR pathway. To measure these interactions, NF-κB activity and inflammatory markers will be measured.

1.7 The use of transgenic mice to measure NF-κB activity

Several methods are available to measure and quantify the NF-κB activity in research. The most common methods are through quantifying NF-κB target gene products such as cytokines or mRNA levels. This is commonly done through Western blotting, immunoassay, or qPCR.

Another method is the use of a reporter gene producing an enzyme (reporter protein) allowing us to monitor the NF-κB gene expression.

In this experiment, multiplex immunoassay is used to perform a cytokine profiling, allowing us to measure cytokine concentrations in the blood. Transgenic mice with a reporter gene producing an enzyme under the control of NF-κB will allow us to measure *in vivo* real-time NF-κB activity.

The mice selected were 3x-kB-luc-transgenic mice, sometimes also referred to as Luc2-reporter mice. Luc2-reporter mice are a transgenic C57BL/6J breed generated by microinjections of the 3x-B-luc plasmid linearized with HindIII and BglI into the Pronuclei of zygotes taken from superovulated female mice (Carlsen et al., 2002). These transgenic mice have a luciferase coding gene incorporated on three NF-κB response elements, resulting in a strong NF-κB regulated expression of luciferase in all cells (Carlsen et al., 2002).
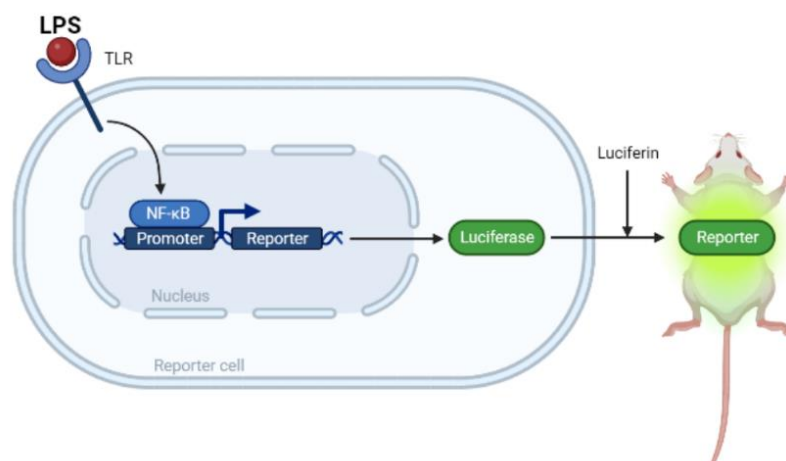
Figure 1.5 – Transcription of reporter gene:

A visual representation of how LPS result in NF-κB activation and transcription of our Luc2 promoter gene.

By injecting luciferin into the transgenic mice, a reaction between luciferin and NF-κB regulated luciferase results in oxyluciferin and light (Figure 1.6). This light emitted from the reaction can then be measured using highly sensitive cameras allowing for real-time *in vivo* measuring of localized NF-κB activity.
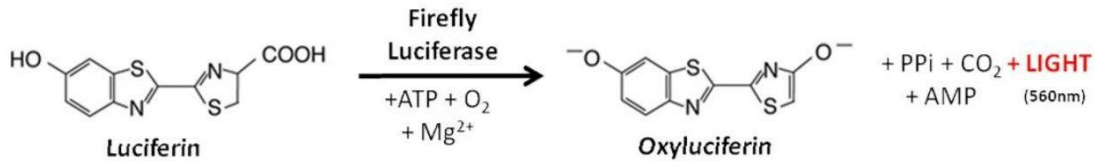
Figure 1.6 – Luciferin-luciferase reaction:

The reaction shows how luciferin and luciferase result in oxyluciferin, amp and light. This light is what will be measured through in vivo imaging. This figure is gathered from Gold Biotechnology's webpage [1].

_____

[1] https://commercio.nyc3.digitaloceanspaces.com/goldbio-2018/pages/luciferase%20reaction%20-%20paint.jpg

1.8   Aim

Many studies have supported the hypothesis that BHB affects inflammation, and connection between BHB, NF-κB, and NLRP3i have been demonstrated. However, most research is either done on mice on a ketogenic diet or in cell cultures. We wanted to explore if injections of BHB influenced inflammation in mice induced by LPS. LPS is often used to create strong and acute inflammation in mice. This approach allowed us to observe the effects of BHB without residual effects from dieting or other factors that could affect the results. Additionally, dose-dependent interactions were easier to observe, as it is assumed that injecting BHB gives higher control over the final BHB concentration.

To our knowledge, no similar experiments have so far been conducted,thus we regarded this experiment as a pilot study. Some small-scale experiments were carried out to help us clarify uncertainties.

The main aim of the experiment was to examine if BHB administered to mice via the intraperitoneal route (IP) affected inflammation induced by LPS.

Sub aims**:**

1) Establish a robust method for assessing BHB in blood samples from C56BL/6J mice to determine the concentration of BHB in blood at different time points following bolus IP injections of BHB.

2) Investigate if NF-κB activity is affected by BHB by injecting four different BHB doses into LPS-treated luc2-repoter mice and measuring NF-κB activity through *in vivo* imaging.

3) Investigate how the inflammatory markers IL-1β, IL-6, IL-10, Il-18, IFN-γ, and TNF-α in blood are impacted by BHB in LPS-treated mice through multiplex immunoassay.

2   Methods

For this thesis, both *in vitro* & *in vivo* experiments involving laboratory mice were conducted. Before injecting different amounts of BHB into the selected mice and measuring NF-κB activity, several small-scale experiments had to be carried out. These experiments were mainly focused on: Genotyping the offspring from bred in advance, observing BHB blood concentration over time after bolus BHB injections, and comparing the accuracy and precision of two methods used to measure BHB. These two methods were an assay kit from Neogen|Megazyme and a handheld tool from Abbot. After conducting these smaller experiments, NF-κB activity in NF-κB-luc transgenic C57BL/J mice could be measured. Due to the nature of the experiment involving animal testing, each aspect had to comply with the European guidelines on animal research as well as be approved by Mattilsynet: The Norwegian Food Safety Authority. This experiment was given FOTS ID 28945. All materials, solutions and instruments used during the project can be found in appendix 1.

2.1   Experimental setup

105 C57BL/J mice were bred using heterozygous NF-κB-luc progenitors and wild-types, resulting in 75 transgenic offspring. Only 24 transgenic mice were needed in this project, as the experiment was planned to include four groups with n=6 transgenic mice in each (three females and three males). The breeding resulted in more transgenic offspring than expected, and due to the layout of the litters, the use of n=26 transgenic mice was favorable. All the groups ended up with age-matched mice and at least three males and three females. Group 3 & 4 included one additional male mouse (See figure 6.1 for a visual representation).

The mice were housed in individually ventilated cages, ranging from 2-5 mice per cage depending on their gender and litter to avoid conflicts of dominance. Each cage included a running wheel, bedding (wood shavings), a piece of paper used for nesting. and a wooden chewing stick. Once a day, the cages would be observed by certified personnel looking for any signs of fighting or discomfort in the mice. When deemed necessary, the cage would be cleaned, and the bedding, paper and chewing stick would be replaced. Until all the mice were between 16 and 21 weeks, they were kept in an animal facility where the temperature and moisture were closely monitored and controlled. This animal facility also included a housing room with 12

hours light/dark cycles. The temperature was held around 25 °C and the relative humidity was set to around 50%. All mice were fed the same standard chow and water in *ab libitum* during the experiment.
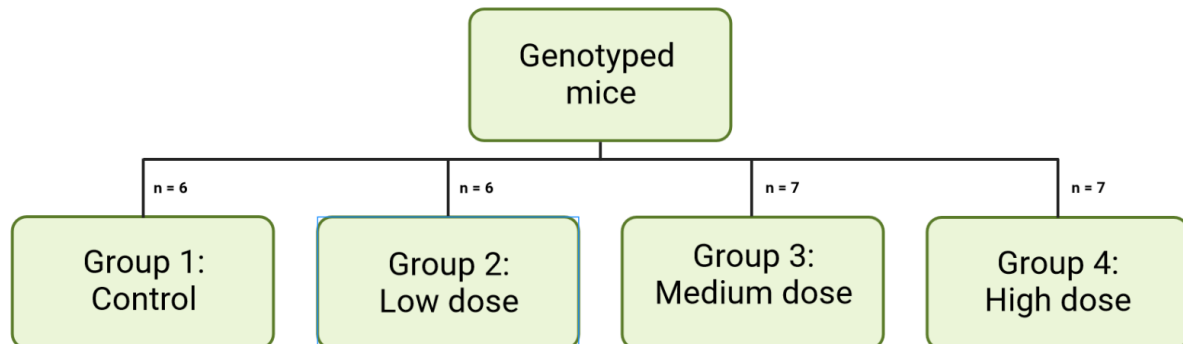
Figure 2.1 – Visual representation of the four groups given different dose BHB:

Group 1: Control was given a control solution. Group 2: Low dose was given 5 mmol/kg BHB. Group 3: Medium dose was given 10 mmol/kg BHB and Group 4: High dose was given 15 mmol/kg BHB.

Figure 2.2 is a visual representation of the timeline, including the uncertainties examined through small-scale experiments.
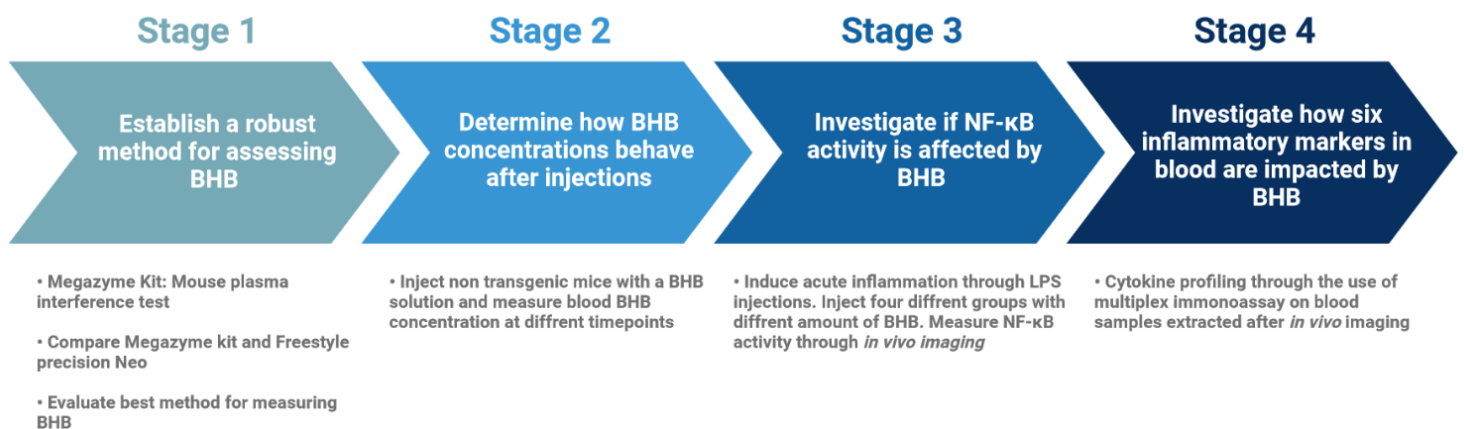
Figure 2.2 – Visual representation of the experiment:

The experiment can be sectioned into four stages. Stage 1 was to establish a robust method for measuring blood BHB concentrations in mice. To accomplish this, several small-scale experiments were done with two different methods of measuring BHB concentrations. Once a robust method for measuring blood BHB concentrations in mice was established, the next stage was the creation of a timeline mapping blood BHB concentrations in mice after BHB injections. This timeline was then used to decide optimal timings for injecting the transgenic mice with LPS, BHB, and luciferin. In stage 3, transgenic mice were injected with LPS, different doses of BHB, and luciferin. NF-kB activity was then measured through in vivo imaging to investigate how the activity is affected by BHB. Stage 4, the last stage, was analyzing six inflammatory markers from blood samples taken at the end of stage 3.

2.2   Megazyme Assay Kit: Mouse plasma interference test

In the weeks leading up to the final experiment, we had to be acquainted with our selected methods of measuring BHB in blood and mice plasma. For measuring BHB in mice plasma, an assay kit from Megazyme (K-HDBA) was selected due to its affordability, availability, and amount of tests it would allow us to perform.

The Megazyme Assay Kit uses colorimetric methods to determine the amount of BHB in the sample (up to 1.2 µg BHB per assay). Two enzymatic processes are utilized to determine the BHB concentrations. Two redox reactions catalyzed by 3-hydroxybutyrate dehydrogenase and diaphorase result in an INT-formazan product that can then be measured using a MicroAssay Absorbance reader.
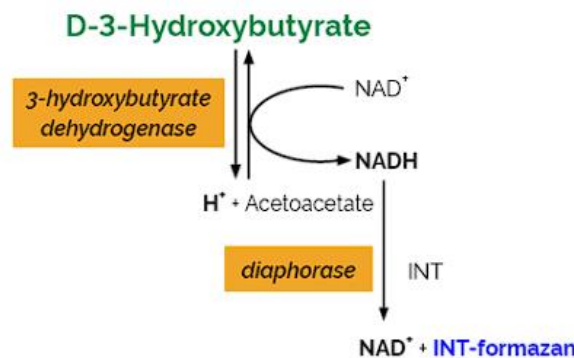
Figure 2.3 – The enzymatic processes used by Megazyme Assay Kit:

First, 3-hydroxybutyrate dehydrogenase (3-HBDH) catalyzes the reaction where BHB is oxidized to acetoacetate. The second enzyme, diaphorase catalyzes the second reaction where iodonitrotetrazolium chloride (INT) is reduced to a formazan product. Since this is a stoichiometric reaction, all the reactants are consumed when the reaction is completed. BHB concentration can be calculated by measuring the amount of INT-formazan. The picture is gathered from the Megazyme product page [1].

_____

[1] https://www.Megazyme.com/d-3-hydroxybutyric-acid-beta-hydroxybutyrate-assay-kit

However, this kit's commercial purpose is mainly to measure D-hydroxybutyric acid in eggs and other food-related products. After contacting the technical support team at Megazyme, it was confirmed that this kit has never been used to test mice plasma. A interference test was necessary to ensure no interference between mouse plasma and the kit.

To do the interference test, plasma was extracted from a random adult non-transgenic mouse. This was done by using a 23G needle containing 90 µL EDTA and cardiac puncture. The content of the needles was then emptied into an Eppendorf tube. To separate the plasma and serum, the Eppendorf tube was spun at 1500 x G in a chilled centrifuge for 10 min. A 96-well microplate was prepared with 10 µL distilled water in wells A1 and B1, 5 µl standard solution from the kit + 5 µl distilled water in the wells A2 and B2, 10 µl Plasma in well A3 and B3, and 5 µl standard solution + 5 µl plasma in wells A4 and B4. See Figure 2.4 for a visual representation of the plate layout.
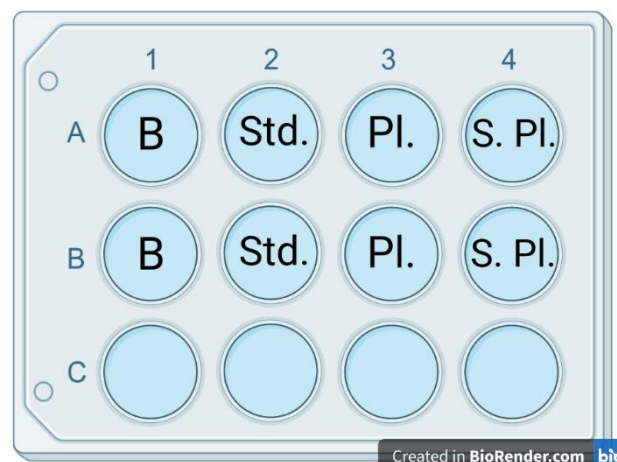
Figure 2.4 - Visual representation of plate layout:

In wells marked B (A1 & B1) no sample or standard was added. In wells marked with St. (A2 & B2) standard solution was added. In the wells marked Pl. (A3 & B3) plasma samples were added. Lastly in the wells marked S. Pl. (A4 & B4) standard solution and plasma samples were added.

272 µL of premade master mix (200 µL dH$_2$O, 50 µL buffer, 20 µL NAD$^+$/INT, and 2 µL Diaphorase) was pipetted into each well, and the microplate was placed on a microplate shaker for 2 min. After 2 min, the absorbance at 492 nm was read using a MicroAssay Absorbance reader. This reading was referred to as A$_1$. The final reaction was then catalyzed by adding 2 µl 3-βhydroxybutyrate dehydrogenase in all wells. The absorbance was then read in two min intervals, starting at 4 min, then 6 min and 8 min etc. This was done to ensure the completion of the reaction, and if completed by 6 min, this absorbance was then noted down as A$_2$.

However, if the reaction was not completed by 6 min and the readings still showed a change in absorbance, the measuring would continue until no change was found, and then that absorbance would be noted down as A_2 instead.

2.3 Comparing and evaluating Megazyme Assay Kit and Freestyle Precision Neo

FreeStyle Precision Neo (FPN) is a 2-in-1 diagnostic tool aimed at diabetics that allows them to test both blood sugar and BHB concentration. By using special strips, Abbott advertises that the tool can measure values up to 8 mM BHB in blood. However, accuracy and precision is not mentioned. An experiment where FPN was compared against the Megazyme kit was done with the aim of getting an indication of the accuracy and precision of FPN.

900 µL blood was extracted from a random non-transgenic mouse and then terminated. This was done by using a 23G needle containing 90 µL EDTA and cardiac puncture. β-Hydroxybutyrate-salt (BHB-sodium) purchased from Sigma-Aldrich was used to create a 600 mM BHB solution. To create the 600 mM BHB solution, 378,3 mg BHB-sodium was weighed and dissolved in 5 mL µL 0.9% NaCl saline solution. Some of this stem solution was then diluted to create 300 mM and 150 mM BHB solutions.

2 µL of the BHB solutions were added to Eppendorf tubes containing 198 µL blood, resulting in three blood samples with theoretically estimated BHB concentrations of 6 mM, 3 mM, and 1.5 mM BHB. The BHB concentrations in the blood samples were then measured using FPN. Plasma from the blood samples was then extracted using the same methods as before and analyzed using the Megazyme kit and FPN. The measured concentrations were then compared against each other.

To test the linearity and precision of FPN, blood from another random non-transgenic mouse was extracted using the same method as before. A new 1200 mM BHB solution was made using 756.6 g BHB-sodium and 5 mL 0.9% NaCl saline solution. A 12 mM BHB solution was created by diluting the 1200 mM BHB solution over several steps.

20 µL blood was pipetted into 5 different Eppendorf tubes. 20 µL 12 mM BHB solution was then added and mixed thoroughly in the first tube marked with "6 mM". 20 µL sample from this tube was pipetted into a new Eppendorf tube marked "3 mM". This step was done two more

times, until a series of blood samples, all theoretically having 6 mM, 3 mM, 1.5 mM, 0.75 mM, and 0 mM BHB were made. The BHB concentration was then measured using FPN.

2.4   Mapping timeline of BHB concentration in blood

Due to the lack of literature on how blood BHB concentration behaves after bolus IP injections of BHB, an experiment with the goal of exploring exactly this was carried out. M. S Yum and colleagues gave bolus IP injection of 20 mmol/kg R-3-Hydroxybutyric acid sodium salt (BHB-sodium) and sampled blood 15 min after the injections. The recorded blood BHB concentration 15 min after injection was measured and calculated to be 4,54 ± 1.99 mM (M. S. Yum et al., 2012). Together with other studies such as (Kraeuter et al., 2020) also injecting 20 mmol/kg intraperitoneally without any mention of complications, the decision was to inject the mice with 22 mmol/kg BHB, aiming to achieve supraphysiological plasma BHB concentrations around 4-7 mM.

A BHB solution at 2,75M was created by adding BHB-sodium to a 0,9% NaCl Saline solution. Three males & three females, random non-transgenic mice ranging from 16-18 weeks, were weighed, and marked on their tails. The baseline BHB concentration was measured using FPN before injecting each mouse with 22 mmol/kg in a staggered fashion. Blood concentration was measured using FPN at 0,15, 30, 45, 60, 75, 120, and 240 minutes after the initial injection. This was done by making a small incision in the tail, allowing a tiny blood drop to be extracted from the tail vein. The tail was then carefully massaged to reopen the incisions each time a new drop of blood was needed.

Measured BHB concentrations were higher than expected, and some were outside the range of what FPN could measure. Combined with the mice showing discomfort, two new solutions with significantly lower concentrations were made by further diluting the BHB solution. The experiment was redone with six new non-transgenic mice. This time four males and two females aged 16-18 weeks were randomly selected and injected with either 3.2 mmol/kg or 1.6 mmol/kg. Blood BHB concentrations were then measured at 0, 15, 30, 45, 60, and 75 min using FPN.

2.5 *In vivo* measuring of NF-κB activity

At week 18 of the project, all selected transgenic mice (n=26) were within the preferred age group (15-25 weeks). By injecting lipopolysaccharide (LPS), a surface membrane component found on most gram-negative bacteria, an acute inflammatory response was triggered. The LPS used in this experiment was purchased from Sigma-Aldrich (Serotype 055:B5). In-Vivo-Imaging-System (IVIS) produced by PerkinElmer, Massachusetts, USA was used to quantify the acute inflammation by measuring the bioluminescence of the transgenic mice. This instrument is capable of measuring both fluorescent and bioluminescent emissions with its extremely sensitive CCD camera.

With our hypothesis that BHB can bind to GPR109a as well as generally impact NF-κB/NLRP3i activation, custom regions of interest (ROI) were made when performing *in vivo* imaging. Two regions were created: ROI 1, a region on the upper abdominal area mainly focusing on the liver, and ROI 2, a region on the lower abdominal area focusing on the intestines (illustrated in Figure 2.5)
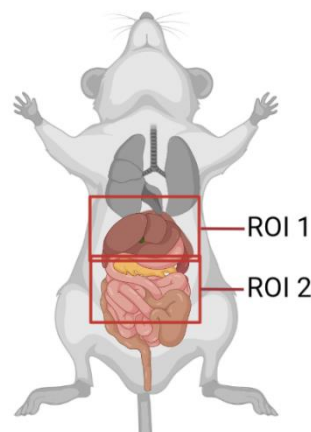
Figure 2.5 – ROI 1 and ROI 2:

Two areas were selected for in vivo imaging. ROI 1 Focuses on measuring NF-κB activity in the liver, while ROI 2 focuses on measuring NF-κB activity in the intestine.

Before the experiment could start, three new BHB solutions at 1.875 M, 1.250 M, and 0.625M were made. The mice were all weighted, individually marked, and then shaved on their thorax-abdominal area to ensure maximal light emission from internal organs through the luciferin-luciferase reaction resulting in bioluminescence. Due to time constraints, this experiment was conducted over two days, using 16 mice on the first day and the remaining 10 on the second day.

The right amount of LPS (100 µL/25g mouse) was calculated and added to individual 1ml syringes with a 25G needle and warmed to room temperature. The LPS was warmed up to room temperature to minimize stress during injections. 3-4 mice were placed into an anesthesia chamber connected to a High-Flow vaporizer containing Isoflurane. The groups of mice were then injected intraperitoneally with LPS in a staggered fashion, 15 minutes between each group, and then put back into their initial cages.

The correct amount of BHB doses (0, 5, 10, 15 mmol/kg) were calculated and then added into individual 1ml syringes with 25G needles and warmed to room temperature. 40 min past the LPS injection, the groups were reintroduced into the anesthesia chamber and anesthetized. When 45 min had passed since the initial IP injection of LPS, the corresponding dose of BHB solution was given through IP injections, and the mice were then placed back into their cage.

The correct dose of luciferin (200 µL /25g mouse) was then calculated and added into 1m syringes with 25G needles and warmed to room temperature. Approximately 10 min before the 2 hours mark since the initial IP injection of LPS, the mice were anesthetized and injected with luciferin intraperitoneally. The mice were then gently placed inside the IVIS. The mice were placed on their backs at predestined locations so that their stomachs were facing the camera and snouts were in the inlets connected to the High-Flow Vaporizer. Extra caution was taken during this step to make sure the correct position of the mice. This is done to ensure they stay under anesthesia for accurate images, but also due to the health of the animals. It is easy to place the mice too far into the inlets, risking contact between the glass tubes surrounding the inlets and their eyes. The bioluminescence was measured over 60 sec using a computer connected to the IVIS running a program called Living Image. The data was first compiled into interactive pictures and then exported to a document. The mice were then placed back into their cages.

Luciferin was then injected again at 3 hours and 50 minutes, and IVIS imaging was taken 10 min later (4 hours from the initial LPS injection). When all measurements were done (5 hours past the initial LPS injection), the mice were terminated, and blood samples were collected. Figure 2.6 shows a visual representation of the experiment's timeline.

Figure 2.6 – Timeline of experiment:

Once all preparations were conducted, the experiment could start. Before every injection the mice were placed under anaesthesia. Between the injections the mice were place back into their cages.

To prepare the mice for termination, each mouse was injected with a ZRF cocktail, a strong sedative mix containing Zoletil Forte, Xylazin, and Fentanyl citrate. This was done in the same staggered fashion as LPS. Using 25G needle and 1ml syringe containing 90 µL EDTA, cardiac puncture was performed, and 50-900 µL blood was extracted from the heart (The aim was to extract 900 µL from all mice). The blood was then transferred to Eppendorf tubes and placed on ice. Cervical dislocation was used to euthanize the mice after the blood sampling was finished. Blood samples were centrifuged at 1500 x G 4^0C for 10 min to extract plasma. The supernatant (plasma) was then pipetted over to new Eppendorf tubes and stored at -20^{0}C in a freezer until further use.

2.6   Cytokine profiling through multiplex immunoassay

Cytokine profiling is commonly performed by multiplex immunoassays, which allow for measurements of several proteins/cytokines from the same plasma sample. Although multiplex immunoassay requires more reagents and expensive machinery, the upside is that several cytokines can be measured at the same time. In the end, less plasma is needed, and the total time ends up being a lot less.

ProcartaPlex^{TM} Multiplex Immunoassay from Invitrogen was purchased from ThermoFischer (**PPX-06**). Explained in their own word how the kit works.

> "ProcartaPlex incorporate magnetic microsphere technology licensed from Luminex^{TM} to enable the simultaneous detection and quantification of multiple protein targets in diverse matrices. …".

ProcartaPlex panel configuration allows users to customize multiplex immunoassays, selecting from over 600 analytes either from humans, rats, mice, non-primates (NHP), canines, or porcupines. A mouse kit for TNF-α, IL-6, IL-1β, IL-10, IL-18 and IFN-γ were chosen for this project. These six were chosen based on compatibility (not all markers can be measured in the same kit) and hypothesized to be most likely affected by introducing BHB through IP injection.

The ProcartaPlex^{TM} multiplex immunoassay kit came as a bundle of a ProcartaPlex Mouse Basic Kit (EPX010-20440-901) and a mouse cytokine simplex kit for each cytokine (See appendix 1). An additional ProcartaPlex Mouse Basic Kit and ProcartaPlex Mouse IL-6 Simplex kit were ordered. This extra kit was used to find a dilution factor that best allow us to observe and measure the six different cytokines within the same standard curve. IL-6 was chosen due to previous experience, showing it to be the cytokine with the highest observed numbers during LPS-induced acute inflammation.

Before using ProcartaPlex Mouse Basic Kit and ProcartaPlex Mouse IL-6 Simplex kit to compare different dilutions, some preparations had to be done. The wash buffer in the basic kit needed to be diluted from 10X to 1X using double distilled water (ddH$_2$O). The IL-6 detection antibody mix from the IL-6 Simplex kit had to be diluted from 50X to 1X using Detection Ab diluent from the mouse basic kit. Lastly, the antigen standard had to be made in advance and diluted. This was done in a 15-step process detailed in the manual that came with the basic kit. The last preparation needed was the creation of a plate map, outlining what well includes plasma samples from mouse, blank or standard. Once all preparations were done, a multistep process based on the five basic steps of sandwich-based assay workflow could begin. These five steps are illustrated in Figure 2.7.

Firstly, a solution containing small (6.6 u) magnetic beads was added to each marked well on a 96-well flat bottom plate. These microsphere magnetic beads are coupled with specific capture antibody and stained with a corresponding fluorescent dye.

When samples or standards are introduced in the next step, the capture antibody can immobilize the targeted analytes after incubating for an appropriate time. Six samples, at eight different dilutions ranging from F=2 to F=256, were added, and the 96-well flat bottom plate was then incubated on a shaker for 120 min.

The third step is the introduction of 1X detection antibodies created during the preparation stages. These biotinylated detection antibodies are analyte-specific and binds to the analyte in

a way that creates the antibody-analyte–antibody sandwich-like structure that the method is named after.

In the 4th step, Streptavidin-Phycoerythrin conjugate (SAPE) gets introduced into each well binding to the biotin, completing the bead complex and acting as indirect immunofluorescent staining. In conjunction with the stained magnetic microsphere bead, this allows for detection, sorting and measurement when the beads pass through a cytometric bead array, like Bio-Plex 200.

The 5th and final is measuring the stained beads using Bio-Plex 200 (a flow cytometry analyzer). The data was compiled and exported into excel documents for further analysis. Between each of these five steps, the 96-well flat bottom plate got placed on a handheld magnetic plate washer and washed three times using 1X wash buffer made during the preparation stages.
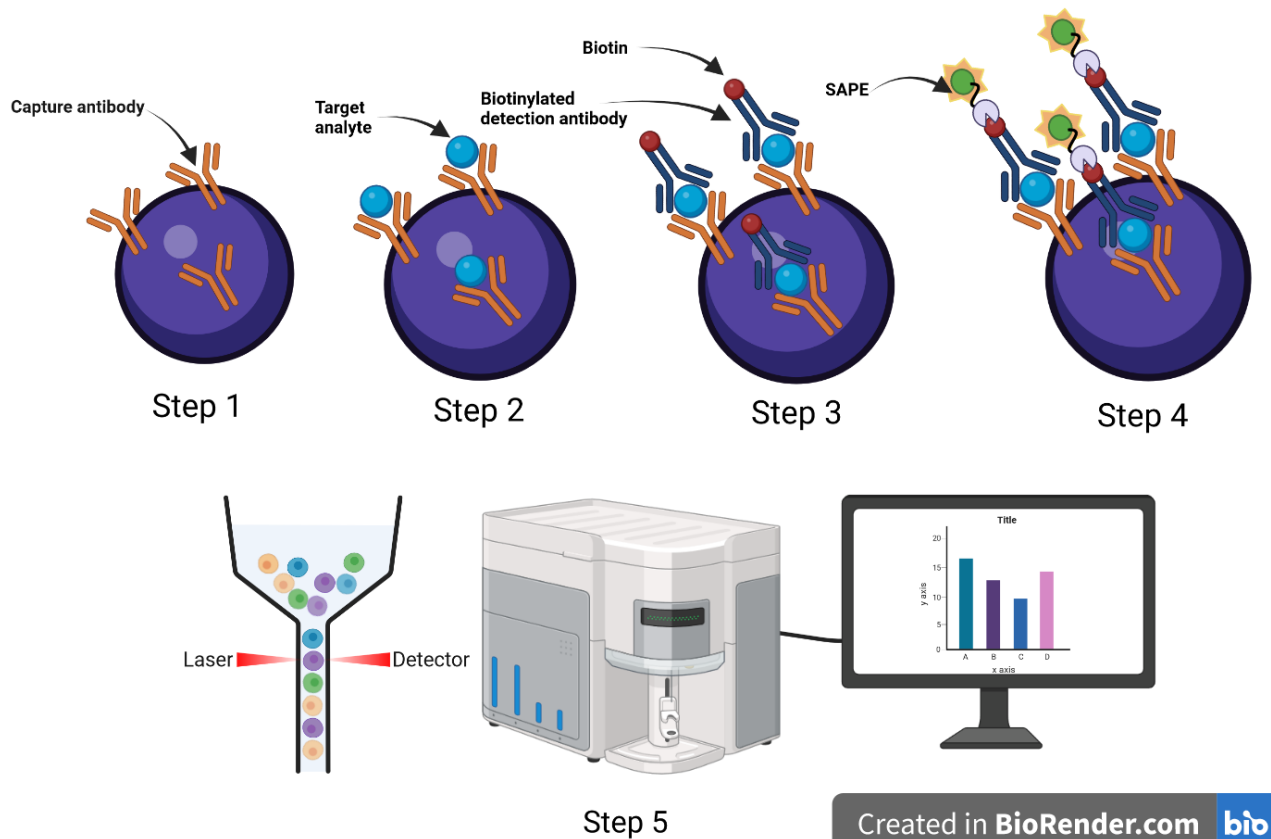
Figure 2.7 – 5 steps of sandwich-based immunoassay:

*This figure illustrates the five main steps of sandwich-based immunoassays. **Step 1** is to dispense color-coded beads with analytic-specific capture antibodies into each well. **Step 2** is the introduction of samples to each well and incubate so the analytic specific capture antibodies can bind to their target analyte. **Step 3**, Biotinylated detection antibodies are added. These antibodies bind to the target analyte. **Step 4**, SAPE (reporter dye) gets added. The biotinylated ends on the detection antibody allow SAPE to connect with the bead complex. **Step 5** is the measurements of the bead-analyte-antibody-reporter dye-complex using a flow cytometry analyzer.*

When all six cytokines were measured at the same time, some necessary changes were made. Each kit came with cytokine-specific 50X bead solution and 50X detection antibody mix. To create a 1X bead solution and a 1X detection antibody mix usable for all six cytokines at the same time, the six different solutions were combined and then diluted to one 1X-multi bead mix as instructed by the accompanied protocol. When samples were added, all samples had a dilution factor of F=16. This was decided from a earlier experiment where several dilution factors were tested on IL-6 (Figure 4.1).

2.7   Data analyses

Data collected from IVIS and Bio-Plex 200 were compiled into an excel document and sorted. The sorted data was then imported to R-studio, and several analytical methods were used. To check if the data met all model assumptions, Shapiro-Wilks test was used to see if the data was normal distributed, and Barlett's test was used to test for equal variance. If these assumptions were not met, data transformations using either log transformation or natural log transformation were applied and checked for normal distribution and equal variance.

If the assumptions of normal distribution and equal variance were met, analysis of variance (ANOVA) was performed to look for any group or gender effect. Linear regression was used to examine how one variable affects the other (How the amount of BHB injected affected different cytokines).

The significance level was set at α=0.05, meaning p-values < 0.05 was considered significant. Data and results with no significance or specific interest have been compiled in Appendix 2.

3 Results

The goal of the thesis was to test the potential anti-inflammatory effects of BHB injections through measurements of NF-κB activity and cytokine profiling. Before injecting BHB into the mice, several small-scale experiments were done to investigate uncertainties. With no data on how plasma or blood BHB concentrations would behave after a bolus BHB IP injection, it was vital that we examined how long BHB would circulate in the blood and when the concentrations would be at their highest. Examining this, would allow us to perform injections at the right time, resulting in the greatest observable effects. Before examining how BHB would behave after a bolus BHB injection, the best method for measuring BHB concentrations in the mice had to be evaluated.

3.1 Establishing method for assessing BHB in blood by comparing two different methods

The first method investigated was the use of an assay kit from Megazyme. It was essential to test for potential interference between mouse plasma and the reagents in the kit. This was done according to the recommendation from Neogen|Megazyme support staff.

Using a MicroAssay Absorbance reader, the absorbance was first read after adding samples and master mix in each well. This absorbance was then noted down as A1. A2 was the absorbance measured at six minutes after adding 3-β-hydroxybutyrate dehydrogenase to each well and making sure that the reaction was complete. The change in absorbance was noted and then compared between the different samples to look for any interaction between mouse plasma and the kit. Table 3.1 shows the average A1, A2, ΔA, and the calculated BHB concentration of the four samples. By comparing calculated BHB concentration between standard and spiked plasma, any interference can be quantified and evaluated if significant. A sample with only plasma is also added to evaluate if the plasma had an initial BHB concentration.

Table 3.1 Megazyme Assay Kit interference test

This table shows average results of two parallels after doing interference test using spiked mice plasma (plasma and standard solution from the kit), Standard solution, mice plasma and blanks. Absorbance was measured at 492 nm using MicroAssay absorbance reader. Marked results (*) are results lower than the linear range of the kit.

	Blank	Spiked Plasma	Standard	Plasma
A1 (Absorbance at start)	0,107	0,126	0,100	0,102
A2 (Absorbance at 6 min)	0,135	0,335	0,279	0,150
Change in absorbance (ΔA)	0,028	0,209	0,179	0,048
Calculated BHB [mg/ml]	---	0,035	0,030	0,008*
Calculated BHB [mM]	---	0,345	0,288	0,077*

With the wells containing master mix & samples having variable baseline absorbance (A1), determining the baseline is necessary to calculate the change in absorbance after starting the reactions by adding 3-β-hydroxybutyrate dehydrogenase. Using the change in absorbance measured between A1 and A2 (ΔA) in the standard and the spiked plasma sample, the concentration of BHB could be calculated in millimolar using two formulas.

$$1: BHB \left[{}^{mg}/_{ml} \right] = \frac{\Delta A_{sample}}{\Delta A_{standard}} * Standard \left[{}^{mg}/_{ml} \right] * Dilution\ factor$$

$$2: BHB\ [mM] = \frac{BHB \left[{}^{mg}/_{ml} \right]}{104,105\ g/mol} * 1000$$

With a calculated difference of 0,06 mM between the spiked sample and the standard solution, it was concluded that there was no significant interference between mice plasma and the Megazyme kit. During the testing of the kit, it was found to be extremely sensitive to methods of pipetting, often with bubbles appearing and impacting the absorbance readings. At the same time, the kit relies on time-sensitive enzymatic reactions, making the kit less desirable to use than first assumed.

The second method of measuring BHB concentrations was a handheld diagnostic tool from Abbot called FreeStyle Precision Neo (FPN). The purpose of this tool is for diabetics to measure BHB concentrations in blood quickly from a small blood sample (≈5 µl).

To compare the Megazyme kit and FPN, blood spiked with a known amount of BHB and diluted with saline was measured using FPN. Plasma was then extracted from the samples and measured with both FPN and the Megazyme kit. The measured values were plotted into a graph against the expected BHB concentration (Figure 3.1). The result showed lower observed concentrations than what was theoretically expected. This disparity between theoretical and observed concentrations did however not impact the validity of the test aimed at comparing the two methods. Comparing blood BHB concentration measured with FPN and the plasma BHB concentrations measured with the Megazyme Kit, the difference was at most 0,315 mM.
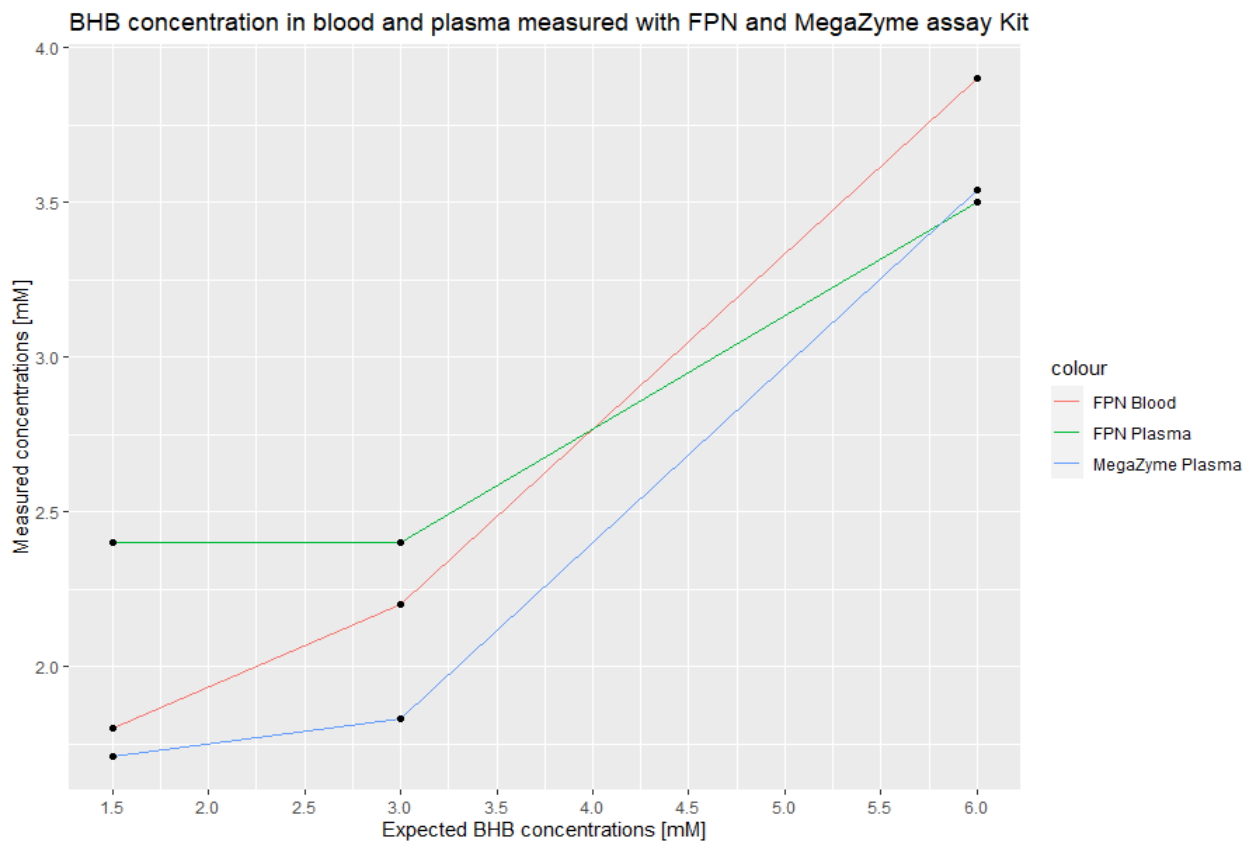
Figure 3.1 - Blood and plasma samples spiked with a known amount of BHB:

The three different lines represent the three different measurements done on blood or plasma spiked with a known amount of BHB. Green line are BHB concentrations in plasma measured using FPN. Red line are BHB concentrations in blood measured using FPN. Blue line are BHB concentrations in plasma measured using Megazyme.

When introducing supraphysiological BHB concentrations, the 0.315 mM difference is tolerated. With the goal to compare the effect of four different doses of BHB, the accuracy of the tool becomes less important, and the precision becomes the primary factor. To evaluate the

precision of FPN, a new dilution series was made, and the linearity of observations was examined using linear regression.

During these tests, it became apparent that the amount of saline solution added to the spiked blood samples had a negative impact on the accuracy of FPN. Adjusting for the amount saline solution in each sample, the observed results came closer to the theoretical ones. These adjusted values can be seen in Table 3.2 and plotted against the theoretical estimated values in Figure 3.2. Linear regression on the adjusted data proved a significant linear relationship (p-value < 0.01) between the adjusted values and expected values. With a linear relationship established, any concentration measured with FPN was assumed to have the same accuracy.

Table 3.2 Adjusted BHB concentrations:

Measured BHB concentrations with FPN in blood adjusted for saline added in each sample and then compared with originally observed and theoretical values.

Adjusted BHB concentrations	0,2 mM	0,62 mM	1,68 mM	2,81 mM	4,98 mM
Theoretical Concentration	0,1 mM	0,75 mM	1,50 mM	3,00 mM	6,00 mM
Originally measured concentrations	0,2 mM	0,60 mM	1,60 mM	2,55 mM	4,15 mM
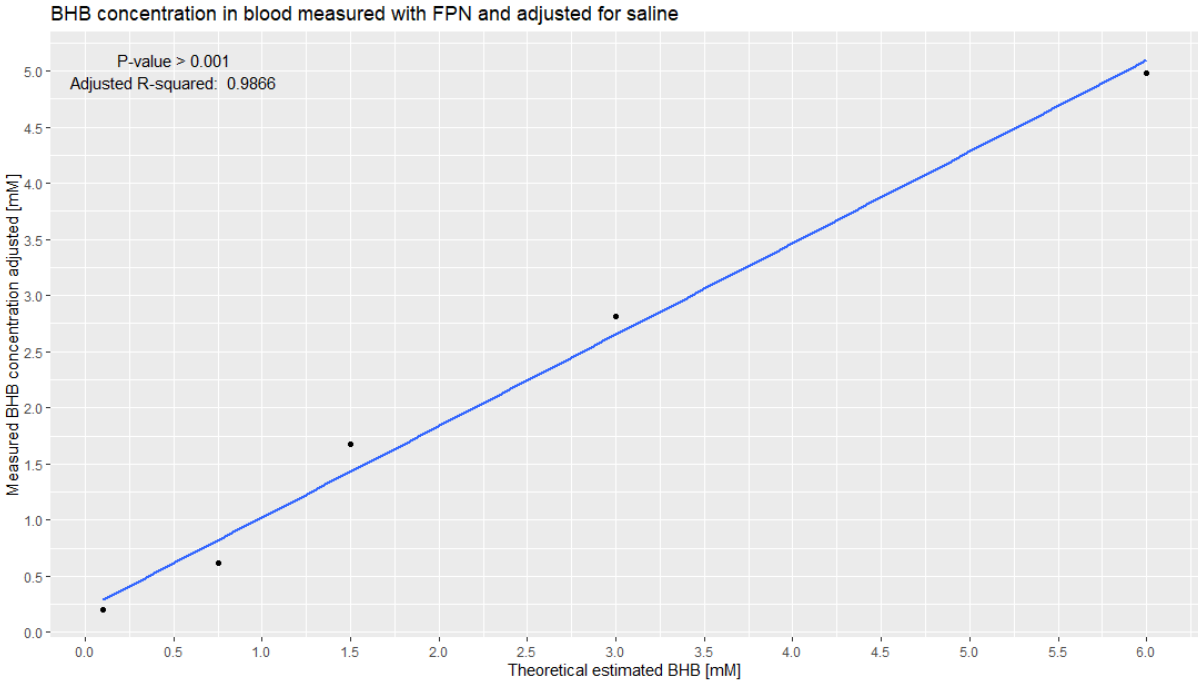
Figure 3.2 - Adjusted BHB concentrations measured by FPN against theoretically estimated BHB concentrations:

The blue line represents the linear regression line with a p-value > 0.001 suggesting the FPN tool measures in a linear fashion.

From these results, it was concluded that FPN was accurate enough when used in blood and that the tool behaves in a linear fashion. Additionally, the fact that FPN only required a small drop of blood (≈5 µl) and a few seconds to measure the BHB concentration made it all clearer that it was the right tool to use.

3.2   Mapping timeline of BHB concentration in blood following a BHB injection

After deciding the best best method for measuring BHB, the investigation into how the BHB concentration behaves after injections and the relationship between mmol/kg given and observed concentration could proceed. Six non-transgenic C57BL/J6 mice were injected with 22 mmol/kg and BHB blood concentrations were measured over a period of four hours (Figure 3.3).
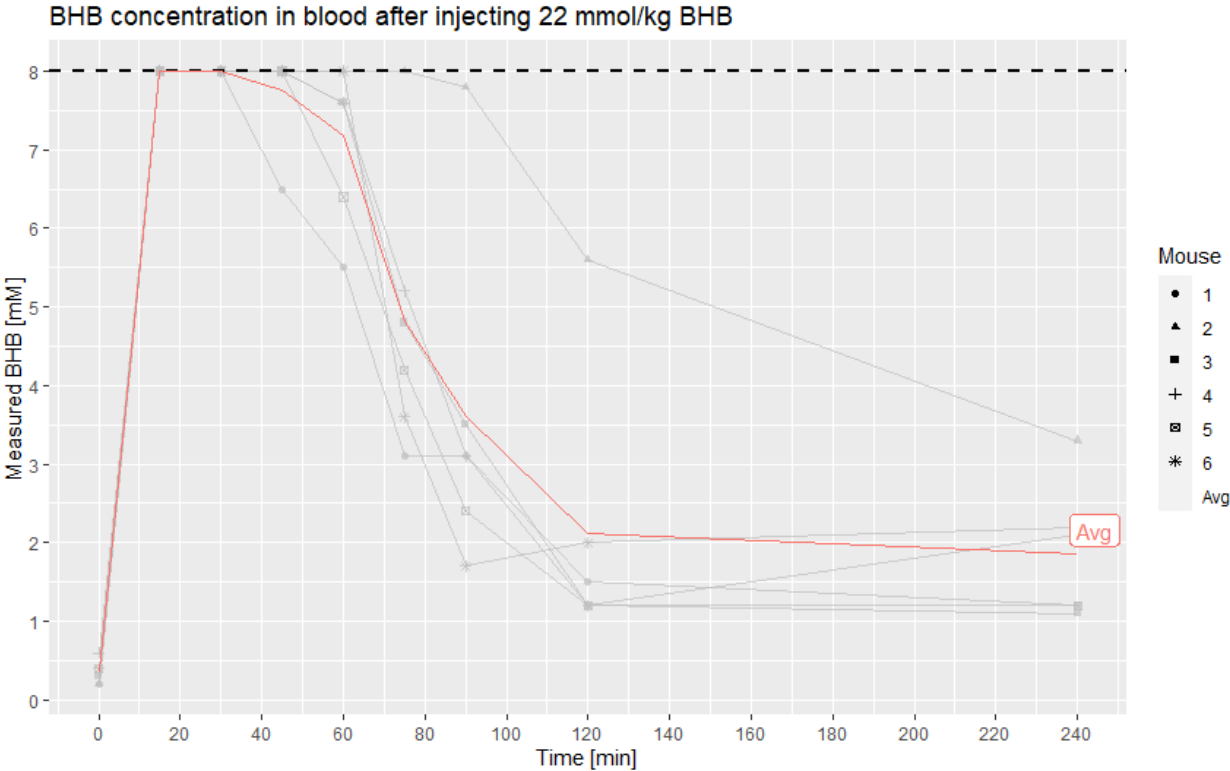
Figure 3.3 - Timeline of BHB concentration after injecting 22 mmol/kg BHB

The red line indicates average values for all mice, with the dashed line illustrating the upper BHB concentration possible to measure using FPN. No concentration measured at 15 or 30 min was under this limit and resulted in the instrument giving error code "Hi".

With most of the early measurements showing "Hi", it is safe to assume that these concentrations were over 8 mM. After 45-75 min from the initial BHB injection most measurements were within the range, and once measurable, the concentrations decreased relatively rapidly and ending up at 1-2 mM after two to four hours.

The measured BHB concentrations differ drastically from the previously mentioned experiment (M.-S. Yum et al., 2012) used as the baseline to calculate the BHB doses. 22 mmol/kg BHB injections were theorized to result in a blood BHB concentration of a maximum 4-7 mM. With these results however, it is reasonably to assume the concentration exceeded 8 mM for a substantial time.

Shortly after the injection, discomfort was observed in all the mice. This was expressed through reduced motor functions, closed eyelids, and hunched backs. These signs were subjectively more severe in females, with their measured concentrations also being higher (mouse 2,4 & 6). After 1-2 hours most mice showed signs of recovery and after six hours the first two mice were back to normal functions. 24 hours after initial BHB injections, all mice except two had fully recovered. These two mice were then terminated (mouse 2 & 6).

With introducing stress through potentially harmful injections being against project's purpose, the BHB doses were reduced. Six new mice were injected with either 3,2 mmol/kg or 1,6 mmol/kg. The result is plotted in Figure 3.4.
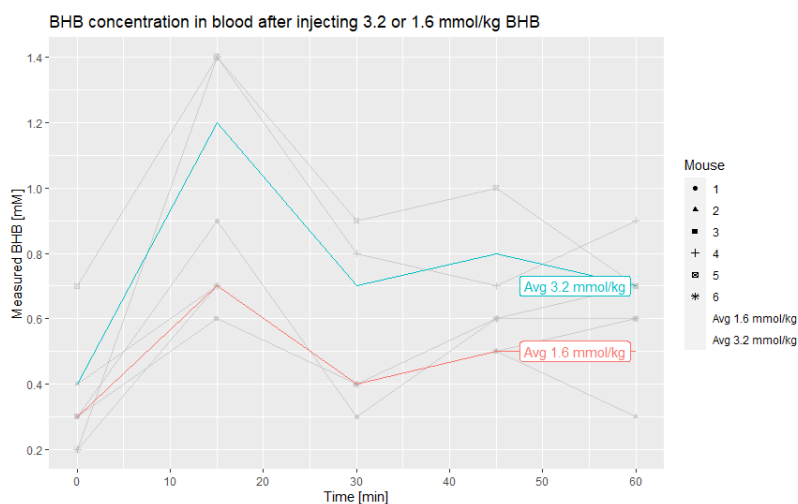
Figure 3.4 - Timeline of BHB concentration after injecting 3.2 mmol/kg and 1.6 mmol/kg BHB solution:

The blue line represents the average BHB concentration measured from mice given 3.2 mmol/kg BHB and the red line represents the average BHB concentration measured from mice given 1.6 mmol/kg.

With no measurements exceeding the limit of FPN, a continuous graph shows a clear rise in blood BHB concentration within the first 15 min. At 30 min, the concentration had decreased almost back to baseline before leveling out slightly higher than baseline.

3.3   BHBs effect on *In vivo* NF-κB activity

Following the *in vivo* imaging, the data on NF-κB mediated light emitted from both ROI 1 and ROI 2 were analyzed (Figure 3.5). No significant difference between the groups given different BHB doses were found. Neither was any dose-dependent relationship between NF-κB activity and the amount of BHB injected found. However, the data shows a strong NF-κB activity in the liver (ROI1), with the measured radiance increasing from 2 to 4 hours, as expected. Comparatively, the NF-κB activity measured from ROI 2, focusing on the lower abdomen and intestines, shows a much weaker NF-κB activity.
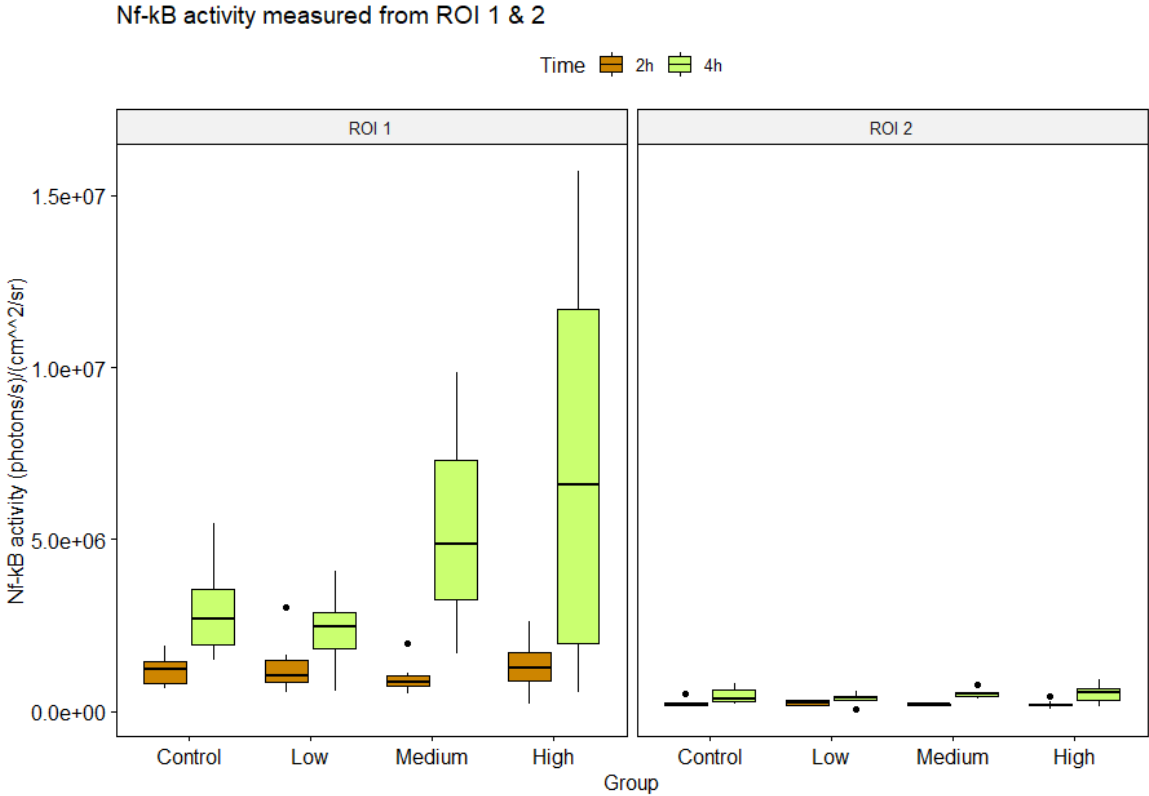
Figure 3.5 – NF-κB activity measured from ROI 1 and ROI2 at two & four hours after initial LPS injection grouped by dosage:

NF-κB activity measured in $(photons/s)/(cm^2/sr)$. The data is grouped by the four different doses BHB injected through a single IP injection. Control - 0 mmol/kg BHB, Low - 5 mmol/kg BHB, Medium - 10 mmol/kg BHB and High - 15 mmol/kg . The whiskers extend to the largest and lowest values observed in each group, excluding outliers which are represented as dots outside the whiskers. Each box represents the interval where 50% of the data resides, with 25% above and 25% below the median line in the box.

Focusing on ROI 1 while grouping based on genders (Figure 3.6), a significant gender-based difference was found (p-value < 0.01). In *in vivo* images taken at both two and four hours showed a significantly higher NF-κB activity in male mice compared to female mice.
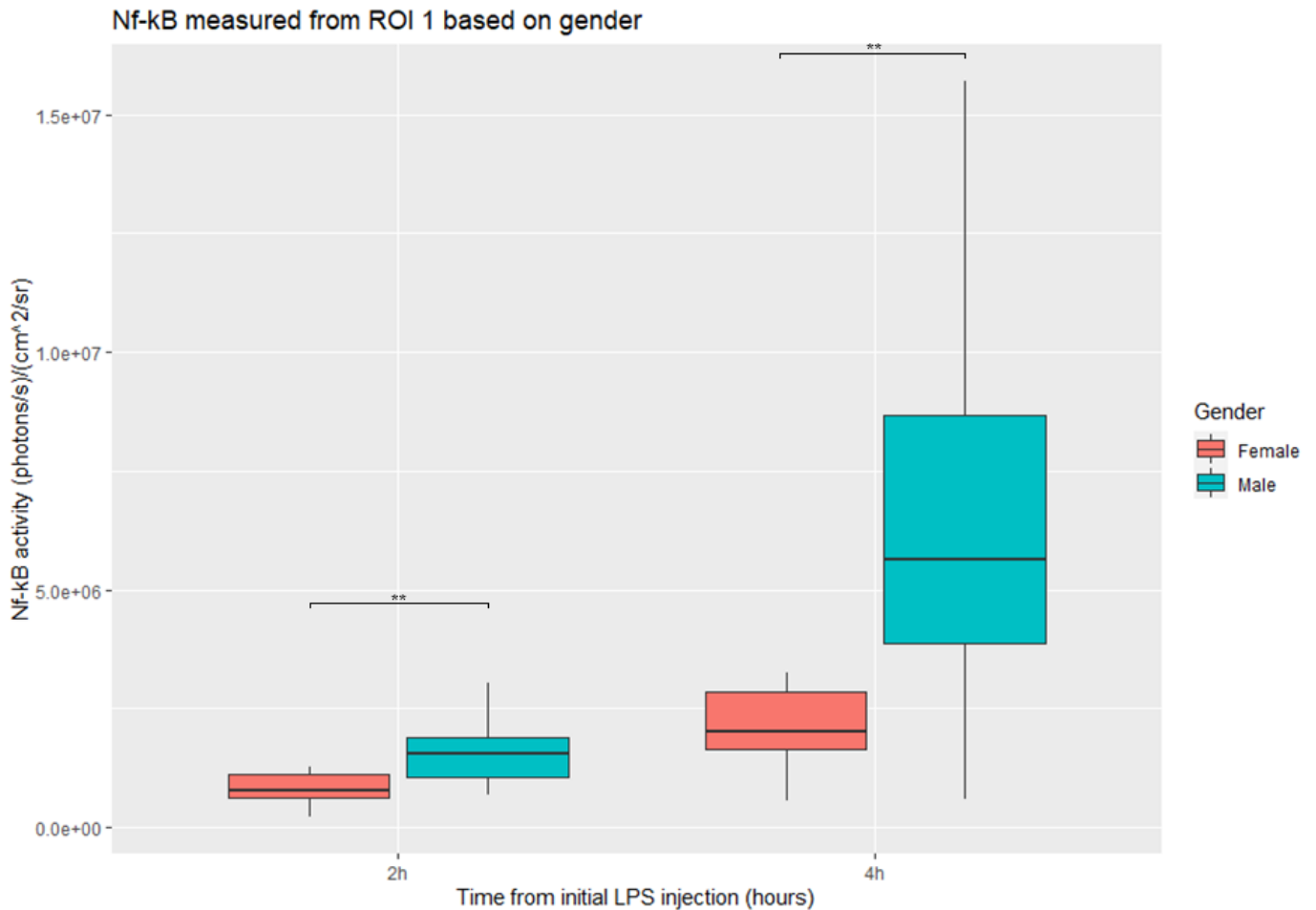
Figure 3.6 - NF-κB activity measured from ROI 1 at 2 and 4 hours after initial LPS injection grouped by genders:

Average radiance measured in $Photons/s \big/ cm^2/sr$ *used as measurement of NF-κB activity. The significant differences between the groups are illustrated as ** (p-value < 0.01). The whiskers extend to the largest and lowest values observed in each group, excluding outliers which are represented as dots outside the whiskers. Each box represents the interval where 50% of the data resides, with 25% above and 25% below the median line in the box.*

3.4 Cytokine profiling through multiplex immunoassay

To investigate potential differences or relationships between the groups given different amount of BHB, multiplex immunoassay was used to perform cytokine profiling. During the blood extraction, complications occurred with mouse #24, causing the mouse to pass before enough blood had been extracted. Results from mouse #24 were therefore excluded for further analysis.

The concentration of each cytokine was quantified using Bio Plex 200. One cytokine, IL-18, was not quantified due to the concentration being too low for detection in any of the samples. Additionally, Well E3, containing samples from mouse #5 did not yield any measurable results. This could potentially be due to a weak contact with the magnetic plate, resulting in all beads being washed out during the washing process.

After analyzing the data, significantly higher IFN-γ concentrations were found in the males than in females. IL-6 concentrations in mice given 15 mmol/kg BHB were significantly higher than in mice given 5 mmol/kg BHB, and in mice given a control solution (0 mmol/kg BHB). Additionally, significantly higher IL-10 concentrations were found in mice given 15 mmol/kg BHB than the mice given 5 mmol/kg BHB, 10 mmol/kg BHB and mice given a control solution (Figure 3.7).
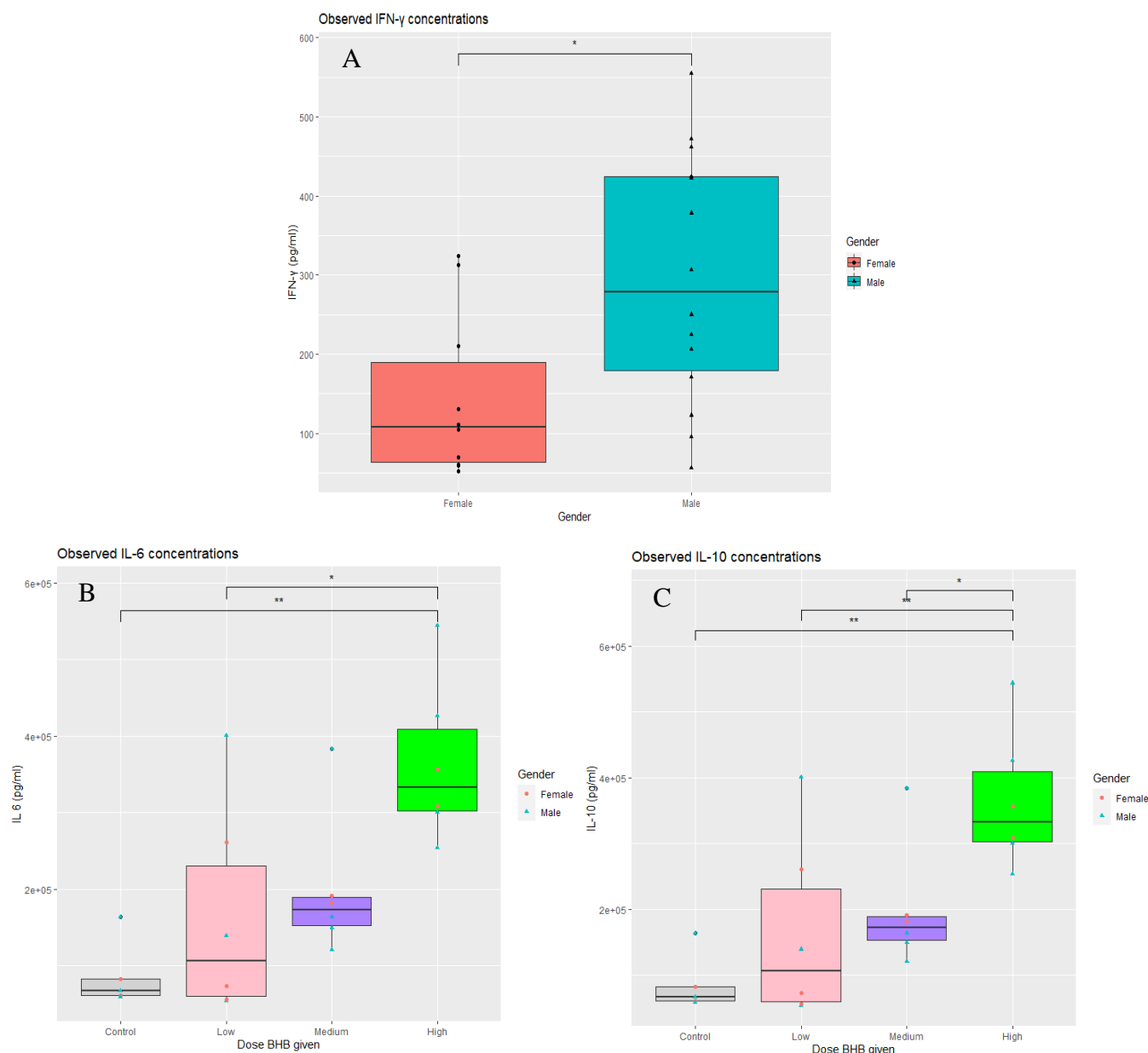
Figure 3.7 – IL6, IL 10 and IFN-γ concentration measured in pg/ml:

*Visual representation of the three cytokines where a significant group or gender effect was found. The significance is annotated with * (p-value < 0.05) or ** (p-value < 0.01). **Boxplot A** illustrates the significantly higher concentration of IFN-γ observed in all male mice compared to all females. **Boxplot B** illustrates the significant higher measured IL-6 concentrations in the group given high dose BHB compared to the groups given low dose and control. **Boxplot C** illustrates the significantly higher measured IL-10 concentrations in the group given a high dose of BHB compared to those given a low dose, medium dose, or a control.*

Red dots are measurements from female mice, and green triangles are measurements from male mice. The whiskers extend to the largest and lowest values observed in each group, excluding outliers which are represented as dots outside the whiskers. Each box represents the interval where 50% of the data resides, with 25% above and 25% below the median.

To examine if measured cytokine concentrations $\left(Ln\left(\frac{pg}{ml}\right)\right)$ could be explained by the amount of BHB injected (mmol/kg), linear regression was used. A significant linear relationship between the amount of BHB injected and cytokine concentration was found for both IL-6 and IL-10 (Figure 3.8). R-squared (R^2) explains to what degree changes in the amount of BHB given explain changes in measured cytokines concentrations. While a significant linear relationship, relatively low R^2 means that much of the variability in measured IL-6 & IL-10 concentration is not explained by our linear regression model.
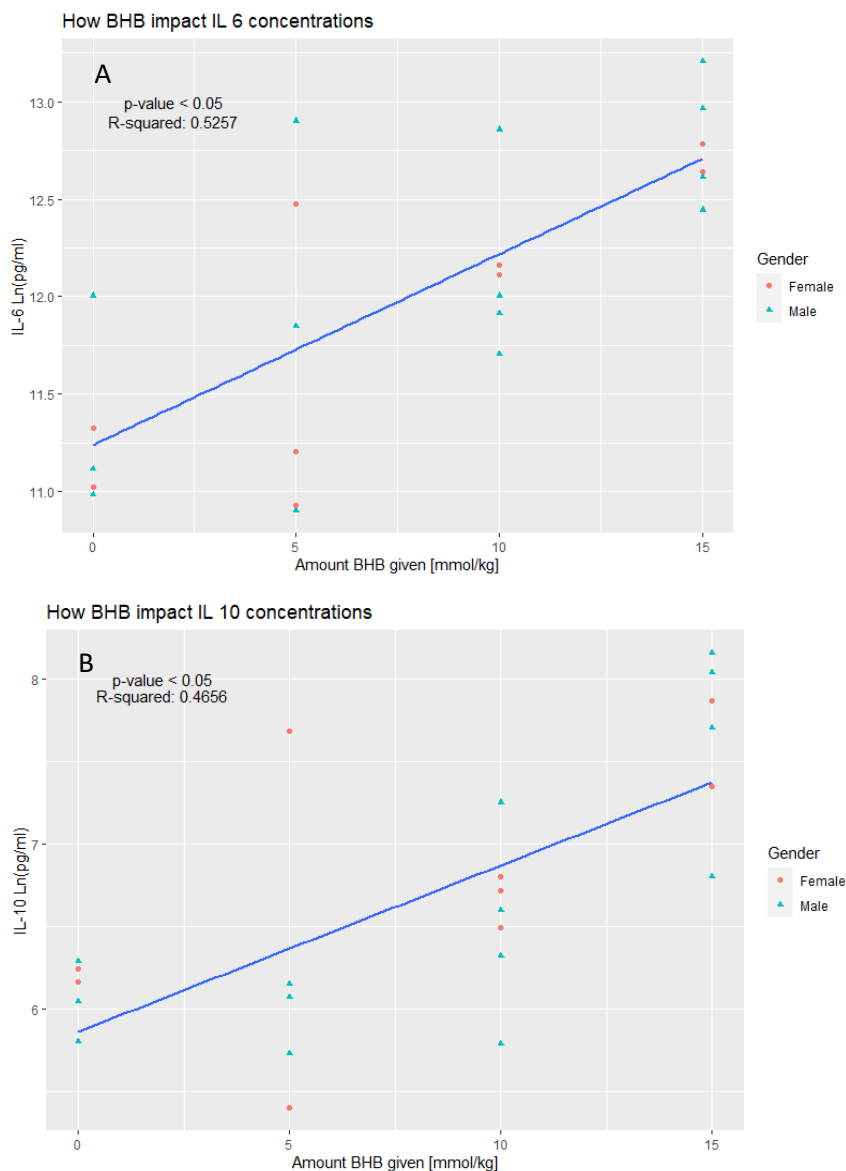
Figure 3.8 - Measured cytokines explained by BHB given:

The amount of BHB given (the independent variable) and measured IL-6 (A) and IL-10(B) (the dependent variable). The blue line illustrates the linear regression line, a line that best fits the linear relationship. Red circles illustrated measurements taken from female mice, and blue triangles illustrated measurements taken from male mice.

4 Discussion

Even though BHB's ability to inhibit NLRP3i activation on LPS mice has previously been demonstrated (Youm et al., 2015), no results suggesting a lower NF-κB activity or inhibition of pro-IL-1β and pro-Il-18 maturation were found. Analyzing data from *in vivo* imaging and cytokine profiling, some significant gender and group effect were found. Male mice were observed to have significantly stronger NF-κB activity in response to LPS injections compared to female mice. Significant linear relationships between the amount BHB injected and the two cytokines IL-10 and Il-6 were also observed.

During the project, different doses of BHB were injected. The first injections of 22 mmol/kg BHB evoked intense discomfort and stress in the mice. As the objective was to investigate potential anti-inflammatory effects, introducing stress through harmful injections was against its purpose. The visual discomfort when injecting BHB was not expected, so previously calculated doses were adjusted before measuring NF-κB activity and performing cytokine profiling. The low dose was reduced to 5 mmol/kg, the medium dose was reduced to 10 mmol/kg, and the high dose was reduced to 15 mmol/kg. When injecting these BHB doses 45 min after the initial LPS injections, no further discomfort was observed.

Due to these results, the focus of the discussion will be:

- Potential harm from BHB injections
- Significant gender and group effects
- Design of experiment and methodological consideration

4.1 BHB doses, potential harm

After weighing six non-transgenic mice and calculating BHB doses, injections were done intraperitoneally. Discomfort was observed following the injections and concentrations measured with FPN showed higher blood BHB concentrations than expected. Based on our results after injecting BHB and a previous study where young humans were given exogenous β-hydroxybutyrate salt supplementations (Stefan et al., 2021), an assumption was made. This assumption was that the BHB concentration in blood increases rapidly depending on the dose

and peaks between 15-30 min. After the peak, the concentration decreases almost as rapid but evens out at concentrations higher than baseline for several hours.

A concern when planning the experiment was the potential detrimental side effects when inducing supraphysiological concentrations of BHB. Natural occurring concentrations of BHB during an intense workout or during two-day fasting are normally 1-2 mM, while consistent values slightly over 2 mM have been observed in humans following a strict ketogenic diet almost devoid of carbohydrates (John C. Newman & Eric Verdin, 2017). Studies on long-term fasting in obese humans have shown concentrations as high as 6 mM after prolonged starvation (38 days) (Owen et al., 1969). Since the plan was to induce supraphysiological BHB concentration, a concern was the potential of inducing ketoacidosis in the mice as a side effect.

4.1.1 Ketoacidosis

Ketoacidosis a life-threatening situation often related to diabetics or people struggling with alcoholism. Often described as an overload of ketones present in your blood. This however is a massive oversimplification. Diabetic ketoacidosis (DKA) is mostly caused by insulin deficit and an increase in plasma glucagon levels. Gluconeogenesis in the liver increases significantly, while the utilization of glucose decreases in muscles, liver, and adipose tissue. With the decreasing amount of insulin, glucose struggles with entering cells, and as a response, the body starts breaking down lipids in adipose tissue as well as muscle proteins. This is done as glucose can no longer act as the primary energy source. The breakdown of lipids creates fatty acids, and these free fatty acids go through β-oxidation in the liver, creating Acetyl-CoA. Through ketogenesis, the production of ketones such as BHB and acetoacetate occurs. Very much like what happens to an individual on the keto-diet or fasting.

These ketones are then used as energy sources, and up to 80% of the total energy is theorized to come from ketogenesis during insulin deficiency (Fedorovich et al., 2018). These ketones accumulate at a rate significantly higher than what the body handles through utilization or renal elimination. In some situations, elevated concentrations of ketones have been shown to reach 20-25 mM in subjects with DKA (Fedorovich et al., 2018).

Hyperketonemia, a state of highly elevated ketone blood levels linked with a decrease in bicarbonate (HCO-), which often results in acidemia, a state where blood pH levels are below 7.35. Some early research attributes this to the fact that hydroxybutyric acid fully dissipates, resulting in the release of H+ that then can bind to the bicarbonate (Laffel, 1999). After looking into every step included in DKA, Green and Bishop suggested that metabolic acidosis is not caused by the acidic nature of ketones but rather by several steps involved in ketogenesis that produce free protons (H^+) (Green & Bishop, 2019). With triacylglycerol hydrolysis, fatty acid activation, β-oxidation of FFA, and an increase in coenzyme A synthesis all producing free protons, they argued that these processes were more likely to be the cause of acidosis observed during DKA. During ketogenesis, BHB the conjugate base form of β-hydroxybutyric acid is produced from acetoacetate, another conjugate base (see figure 5.4 Ketogenesis). With the ketones appearing in their base form, it is rather obvious that the original hypothesis is likely wrong and that the ketones produced likely are not the cause of the acidosis observed during hyperketonemia.

Hyperglycemia on the other hand, is a state where blood sugar levels are significantly elevated that can occur during DKA when the glucose in the blood is unable to be metabolized. The high blood glucose levels create an osmolar gradient. The osmolar gradient, coupled with hypertonicity and acidosis, drive potassium out of the intracellular space, leading to hyperkalemia. This a medical term describing elevated potassium levels in blood over the normal (Umpierrez et al., 2002).

The BHB doses used in our experiment were created by β-hydroxybutyrate-sodium-salt (BHB-sodium) (H6501) purchased from Sigma-Aldrich dissolved in 0.9% NaCl saline. When fully dissolved, the result is a solution with BHB and natrium-ions. No significant metabolic acidosis was expected to occur after BHB injections due to no H^+ from the dissipation of β-hydroxybutyric acid or free protons from ketogenesis. Ketoacidosis from hyperketonemia was therefore not considered a potential risk. With the mice all healthy, having *ad libitum* access to standard chow and assumedly normal insulin production, hyperglycemia was also not considered a potential risk.

Although ketoacidosis was not considered a risk, substantial discomfort was still observed in the mice injected with 22 mmol/kg BHB leading to further investigation of BHB-sodium being potentially toxic.

A recent study investigating the toxicity of BHB-sodium used a stepwise increase or decrease in the amount of BHB-sodium given to mice. This was done so an effective dose range and potential lethal threshold could be investigated. Increasing the dose to 300 mg/day from 150 mg/day increased the severity of onset illness 2.2-fold and increased the mortality rate by 50% (from 30.4 to 87.5%) (Weckx et al., 2021). Doses such as 180 mg/day and 225 mg/day were also tried, showing an increase in severity. Their conclusion was that 150 mg/day BHB-sodium given through subcutaneous bolus injections were close to the toxic threshold of BHB-sodium.

Tracking BHB concentration over time, a quick increase in blood BHB levels were observed, as well as a rapid decline. This suggests that BHB was relatively quickly removed from circulation, leaving the accompanying Na^+ to potentially circulate longer, resulting in acid/base imbalance. The fact that intracellular uptake and metabolism of BHB requires protons as co-factors, this might contribute to the acid/base imbalance (Felmlee et al., 2020)

Comparing the amount of BHB given in the experiment done by Weckx and colleagues with our own, a 25g mouse injected with 22 mmol/kg BHB solution would be given a total of 50 mg BHB-sodium. That is less than half the suggested toxic threshold (Weckx et al., 2021). Importantly there is a distinctive difference in the method of injection in our experiment. Instead of using subcutaneous injections, intraperitoneal (IP) injections were used. This is noteworthy due to the fact that IP injections often have higher absolute bioavailability compared to subcutaneous injections (Al Shoyaib et al., 2019). Due to higher absolute bioavailability, a smaller IP injection of BHB could potentially lead to the same circulating concentration as a bigger subcutaneous, meaning our injections might have been closer to the toxic threshold than assumed.

22 mmol/kg BHB solution also equals 506 mg/kg Na^+. LD50 for injecting mice with NaCl is 2602 mg/kg (Information, 2022). This is five times more circulating Na^+ than introduced through 22 mmol/kg BHB injections. This, coupled with the fact that research discussing complications of introducing Na+ and Cl- through 0.9% NaCl saline solution, mainly focus on hyperchloremia and hyperchloremic acidosis (Li et al., 2016). The concentration was assumed to be nontoxic in this regard. However, in retrospect, the effect of hypernatremia should have been investigated more.

4.1.3 Hypernatremia: Increased circulating Na$^+$ levels impacting Ion difference, Na$^+$ Influx, and acting pro-inflammatory

Assuming extracellular fluids (ECF) make up 20% of a mouse's bodyweight, a 25-gram mouse has 5 ml ECF. Measurements on several strands of mice have shown plasma sodium concentration around 140-160 mM when eating a regular salt diet (Mérillat et al., 2009). Rough calculations estimating the change of plasma sodium after injecting 22 mmol/kg BHB solution results in an estimated plasma concentration of around 240 mM. In humans, this would be defined as extreme hypernatremia associated with a mortality rate over 60% (Arambewela et al., 2016).

With higher doses of BHB meaning more Na$^+$, higher doses of BHB results in a higher risk of hypernatremia. The hypothesis that hypernatremia might have occurred is supported when our results are compared to a clinical study where immune stimulation responses was examined in patients with sepsis. They observed higher TNF-α, IL-6, and IL-10 in patients acquiring hypernatremia compared to those with sustained eunatremia (Lin et al., 2022). The same two cytokines found to significant have linear relationship with the amount of BHB given (IL-6 & IL-10).

The Stewart approach to acid-base balance is a method focused on three variables: Strong ion difference (SID), total concentration of weak acids (A$_{Tot}$), and partial pressure of carbon dioxide ($_p$CO2). Using this method, it becomes clear that an increase in SID or reduction of A$_{Tot}$ results in a higher pH in the blood. With a big enough change leading to metabolic alkalosis (Morgan, 2009). Going back to the experiment done by Weckx and colleagues, where they measured pH in the blood, mice given 150 mg/day or more BHB-sodium showed signs of alkalosis (Weckx et al., 2021). This observed alkalosis could be explained by the sudden increase of circulatory Na$^+$-ions following a bolus injection of BHB-sodium, increasing the SID.

In hindsight, closely monitoring the blood pH levels in mice after injecting BHB or using additional BHB-salt bound to calcium or magnesium could have given valuable additional data. This additional data would help when assessing to what degree the potential alkalosis is caused by sudden influx of circulating Na$^+$. Plenty of data suggest that sodium is implicated in NLRP3i activation through Na$^+$ influx and through increasing the intracellular osmolarity. The increase in intracellular osmolarity results in cellular swelling and a decrease in K$^+$, much like that of K$^+$ efflux (Schorn et al., 2011). The choice of using BHB-sodium might have turned out to be an unfortunate choice when examining the interactions between BHB and inflammation. In

retrospect, we now know that the use of several different BHB salts could give a better grasp of the interaction between the sodium and the inflammatory processes measured.

Traditionally, Na^+ accumulation in tissue has been focused on the kidney, where increased levels of electrolytes have been found to impact expression of phagocytes, known stimulators of inflammatory T-cells (Chessa et al., 2016; Hochheiser et al., 2013). There are several studies suggesting that changes in osmolarity might be part of ancient danger signaling in other tissue as well. With the accumulation of Na^+ being observed in the skin of humans and other animals, research using high salt conditions on skin cells found that these conditions impaired the development of anti-inflammatory macrophage activation needed for tissue repair and instead promoted inflammatory responses (Binger et al., 2015; Ivanova et al., 1978; Szabó & Magyar, 1982; Wiig et al., 2013). This can also be seen with T-cells, where high local Na^+ content affects the activation of T-cells. This results in increased production of TH17 and the restoration of IL-2-producing T-cells suppressed by anti-inflammatory cytokines such as IL-4 or IL-10 (Binger et al., 2015; Loomis et al., 2001). With hypernatremia sometimes being a secondary effect of infections (Królicka et al., 2020), the occurrence of hypertonic salty microenvironments might be a beneficial response against microbial pathogens. With Na^+ especially taking a big part in strengthening the skin barrier (Schatz et al., 2017).

As much as we tried to optimize the timing of BHB injections to have a maximal effect, the result showed a rapid increase and decrease in blood BHB concentration after the injections. While the NF-κB activity model takes this somewhat into account, there is a high probability that the cytokine profiling of blood samples taken 4 hours and 15 min after BHB injections does not take this into account. Thus, any effects BHB potentially exert on the inflammation process is not captured, but rather the effect of metabolic alkalosis caused by hypernatremia or potential pro-inflammatory effects from high levels of circulating Na^+.

4.2   Group and gender effect observed through NF-κB activity and Cytokine Profiling

Other previous experiments on C57BL/6J mice given IP injection of LPS and euthanized at 1, 3, 6, 12, and 24 hours after initial LPS injection showed clear peaks at the 1-hour mark when IL-6, IL-10, and TNF-α were measured using LiquiChip [tm] technology. The only cytokine measured with a different trend was IFN-γ, which increased slowly and peaked at 12 hours (J. Liu et al., 2017). Studies looking at IL-1β in adult mice show a rapid increase in the first hour

and a peak around 4 hours after subcutaneous LPS injections (Cusumano et al., 1997). IP injections generally have higher bioavailability (Al Shoyaib et al., 2019). It is reasonable to assume that the time until peak plasma levels of IL-1β is considerably faster when treating mice with IP LPS injections. Based on these results and assumptions derived from our own BHB - timeline experiment, the optimal time of BHB injection was determined to be around 45 min after LPS injection. This was done to optimize the potential effect BHB could have on the acute inflammation caused by LPS.

Pictures taken with IVIS showed a clear activation of NF-κB in both ROI 1 and ROI 2 as well at two hours, and with a significant increase in activity at taken at four. No group effect between BHB dose and NF-κB activity was found, but ROI 1 focusing on the liver showed significant gender differences.

4.2.1 Gender difference impacting NF-κB activity

LPS has been shown to induce a slightly greater response in male mice. When both female and male mice were injected with a lethal dose of 20 mg/kg LPS the female mice were shown to be more resilient through higher survival rate and significantly longer onset until fatality (Ivan et al., 2021). Gender differences in mice immune responses are documented as early as 1972 (Eidinger & Garrett, 1972), and today it is widely agreed that mammals express sexual dimorphism in both innate and adaptive immune responses. The interaction between the immune system and secreted sex hormones from endocrine glands is suggested as the main driver. Female sex hormones produced in the ovary placenta, such as estrogen and progesterone, stimulate the innate and adaptive immune response differently than testosterone, mainly produced in the testis. While sex hormones often are the focus when discussing sexual dimorphism observed in immune responses between genders, differences in innate immune responses in mammals suggest that some of the difference might be germline encoded.

Data collected from adult humans, rodents, and cell cultures confirm that TLR4 expression on macrophages is greater in males than females (Klein & Flanagan, 2016). In this project, LPS was used to induce systemic inflammation and activate NF-κB gene expression. CD14, a pattern-recognizing receptor, binds to LPS, and MD-2, a lymphocyte antigen, creates a complex with TLR4 allowing for LPS to bind and stimulate downstream adaptor molecules, and starting signal pathways converging at NF-κB (Yesudhas et al., 2014). Macrophages, the most abundant

liver immune cell, and males expressing more TLR4 is likely one of the explaining factors in the significant gender difference in NF-κB expression measured through *in vivo* imaging for ROI 1.

As mentioned earlier, sex hormones are often considered the biggest driver for observation showing higher immunocompetence in females. While often linked to differences in the adaptive immune response, estrogen has also been shown to have a strong influence on NF-κB signaling. Several mechanisms are suggested for this nonclassical anti-inflammatory effect. The most common suggestions are inhibition of NF-κB DNA binding, induction of IκB expression, or direct protein-to-protein interaction (Chadwick et al., 2005). The estrogen E2 (estradiol) has been shown to inhibit the inflammatory effects of LPS. Studies on LPS-treated mice cells showed that E2 blocks the intracellular transport of NF-κB (Ghisletti et al., 2005). Similar experiments on rat cells showed E2 also promoting the production of IκB-α, reducing levels of phosphorylated IκB-α creating a negative feedback loop (Xing et al., 2012). The hormonal difference in the mice is another likely factor in the observed gender differences when measuring the NF-κB activity.

4.2.2   Cytokine profiling

A clear gender difference was observed in NF-κB activity, however when analyzing the data from the immunoassay, only a significant gender difference for IFN-γ concentrations were observed. Significant gender differences in several pro-inflammatory cytokines have been observed previously in similar experiments treating mice with LPS (Aulock et al., 2007; Kuo, 2016). When specifically looking at IFN-γ, most studies show a higher response in females than males, with some not finding a significant difference at all. The commonly suggested mechanism behind the difference often observed is the fact that naive CD4+ cells in female produce mostly IFN-γ upon specific stimulation, while the same cells in males tend to produce more IL-17 (Zhang et al., 2012). Additionally, the female sex hormone E2 can upregulate expression of the IFN-γ gene (Fox et al., 1991). While theory suggests that females produce more IFN-γ than males, our findings show a significantly higher IFN-γ concentration in male mice, rather than in the female mice. The interactions resulting in IFN-γ production when treating mice with LPS are likely more complex and the suggested mechanisms leading to higher IFN-γ concentrations in females might not be the dominating ones. This is supported by

others also observing a higher IFN-γ in male mice rather than in the female mice when treating mice with LPS (Erickson et al., 2018).

4.3 Design of experiment and methodological consideration

4.3.1 The breeding process

At the start of the project, non-transgenic homozygotes were bred with transgenic heterozygotes. The result was 105 offspring, out of which 75 were transgenic. The probability of getting 75 transgenic offspring when breeding a heterozygote with wildtype is close to zero, questioning if at some point, two heterozygotes' mice bred. If this was the case, it might impact the results through the "gene dosage effect".

When discussing this potential issue with people having prior experience using the same breed of luc2-transgenic mice, homozygotes transgenic mice were assumed and partly proven to have a 100% mortality rate. In the case of two heterozygous breeding, no homozygote transgenic mice would be expected to survive long enough to impact the results of the experiment. Considering this, the results of our breeding were no longer statistically impossible.

4.3.2 Impact of using both genders

The aim was to investigate if NF-κB activity was affected by BHB, but our result only showed a significant gender difference in NF-κB activity. While somewhat interesting, limiting our experiment to one gender would most likely have been beneficial.

The effect of significantly higher NF-κB activity in male mice compared to female mice also results in higher variability within each group. With the increased spread in measured NF-κB activity (variability), our ability to detect significant group effects is reduced. Excluding a gender could result in less variability, but it also greatly reduces our sample size. To avoid this, some studies use male mice only. This is done to avoid variability caused by gender differences, such as different sex hormones. The reason male mice are selected over female, is the inherent variability between female mice due to the estrous cycle.

4.3.3   The Megazyme kit

The first small-scale experiment carried out was to test sample interference between mouse plasma and the Megazyme kit. These tests were done with no pre-existing experience with the kits or protocols and with limited experience handling some of the tools. Time was therefore invested to fully understanding each step of the protocol, testing them out, and improving them when necessary.

When getting acquainted with the Megazyme kit, some obstacles appeared when following the accompanying instructions. The main obstacle resulted from the fact that the buffer in the kit was prone to make bubbles, impacting the absorbance readings. Several methods were tried to overcome this issue. In the end, the most effective solution was premixing several of the reagents into a master mix and then use a single pipette in every step.

This introduced additional time investments, and the accompanying instructions made it clear that the enzymatic process is time sensitive. It states that the readings must be done at two and six min after adding the reagents. A test to examine what happens if these instructions are not followed was done by testing the absorbance of the master mix over one hour. The absorbance at 492 nm did not change at all the first 15 min, leaving us with some wriggle room. It was concluded that pre-making the master mix and carefully pipetting with a single pipette did not negatively impact the results. Even though it took a little longer.

With only a 0.005 mg/ml difference between the spiked sample and the standard, it was decided that there was no significant interference between mouse plasma and the Megazyme kit. When getting acquainted with the protocol, more significant differences attributed to the bubbles or issues with pipetting were observed.

Overall, the method was still time-consuming. With each sample tested requiring 10 µL plasma, a minimum of 20 µL blood would be needed when assuming 50-55% of whole blood is plasma. In reality, more than 20 µL would be needed, as each sample would include a parallel, and some redundancy would also be necessary.

Using the Megazyme kit to measure BHB concentrations at eight different time points following BHB injections would not have been compliant with the European guidelines on animal research regarding the maximal volume of blood sampled from mice without fluid replacement. With the Megazyme kit not ideal for measuring several concentrations from samples taken in a short period (<24 hours), a handheld diagnostic tool was suggested. Several

diagnostic tools were researched, and Freestyle Precision Neo from Abbot was chosen because it was readily available and within the budget.

4.3.4 FreeStyle Precision Neo

Due to FPN being a diagnostic tool aimed at people with diabetics, its usability to measure blood BHB concentration in mice was not documented. Uncertainties about the accuracy and precision of FPN measurements meant that tests were necessary to examine this precisely.

Creating a set of blood and plasma samples by adding BHB solutions was done in order to compare the results from FPN with the Megazyme kit. The Megazyme kit was considered the "golden standard", as the improved protocol allowed consistent and accurate results.

Comparing our two methods of measuring BHB concentration, no impactful difference was observed between blood BHB concentration measured with FPN and plasma BHB concentrations measured with Megazyme.

Further tests showed that FPN's accuracy was negatively impacted by the saline in the BHB solution used to spike the blood sample. After adjusting for the saline in each sample, linear regression proved a significant linear relationship, and it was concluded that the accuracy of FPN was consistent between 0-8 mM. With FPN only requiring a small blood sample ($\approx$5 µl) to measure the BHB concentrations in seconds, made it the obvious choice going forward.

4.3.5 BHB solutions

During the tests aimed at comparing FPN with the Megazyme kit, measured concentrations differed from the theoretically calculated BHB concentrations. The measured concentration in our samples was consistently lower than what was expected. This was mainly attributed to the methods used to create our BHB solutions. At first, BHB-sodium was weighted to the nearest milligram in a plastic container. The BHB-sodium powder was then transferred to a beaker, and 0,9% NaCl Saline solution was added. With the BHB-sodium powder having small grains, some residue was left in the plastic container used for measuring. In addition, the volume of the BHB-sodium was not accounted for when adding 0,9% NaCl Saline solution.

Several adjustments were made in the subsequent tests to reduce the disparity between measured and expected concentration.

When creating the BHB solution, a larger solution was created to reduce any effects from potential inaccuracies in the weighting. The BHB-sodium was added directly to a graduated cylinder, and saline solution was carefully added until the correct volume was observed. The cylinder was periodically placed on a shaker while adding the saline solution to ensure the full dissolvement of BHB-sodium. These adjustments yielded significantly closer measured concentrations to the expected ones.

4.3.6 *In vivo* imaging to measure NF-κB activity.

NF-κB activity in LPS-treated C57BL/6 mice has been shown to be fluctuating over time. Sakai and colleagues found that when treating C57BL/6 mice with LPS, nuclear translocation of NF-κB occurred within 10 min and that the activity reached its peak at 25 min past LPS stimulation. Following the first peak, a second and third peak was observed approximately 80 & 160 min later (Sakai et al., 2017).

This fluctuation in NF-κB activity could be a problem when wanting to examine the strength of the NF-κB activity. However, it was not of concern in our Luc2-reporter mice. Luciferase is a cytosolic protein, meaning the NF-κB regulated synthesis of luciferase occurs relatively quickly. Luciferase also has a half-time of around 160 min (Heo et al., 2019). This means that LPS-stimulated NF-κB activation results in a relatively quick synthesis of luciferase that accumulates over time.

The *in vivo* images taken at two and four hours does therefore not show a snapshot of the NF-κB activity but instead gives an indication of the overall activity up to the time the *in vivo* imaging is done. Theoretically, any impact on the NF-κB activity happening in the first two hours, is expected to be reflected in the data from *in vivo* imaging at two hours. Similarly, any impact on the activity during the last 4-hour period is expected to be observable in the *in vivo* image taken at four hours, with NF-κB activity during the first 2 hours having less impact due to luciferase degrading over time.

4.3.7 Cytokine Profiling

4.3.7.1 Excluding datapoints

During cytokine profiling, some cytokines were not detected due to the bead number being too low in the well. When the bead number was under a certain value, the cytokine concentration would not be calculated and instead be reported as error (OOR <). These data points were then excluded from any further analysis.

While equal sample size in every group is not an assumption made in ANOVA, sample size does play an important role when examining significant differences. With a sample size of six or seven in each group, any excluded samples have a relatively big impact. Generally, a bigger sample size is preferred as the variability of sampling distribution tends to decrease and analyses become more statistically significant. In other word, there is less chance our results happened by coincidence. By also excluding samples with concentrations too low to calculate, we are excluding samples that likely would have had low concentrations, further impacting the data.

To avoid this, concentrations with error (OOR<) could have been changed to the lowest quantifiable concentration instead of being excluded. The use of parallel samples is also something that could reduce the risk of samples with quantifiable data points. The use of parallel samples was discussed, but due to the number of samples measured, there were not enough reagents and purchasing another set of ProcartaPlex kits was not within the budget.

4.3.7.2 The matrix effect

When extracting blood for cytokine profiling, an uneven amount of blood was extracted from each mouse. This caused each blood sample to be diluted differently by the EDTA already added to each syringe. Our solution was to adjust for this difference in dilution. After extracting plasma from the blood samples, both the plasma and red blood cells were measured. Based on some rough calculations and an assumption that EDTA would remain in the supernatant (Plasma), the values were adjusted according to the EDTA dilution. While the goal of this was to minimize any effects of the different dilutions, these adjustments introduced even more uncertainty through something called the matrix effect.

When performing IL-6 cytokine profiling on different dilutions, an effect called the matrix effect occurred (Figure 4.1). The matrix effect happens due to biological samples haveing many components, such as proteins, carbohydrates, and phospholipids, that interfere with the binding of the antibodies. Therefore, more diluted samples often lead to better binding affinity, and hence it is often smart to map the matrix effect before doing the final analysis. Figure 4.1 shows the IL-6 concentration measured from different dilution series of six samples. The measured IL-6 concentration increased significantly until the samples were diluted by a factor of 16. Dilutions of IL-6 past a factor of 16 did not affect the result nearly as much as the dilutions did up to 16.

In practice, this means that samples with different dilutions often result in different concentrations. Without mapping the matrix effect, the results should not be used to confirm absolute values. Checking the matrix effect for every single cytokine is both expensive and time-consuming, however if all the samples are diluted by the same factor, the results can be used comparatively.
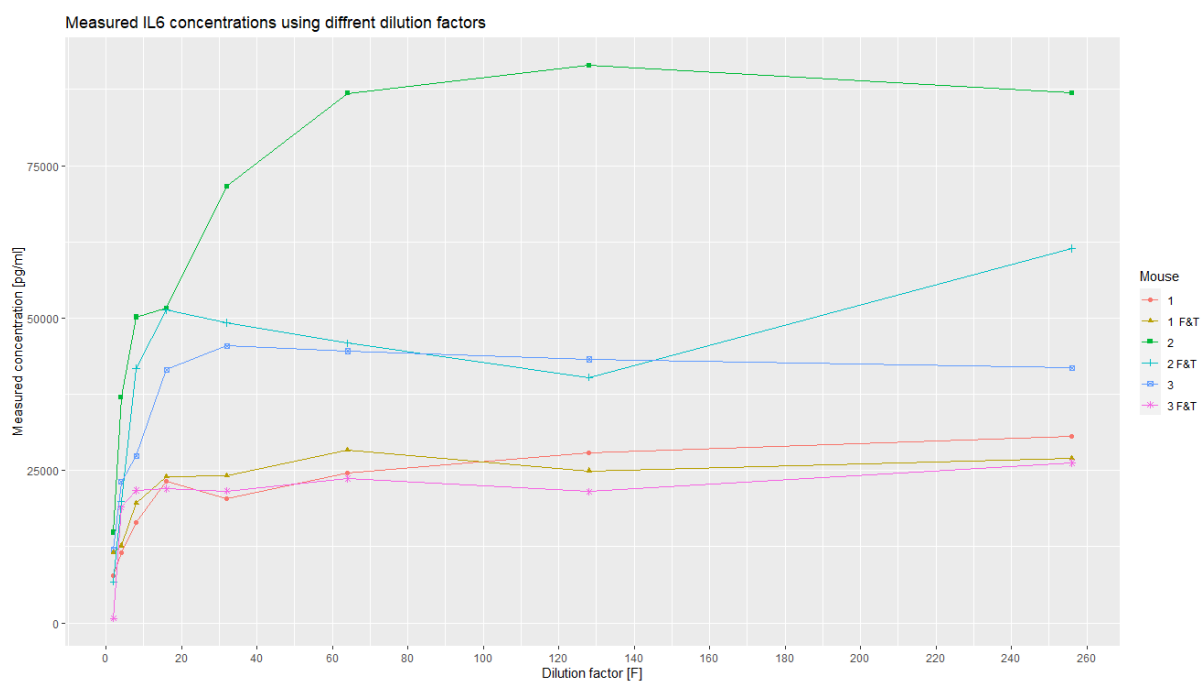
Figure 4.1 – Measured IL-6 concentration using different dilution factors [F]:

Samples from three different mouse (1,2 & 3). F&T is noted on samples that were frozen with liquid nitrogen and then thawed again. No significant difference in how the samples behaved can be observed.

As mentioned, a varying amount of blood was extracted from each mouse. While most blood samples were around 500-600 µL, the total sample size ranged from 50-900 µL. This led to a

wide spectrum of dilutions. It is impossible to determine how the different dilutions is affected by the matrix effect, and therefore any conclusion drawn from the cytokine profiling must be met with some skepticism.

5   Summary and conclusion

No data supporting the hypothesis that BHB acts anti-inflammatory was found. No reduction in IL-1β or IL-18 concentration indicates that our BHB injections were not able to inhibit NLRP3i activation at a significant level. Measured NF-κB activity showed no significant difference between the groups. Therefore, the hypothesis that BHB could reduce inflammation due to the phosphorylation of NF-κB-subunits or by binding to GPR109a could not be confirmed. Instead, a significant gender difference in NF-κB activity was found. Additionally, a linear dose-dependent relationship between the amount of BHB injected and IL-10 and Il-6 concentrations were observed.

6   Future perspectives

While no data confirming the hypothesis was found, it raised several interesting questions. The use of different or additional BHB salts could give valuable data when investigating the potential impacts of introducing a huge influx of Na^+. With literature suggesting Na^+ influx as a mechanism able to activate NLRP3i, any BHB injections involving Na^+ should be avoided when investigating BHBs anti-inflammatory properties.

To further investigate any potential alkalosis or hypernatremia caused by BHB injections. PH-values in blood and circulatory Na^+ should be measured at several time points following bolus IP injections of BHB. This could help determine if it was indeed the sodium in BHB-sodium that caused the discomfort observed when injecting higher doses in the mice.

With the data clearly showing a significant gender difference observed in NF-κB activity, the use of only one gender could reduce this variance by eliminating any variance caused by a difference in gender. Less variance results in a higher chance of significant findings. Increasing the sample size to further reduce variance is another suggestion for any further studies.

References

Al Shoyaib, A., Archie, S. R., & Karamyan, V. T. (2019). Intraperitoneal Route of Drug Administration: Should it Be Used in Experimental Animal Studies? *Pharm Res*, *37*(1), 12. https://doi.org/10.1007/s11095-019-2745-x

Amin, M. N., Siddiqui, S. A., Ibrahim, M., Hakim, M. L., Ahammed, M. S., Kabir, A., & Sultana, F. (2020). Inflammatory cytokines in the pathogenesis of cardiovascular disease and cancer. *SAGE Open Med*, *8*, 2050312120965752. https://doi.org/10.1177/2050312120965752

Angeloni, C., Businaro, R., & Vauzour, D. (2020). The role of diet in preventing and reducing cognitive decline. *Curr Opin Psychiatry*, *33*(4), 432-438. https://doi.org/10.1097/yco.0000000000000605

Arambewela, M. H., Somasundaram, N. P., & Garusinghe, C. (2016). Extreme hypernatremia as a probable cause of fatal arrhythmia: a case report. *J Med Case Rep*, *10*(1), 272. https://doi.org/10.1186/s13256-016-1062-9

Aulock, S., Deininger, S., Draing, C., Gueinzius, K., Dehus, O., & Hermann, C. (2007). Gender Difference in Cytokine Secretion on Immune Stimulation with LPS and LTA. *Journal of interferon & cytokine research : the official journal of the International Society for Interferon and Cytokine Research*, *26*, 887-892. https://doi.org/10.1089/jir.2006.26.887

Batch, J. T., Lamsal, S. P., Adkins, M., Sultan, S., & Ramirez, M. N. (2020). Advantages and Disadvantages of the Ketogenic Diet: A Review Article. *Cureus*, *12*(8), e9639. https://doi.org/10.7759/cureus.9639

Bełtowski, J. (2003). Adiponectin and resistin--new hormones of white adipose tissue. *Med Sci Monit*, *9*(2), Ra55-61.

Bianchi, V. E. (2019). The Anti-Inflammatory Effects of Testosterone. *J Endocr Soc*, *3*(1), 91-107. https://doi.org/10.1210/js.2018-00186

Binger, K. J., Gebhardt, M., Heinig, M., Rintisch, C., Schroeder, A., Neuhofer, W., Hilgers, K., Manzel, A., Schwartz, C., Kleinewietfeld, M., Voelkl, J., Schatz, V., Linker, R. A., Lang, F., Voehringer, D., Wright, M. D., Hubner, N., Dechend, R., Jantsch, J., . . . Müller, D. N. (2015). High salt reduces the activation of IL-4- and IL-13-stimulated macrophages. *J Clin Invest*, *125*(11), 4223-4238. https://doi.org/10.1172/jci80919

Broz, P., & Dixit, V. M. (2016). Inflammasomes: mechanism of assembly, regulation and signalling. *Nature Reviews Immunology*, *16*(7), 407-420. https://doi.org/10.1038/nri.2016.58

Calao, M., Burny, A., Quivy, V., Dekoninck, A., & Van Lint, C. (2008). A pervasive role of histone acetyltransferases and deacetylases in an NF-kappaB-signaling code. *Trends Biochem Sci*, *33*(7), 339-349. https://doi.org/10.1016/j.tibs.2008.04.015

Cantrell CB, M. S. (2022). *Biochemistry, Ketone Metabolism* https://doi.org/https://www.ncbi.nlm.nih.gov/books/NBK554523/

Carlsen, H., Moskaug, J. Ø., Fromm, S. H., & Blomhoff, R. (2002). In Vivo Imaging of NF-κB Activity. *The Journal of Immunology*, *168*(3), 1441-1446. https://doi.org/10.4049/jimmunol.168.3.1441

Chadwick, C. C., Chippari, S., Matelan, E., Borges-Marcucci, L., Eckert, A. M., Keith, J. C., Jr., Albert, L. M., Leathurby, Y., Harris, H. A., Bhat, R. A., Ashwell, M., Trybulski, E., Winneker, R. C., Adelman, S. J., Steffan, R. J., & Harnish, D. C. (2005). Identification of pathway-selective estrogen receptor ligands that inhibit NF-kappaB transcriptional activity. *Proc Natl Acad Sci U S A*, *102*(7), 2543-2548. https://doi.org/10.1073/pnas.0405841102

Chandran, M., Phillips, S. A., Ciaraldi, T., & Henry, R. R. (2003). Adiponectin: More Than Just Another Fat Cell Hormone? *Diabetes Care*, *26*(8), 2442-2450. https://doi.org/10.2337/diacare.26.8.2442

Chessa, F., Mathow, D., Wang, S., Hielscher, T., Atzberger, A., Porubsky, S., Gretz, N., Burgdorf, S., Gröne, H. J., & Popovic, Z. V. (2016). The renal microenvironment modifies dendritic cell phenotype. *Kidney Int*, *89*(1), 82-94. https://doi.org/10.1038/ki.2015.292

Clément, K., Vaisse, C., Lahlou, N., Cabrol, S., Pelloux, V., Cassuto, D., Gourmelen, M., Dina, C., Chambaz, J., Lacorte, J. M., Basdevant, A., Bougnères, P., Lebouc, Y., Froguel, P., & Guy-Grand, B. (1998). A mutation in the human leptin receptor gene causes obesity and pituitary dysfunction. *Nature*, *392*(6674), 398-401. https://doi.org/10.1038/32911

Cruz, C. M., Rinna, A., Forman, H. J., Ventura, A. L., Persechini, P. M., & Ojcius, D. M. (2007). ATP activates a reactive oxygen species-dependent oxidative stress response and secretion of proinflammatory cytokines in macrophages. *J Biol Chem*, *282*(5), 2871-2879. https://doi.org/10.1074/jbc.M608083200

Cusumano, V., Mancuso, G., Genovese, F., Cuzzola, M., Carbone, M., Cook, James A., Cochran, Joel B., & Teti, G. (1997). Neonatal Hypersusceptibility to Endotoxin Correlates with Increased Tumor Necrosis Factor Production in Mice. *The Journal of Infectious Diseases*, *176*, 168-176. https://doi.org/10.1086/514019

de Kloet, A. D., Pacheco-López, G., Langhans, W., & Brown, L. M. (2011). The effect of TNFα on food intake and central insulin sensitivity in rats. *Physiol Behav*, *103*(1), 17-20. https://doi.org/10.1016/j.physbeh.2010.11.037

Dhillion KK, G. S. (2022). *Biochemistry, Ketogenesis* https://doi.org/https://www.ncbi.nlm.nih.gov/books/NBK493179/

Dostert, C., Pétrilli, V., Van Bruggen, R., Steele, C., Mossman, B. T., & Tschopp, J. (2008). Innate immune activation through Nalp3 inflammasome sensing of asbestos and silica. *Science*, *320*(5876), 674-677. https://doi.org/10.1126/science.1156995

Eidinger, D., & Garrett, T. J. (1972). Studies of the regulatory effects of the sex hormones on antibody formation and stem cell differentiation. *J Exp Med*, *136*(5), 1098-1116. https://doi.org/10.1084/jem.136.5.1098

Ellulu, M. S., Patimah, I., Khaza'ai, H., Rahmat, A., & Abed, Y. (2017). Obesity and inflammation: the linking mechanism and the complications. *Arch Med Sci*, *13*(4), 851-863. https://doi.org/10.5114/aoms.2016.58928

Elmallah, M., & Micheau, O. (2019). Epigenetic Regulation of TRAIL Signaling: Implication for Cancer Therapy. *Cancers*, *11*, 850. https://doi.org/10.3390/cancers11060850

Erickson, M. A., Liang, W. S., Fernandez, E. G., Bullock, K. M., Thysell, J. A., & Banks, W. A. (2018). Genetics and sex influence peripheral and central innate immune responses and blood-brain barrier integrity. *PLoS One*, *13*(10), e0205769. https://doi.org/10.1371/journal.pone.0205769

Evans, M., Cogan, K., & Egan, B. (2017). Metabolism of ketone bodies during exercise and training: physiological basis for exogenous supplementation. *The Journal of Physiology*, *595*, 2857-2871. https://doi.org/10.1113/JP273185

Fantuzzi, G. (2005). Adipose tissue, adipokines, and inflammation. *J Allergy Clin Immunol*, *115*(5), 911-919; quiz 920. https://doi.org/10.1016/j.jaci.2005.02.023

Fantuzzi, G., & Faggioni, R. (2000). Leptin in the regulation of immunity, inflammation, and hematopoiesis. *Journal of Leukocyte Biology*, *68*(4), 437-446. https://doi.org/https://doi.org/10.1189/jlb.68.4.437

Fedorovich, S. V., Voronina, P. P., & Waseem, T. V. (2018). Ketogenic diet versus ketoacidosis: what determines the influence of ketone bodies on neurons? *Neural Regen Res*, *13*(12), 2060-2063. https://doi.org/10.4103/1673-5374.241442

Felmlee, M. A., Jones, R. S., Rodriguez-Cruz, V., Follman, K. E., & Morris, M. E. (2020). Monocarboxylate Transporters (SLC16): Function, Regulation, and Role in Health and Disease. *Pharmacological Reviews*, *72*(2), 466-485. https://doi.org/10.1124/pr.119.018762

Fletcher, J. A., Deja, S., Satapati, S., Fu, X., Burgess, S. C., & Browning, J. D. (2019). Impaired ketogenesis and increased acetyl-CoA oxidation promote hyperglycemia in human fatty liver. *JCI Insight*, *5*(11). https://doi.org/10.1172/jci.insight.127737

Fox, H. S., Bond, B. L., & Parslow, T. G. (1991). Estrogen regulates the IFN-gamma promoter. *J Immunol*, *146*(12), 4362-4367.

Franchi, L., Eigenbrod, T., Muñoz-Planillo, R., & Nuñez, G. (2009). The inflammasome: a caspase-1-activation platform that regulates immune responses and disease pathogenesis. *Nat Immunol*, *10*(3), 241-247. https://doi.org/10.1038/ni.1703

Franchi, L., Warner, N., Viani, K., & Nuñez, G. (2009). Function of Nod-like receptors in microbial recognition and host defense. *Immunological reviews*, *227*(1), 106-128. https://doi.org/10.1111/j.1600-065X.2008.00734.x

Furman, D., Campisi, J., Verdin, E., Carrera-Bastos, P., Targ, S., Franceschi, C., Ferrucci, L., Gilroy, D. W., Fasano, A., Miller, G. W., Miller, A. H., Mantovani, A., Weyand, C. M., Barzilai, N., Goronzy, J. J., Rando, T. A., Effros, R. B., Lucia, A., Kleinstreuer, N., & Slavich, G. M. (2019). Chronic inflammation in the etiology of disease across the life span. *Nature medicine*, *25*(12), 1822-1832. https://doi.org/10.1038/s41591-019-0675-0

Ghisletti, S., Meda, C., Maggi, A., & Vegeto, E. (2005). 17beta-estradiol inhibits inflammatory gene expression by controlling NF-kappaB intracellular localization. *Mol Cell Biol*, *25*(8), 2957-2968. https://doi.org/10.1128/mcb.25.8.2957-2968.2005

Graff, E. C., Fang, H., Wanders, D., & Judd, R. L. (2016). Anti-inflammatory effects of the hydroxycarboxylic acid receptor 2. *Metabolism*, *65*(2), 102-113. https://doi.org/10.1016/j.metabol.2015.10.001

Green, A., & Bishop, R. E. (2019). Ketoacidosis – Where Do the Protons Come From? *Trends in Biochemical Sciences*, *44*(6), 484-489. https://doi.org/https://doi.org/10.1016/j.tibs.2019.01.005

Grimm, S., & Baeuerle, P. (1993). The inducible transcription factor NF-??B: Structure-function relationship of its protein subunits. *The Biochemical journal*, *290 (Pt 2)*, 297-308. https://doi.org/10.1042/bj2900297

Hayden, M. S., & Ghosh, S. (2014). Regulation of NF-κB by TNF family cytokines. *Semin Immunol*, *26*(3), 253-266. https://doi.org/10.1016/j.smim.2014.05.004

Heo, H., Jo, J., Jung, J. I., Han, Y. M., Lee, S., Kim, S. R., Kwon, S. H., Kim, K. N., Hwang, B. J., Kee, Y., Lee, B. D., Kang, D., & Her, S. (2019). Improved dynamic monitoring of transcriptional activity during longitudinal analysis in the mouse brain. *Biol Open*, *8*(1). https://doi.org/10.1242/bio.037168

Herrero, M. T., Estrada, C., Maatouk, L., & Vyas, S. (2015). Inflammation in Parkinson's disease: role of glucocorticoids. *Front Neuroanat*, *9*, 32. https://doi.org/10.3389/fnana.2015.00032

Hochheiser, K., Heuser, C., Krause, T. A., Teteris, S., Ilias, A., Weisheit, C., Hoss, F., Tittel, A. P., Knolle, P. A., Panzer, U., Engel, D. R., Tharaux, P. L., & Kurts, C. (2013). Exclusive CX3CR1 dependence of kidney DCs impacts glomerulonephritis progression. *J Clin Invest*, *123*(10), 4242-4254. https://doi.org/10.1172/jci70143

Hugo, S. E., Cruz-Garcia, L., Karanth, S., Anderson, R. M., Stainier, D. Y., & Schlegel, A. (2012). A monocarboxylate transporter required for hepatocyte secretion of ketone bodies during fasting. *Genes Dev*, *26*(3), 282-293. https://doi.org/10.1101/gad.180968.111

Irwin, M. R., Olmstead, R., & Carroll, J. E. (2016). Sleep Disturbance, Sleep Duration, and Inflammation: A Systematic Review and Meta-Analysis of Cohort Studies and Experimental Sleep Deprivation. *Biol Psychiatry*, *80*(1), 40-52. https://doi.org/10.1016/j.biopsych.2015.05.014

Irwin, M. R., Witarama, T., Caudill, M., Olmstead, R., & Breen, E. C. (2015). Sleep loss activates cellular inflammation and signal transducer and activator of transcription (STAT) family proteins in humans. *Brain Behav Immun*, *47*, 86-92. https://doi.org/10.1016/j.bbi.2014.09.017

Ivan, G., Eric, T., Edson, L., Chilly Gay, R., Se Jin, J., & and Chan Young, S. (2021). Strain, Age, and Gender Differences in Response to Lipopolysaccharide (LPS) Animal Model of Sepsis in Mice. *YAKHAK HOEJI*, *65*(1), 17-22. https://doi.org/10.17480/psk.2021.65.1.17

Ivanova, L. N., Archibasova, V. K., & Shterental, I. (1978). [Sodium-depositing function of the skin in white rats]. *Fiziol Zh SSSR Im I M Sechenova*, *64*(3), 358-363. (Natriĭ-deponiruiushchaia funktsiia kozhi u belykh krys.)

Kabel, A. M. (2014). Relationship between Cancer and Cytokines. *Journal of Cancer Research and Treatment*, *2*(2), 41-43. http://pubs.sciepub.com/jcrt/2/2/3

Kany, S., Vollrath, J. T., & Relja, B. (2019). Cytokines in Inflammatory Disease. *International journal of molecular sciences*, *20*(23), 6008. https://doi.org/10.3390/ijms20236008

Kelley, N., Jeltema, D., Duan, Y., & He, Y. (2019). The NLRP3 Inflammasome: An Overview of Mechanisms of Activation and Regulation. *International journal of molecular sciences*, *20*(13). https://doi.org/10.3390/ijms20133328

Klein, S. L., & Flanagan, K. L. (2016). Sex differences in immune responses. *Nature Reviews Immunology*, *16*(10), 626-638. https://doi.org/10.1038/nri.2016.90

Kraeuter, A. K., Mashavave, T., Suvarna, A., van den Buuse, M., & Sarnyai, Z. (2020). Effects of beta-hydroxybutyrate administration on MK-801-induced schizophrenia-like behaviour in mice. *Psychopharmacology (Berl)*, *237*(5), 1397-1405. https://doi.org/10.1007/s00213-020-05467-2

Królicka, A. L., Kruczkowska, A., Krajewska, M., & Kusztal, M. A. (2020). Hyponatremia in Infectious Diseases-A Literature Review. *Int J Environ Res Public Health*, *17*(15). https://doi.org/10.3390/ijerph17155320

Kumar, H., Kawai, T., & Akira, S. (2011). Pathogen Recognition by the Innate Immune System. *International Reviews of Immunology*, *30*(1), 16-34. https://doi.org/10.3109/08830185.2010.529976

Kuo, S. M. (2016). Gender Difference in Bacteria Endotoxin-Induced Inflammatory and Anorexic Responses. *PLoS One*, *11*(9), e0162971. https://doi.org/10.1371/journal.pone.0162971

Laffel, L. (1999). Ketone bodies: a review of physiology, pathophysiology and application of monitoring to diabetes. *Diabetes/Metabolism Research and Reviews*, *15*(6), 412-426. https://doi.org/https://doi.org/10.1002/(SICI)1520-7560(199911/12)15:6<412::AID-DMRR72>3.0.CO;2-8

Lawrence, T. (2009). The nuclear factor NF-kappaB pathway in inflammation. *Cold Spring Harbor perspectives in biology*, *1*(6), a001651-a001651. https://doi.org/10.1101/cshperspect.a001651

Li, H., Sun, S. R., Yap, J. Q., Chen, J. H., & Qian, Q. (2016). 0.9% saline is neither normal nor physiological. *J Zhejiang Univ Sci B*, *17*(3), 181-187. https://doi.org/10.1631/jzus.B1500201

Lin, C. Y., Chen, Y. M., Tsai, Y. H., Hung, K. Y., Fang, Y. T., Chang, Y. P., Tsai, M. Y., Wu, H. F., Lin, M. C., & Fang, W. F. (2022). Association of Hypernatremia with Immune Profiles and Clinical Outcomes in Adult Intensive Care Unit Patients with Sepsis. *Biomedicines*, *10*(9). https://doi.org/10.3390/biomedicines10092285

Liu, J., Wang, J., Luo, H., Li, Z., Zhong, T.-Y., Tang, J., & Jiang, Y. (2017). Screening cytokine/chemokine profiles in serum and organs from an endotoxic shock mouse model by LiquiChip. *Science China. Life sciences*, *60*. https://doi.org/10.1007/s11427-016-9016-6

Liu, T., Zhang, L., Joo, D., & Sun, S. C. (2017). NF-κB signaling in inflammation. *Signal Transduct Target Ther*, *2*, 17023-. https://doi.org/10.1038/sigtrans.2017.23

Loomis, W. H., Namiki, S., Hoyt, D. B., & Junger, W. G. (2001). Hypertonicity rescues T cells from suppression by trauma-induced anti-inflammatory mediators. *American Journal of Physiology-Cell Physiology*, *281*(3), C840-C848. https://doi.org/10.1152/ajpcell.2001.281.3.C840

Ma, M. W., Wang, J., Dhandapani, K. M., & Brann, D. W. (2017). NADPH Oxidase 2 Regulates NLRP3 Inflammasome Activation in the Brain after Traumatic Brain Injury. *Oxid Med Cell Longev*, *2017*, 6057609. https://doi.org/10.1155/2017/6057609

Maffei, M., Stoffel, M., Barone, M., Moon, B., Dammerman, M., Ravussin, E., Bogardus, C., Ludwig, D. S., Flier, J. S., Talley, M., Auerbach, S., & Friedman, J. M. (1996). Absence of Mutations in the Human OB Gene in Obese/Diabetic Subjects. *Diabetes*, *45*(5), 679-682. https://doi.org/10.2337/diab.45.5.679

Marsland, A. L., Walsh, C., Lockwood, K., & John-Henderson, N. A. (2017). The effects of acute psychological stress on circulating and stimulated inflammatory markers: A systematic review and meta-analysis. *Brain, Behavior, and Immunity*, *64*, 208-219. https://doi.org/https://doi.org/10.1016/j.bbi.2017.01.011

Masaki, T., Chiba, S., Tatsukawa, H., Yasuda, T., Noguchi, H., Seike, M., & Yoshimatsu, H. (2004). Adiponectin protects LPS-induced liver injury through modulation of TNF-α in KK-Ay obese mice. *Hepatology*, *40*(1), 177-184. https://doi.org/https://doi.org/10.1002/hep.20282

Matzinger, P. (1994). Tolerance, Danger and the Extended Family. *Annual Review of Immunology*, *12*, 991-1045. https://doi.org/10.1146/annurev.iy.12.040194.005015

Mérillat, A.-M., Charles, R.-P., Porret, A., Maillard, M., Rossier, B., Beermann, F., & Hummler, E. (2009). Conditional gene targeting of the ENaC subunit genes Scnn1b and Scnn1g. *American Journal of Physiology-Renal Physiology*, *296*(2), F249-F256. https://doi.org/10.1152/ajprenal.00612.2007

Minutoli, L., Puzzolo, D., Rinaldi, M., Irrera, N., Marini, H., Arcoraci, V., Bitto, A., Crea, G., Pisani, A., Squadrito, F., Trichilo, V., Bruschetta, D., Micali, A., & Altavilla, D. (2016). ROS-Mediated NLRP3 Inflammasome Activation in Brain, Heart, Kidney, and Testis Ischemia/Reperfusion Injury. *Oxid Med Cell Longev*, *2016*, 2183026. https://doi.org/10.1155/2016/2183026

Mogi, M., Harada, M., Kondo, T., Riederer, P., Inagaki, H., Minami, M., & Nagatsu, T. (1994). Interleukin-1 beta, interleukin-6, epidermal growth factor and transforming growth factor-alpha are elevated in the brain from parkinsonian patients. *Neurosci Lett*, *180*(2), 147-150. https://doi.org/10.1016/0304-3940(94)90508-8

Morgan, T. J. (2009). The Stewart approach--one clinician's perspective. *Clin Biochem Rev*, *30*(2), 41-54.

Muñoz-Planillo, R., Kuffa, P., Martínez-Colón, G., Smith, B. L., Rajendiran, T. M., & Núñez, G. (2013). K^+ efflux is the common trigger of NLRP3 inflammasome activation by bacterial toxins and particulate matter. *Immunity*, *38*(6), 1142-1153. https://doi.org/10.1016/j.immuni.2013.05.016

Nakahira, K., Haspel, J. A., Rathinam, V. A., Lee, S. J., Dolinay, T., Lam, H. C., Englert, J. A., Rabinovitch, M., Cernadas, M., Kim, H. P., Fitzgerald, K. A., Ryter, S. W., & Choi, A. M. (2011). Autophagy proteins regulate innate immune responses by inhibiting the release of mitochondrial DNA mediated by the NALP3 inflammasome. *Nat Immunol*, *12*(3), 222-230. https://doi.org/10.1038/ni.1980

Newman, J. C., & Verdin, E. (2017). β-Hydroxybutyrate: A Signaling Metabolite. *Annual review of nutrition*, *37*, 51-76. https://doi.org/10.1146/annurev-nutr-071816-064916

Newman, J. C., & Verdin, E. (2017). β-Hydroxybutyrate: A Signaling Metabolite. *Annu Rev Nutr*, *37*, 51-76. https://doi.org/10.1146/annurev-nutr-071816-064916

Nunes-Alves, C. (2014). New LPS receptors discovered. *Nature Reviews Immunology*, *14*(9), 583-583. https://doi.org/10.1038/nri3736

O'Neill, L. A. J., & Bowie, A. G. (2007). The family of five: TIR-domain-containing adaptors in Toll-like receptor signalling. *Nature Reviews Immunology*, *7*(5), 353-364. https://doi.org/10.1038/nri2079

Owen, O. E., Felig, P., Morgan, A. P., Wahren, J., & Cahill, G. F., Jr. (1969). Liver and kidney metabolism during prolonged starvation. *J Clin Invest*, *48*(3), 574-583. https://doi.org/10.1172/jci106016

Pahwa R, G. A., Jialal I. (2022). *Chronic Inflammation* https://www.ncbi.nlm.nih.gov/books/NBK493173/

Paik, S., Kim, J. K., Silwal, P., Sasakawa, C., & Jo, E.-K. (2021). An update on the regulatory mechanisms of NLRP3 inflammasome activation. *Cellular & Molecular Immunology*, *18*(5), 1141-1160. https://doi.org/10.1038/s41423-021-00670-3

Pellerin, L., Halestrap, A. P., & Pierre, K. (2005). Cellular and subcellular distribution of monocarboxylate transporters in cultured brain cells and in the adult brain. *Journal of Neuroscience Research*, *79*(1-2), 55-64. https://doi.org/https://doi.org/10.1002/jnr.20307

Perregaux, D., & Gabel, C. A. (1994). Interleukin-1 beta maturation and release in response to ATP and nigericin. Evidence that potassium depletion mediated by these agents is a necessary and common feature of their activity. *J Biol Chem*, *269*(21), 15195-15203.

Pistorio, V., Tokgozoglu, J., Ratziu, V., & Gautheron, J. (2022). The scaffold-dependent function of RIPK1 in experimental non-alcoholic steatohepatitis. *Journal of Molecular Medicine*, *100*(7), 1039-1042. https://doi.org/10.1007/s00109-022-02217-z

Pizzino, G., Irrera, N., Cucinotta, M., Pallio, G., Mannino, F., Arcoraci, V., Squadrito, F., Altavilla, D., & Bitto, A. (2017). Oxidative Stress: Harms and Benefits for Human Health. *Oxid Med Cell Longev*, *2017*, 8416763. https://doi.org/10.1155/2017/8416763

Ray, P. D., Huang, B. W., & Tsuji, Y. (2012). Reactive oxygen species (ROS) homeostasis and redox regulation in cellular signaling. *Cell Signal*, *24*(5), 981-990. https://doi.org/10.1016/j.cellsig.2012.01.008

Roh, J. S., & Sohn, D. H. (2018). Damage-Associated Molecular Patterns in Inflammatory Diseases. *Immune network*, *18*(4), e27-e27. https://doi.org/10.4110/in.2018.18.e27

Roma, P., Amandeep, G., Pankaj, B., & Ishwarlal, J. (2021). *Chronic Inflammation*. StatPearls https://www.ncbi.nlm.nih.gov/books/NBK493173/

Roma, P., Lindsey, R., Joanna, P., & William, M. C. (2017). Reactive Oxygen Species: The Good and the Bad. In F. Cristiana & A. Elena (Eds.), *Reactive Oxygen Species (ROS) in Living Cells* (pp. Ch. 2). IntechOpen. https://doi.org/10.5772/intechopen.71547

Rusek, M., Pluta, R., Ułamek-Kozioł, M., & Czuczwar, S. J. (2019). Ketogenic Diet in Alzheimer's Disease. *International journal of molecular sciences*, *20*(16). https://doi.org/10.3390/ijms20163892

Sakai, J., Cammarota, E., Wright, J. A., Cicuta, P., Gottschalk, R. A., Li, N., Fraser, I. D. C., & Bryant, C. E. (2017). Lipopolysaccharide-induced NF-κB nuclear translocation is primarily dependent on MyD88, but TNFα expression requires TRIF and MyD88. *Sci Rep*, *7*(1), 1428. https://doi.org/10.1038/s41598-017-01600-y

Schatz, V., Neubert, P., Schröder, A., Binger, K., Gebhard, M., Müller, D. N., Luft, F. C., Titze, J., & Jantsch, J. (2017). Elementary immunology: Na(+) as a regulator of immunity. *Pediatr Nephrol*, *32*(2), 201-210. https://doi.org/10.1007/s00467-016-3349-x

Schorn, C., Frey, B., Lauber, K., Janko, C., Strysio, M., Keppeler, H., Gaipl, U. S., Voll, R. E., Springer, E., Munoz, L. E., Schett, G., & Herrmann, M. (2011). Sodium overload and water influx activate the NALP3 inflammasome. *J Biol Chem*, *286*(1), 35-41. https://doi.org/10.1074/jbc.M110.139048

Schroder, K., & Tschopp, J. (2010). The inflammasomes. *Cell*, *140*(6), 821-832. https://doi.org/10.1016/j.cell.2010.01.040

Schröfelbauer, B., Polley, S., Behar, M., Ghosh, G., & Hoffmann, A. (2012). NEMO ensures signaling specificity of the pleiotropic IKKβ by directing its kinase activity toward IκBα. *Mol Cell*, *47*(1), 111-121. https://doi.org/10.1016/j.molcel.2012.04.020

Shimada, K., Crother, T. R., Karlin, J., Dagvadorj, J., Chiba, N., Chen, S., Ramanujan, V. K., Wolf, A. J., Vergnes, L., Ojcius, D. M., Rentsendorj, A., Vargas, M., Guerrero, C., Wang, Y., Fitzgerald, K. A., Underhill, D. M., Town, T., & Arditi, M. (2012). Oxidized mitochondrial DNA activates the NLRP3 inflammasome during apoptosis. *Immunity*, *36*(3), 401-414. https://doi.org/10.1016/j.immuni.2012.01.009

Shimazu, T., Hirschey, M. D., Newman, J., He, W., Shirakawa, K., Le Moan, N., Grueter, C. A., Lim, H., Saunders, L. R., Stevens, R. D., Newgard, C. B., Farese, R. V., Jr., de Cabo, R., Ulrich, S., Akassoglou, K., & Verdin, E. (2013). Suppression of oxidative stress by β-hydroxybutyrate, an endogenous histone deacetylase inhibitor. *Science*, *339*(6116), 211-214. https://doi.org/10.1126/science.1227166

Singh, N., Gurav, A., Sivaprakasam, S., Brady, E., Padia, R., Shi, H., Thangaraju, M., Prasad, P. D., Manicassamy, S., Munn, D. H., Lee, J. R., Offermanns, S., & Ganapathy, V. (2014). Activation of Gpr109a, receptor for niacin and the commensal metabolite butyrate, suppresses colonic inflammation and carcinogenesis. *Immunity*, *40*(1), 128-139. https://doi.org/10.1016/j.immuni.2013.12.007

Singh, T., & Newman, A. B. (2011). Inflammatory markers in population studies of aging. *Ageing Res Rev*, *10*(3), 319-329. https://doi.org/10.1016/j.arr.2010.11.002

Sirotkovic-Skerlev, M., Kulić, A., Bradić, L., & Cacev, T. (2012). Protumor effects of proinflammatory mediators in breast cancer. *Periodicum Biologorum*, *114*, 489.

Stefan, M., Sharp, M., Gheith, R., Lowery, R., & Wilson, J. (2021). The Effect of Exogenous Beta-Hydroxybutyrate Salt Supplementation on Metrics of Safety and Health in Adolescents. *Nutrients*, *13*(3). https://doi.org/10.3390/nu13030854

Stefanetti, R. J., Voisin, S., Russell, A., & Lamon, S. (2018). Recent advances in understanding the role of FOXO3. *F1000Res*, *7*. https://doi.org/10.12688/f1000research.15258.1

Sun, S. C. (2011). Non-canonical NF-κB signaling pathway. *Cell Res*, *21*(1), 71-85. https://doi.org/10.1038/cr.2010.177

Sun, S. C. (2017). The non-canonical NF-κB pathway in immunity and inflammation. *Nat Rev Immunol*, *17*(9), 545-558. https://doi.org/10.1038/nri.2017.52

Sun, S. C., & Ley, S. C. (2008). New insights into NF-kappaB regulation and function. *Trends Immunol*, *29*(10), 469-478. https://doi.org/10.1016/j.it.2008.07.003

Swanson, K. V., Deng, M., & Ting, J. P. (2019). The NLRP3 inflammasome: molecular activation and regulation to therapeutics. *Nat Rev Immunol*, *19*(8), 477-489. https://doi.org/10.1038/s41577-019-0165-0

Szabó, G., & Magyar, Z. (1982). Electrolyte concentrations in subcutaneous tissue fluid and lymph. *Lymphology*, *15*(4), 174-177.

Taggart, A. K., Kero, J., Gan, X., Cai, T. Q., Cheng, K., Ippolito, M., Ren, N., Kaplan, R., Wu, K., Wu, T. J., Jin, L., Liaw, C., Chen, R., Richman, J., Connolly, D., Offermanns, S., Wright, S. D., & Waters, M. G. (2005). (D)-beta-Hydroxybutyrate inhibits adipocyte lipolysis via the nicotinic acid receptor PUMA-G. *J Biol Chem*, *280*(29), 26649-26652. https://doi.org/10.1074/jbc.C500213200

Taniyama, Y., & Griendling, K. K. (2003). Reactive Oxygen Species in the Vasculature. *Hypertension*, *42*(6), 1075-1081. https://doi.org/doi:10.1161/01.HYP.0000100443.09293.4F

Thangaraju, M., Cresci, G. A., Liu, K., Ananth, S., Gnanaprakasam, J. P., Browning, D. D., Mellinger, J. D., Smith, S. B., Digby, G. J., Lambert, N. A., Prasad, P. D., & Ganapathy, V. (2009). GPR109A is a G-protein-coupled receptor for the bacterial fermentation product butyrate and functions as a tumor suppressor in colon. *Cancer Res*, *69*(7), 2826-2832. https://doi.org/10.1158/0008-5472.Can-08-4466

Tian, R., Hou, G., Li, D., & Yuan, T. F. (2014). A possible change process of inflammatory cytokines in the prolonged chronic stress and its ultimate implications for health. *ScientificWorldJournal*, *2014*, 780616. https://doi.org/10.1155/2014/780616

Tulotta, C., & Ottewell, P. (2018). The role of IL-1B in breast cancer bone metastasis. *Endocr Relat Cancer*, *25*(7), R421-r434. https://doi.org/10.1530/erc-17-0309

Tunaru, S., Kero, J., Schaub, A., Wufka, C., Blaukat, A., Pfeffer, K., & Offermanns, S. (2003). PUMA-G and HM74 are receptors for nicotinic acid and mediate its anti-lipolytic effect. *Nature medicine*, *9*(3), 352-355. https://doi.org/10.1038/nm824

Ułamek-Kozioł, M., Czuczwar, S. J., Januszewski, S., & Pluta, R. (2019). Ketogenic Diet and Epilepsy. *Nutrients*, *11*(10). https://doi.org/10.3390/nu11102510

Umpierrez, G. E., Murphy, M. B., & Kitabchi, A. E. (2002). Diabetic Ketoacidosis and Hyperglycemic Hyperosmolar Syndrome. *Diabetes Spectrum*, *15*(1), 28-36. https://doi.org/10.2337/diaspect.15.1.28

van Bruggen, R., Köker, M. Y., Jansen, M., van Houdt, M., Roos, D., Kuijpers, T. W., & van den Berg, T. K. (2010). Human NLRP3 inflammasome activation is Nox1-4 independent. *Blood*, *115*(26), 5398-5400. https://doi.org/10.1182/blood-2009-10-250803

W.H.O. (2020). *The top 10 causes of death*. WHO. https://www.who.int/news-room/fact-sheets/detail/the-top-10-causes-of-death

Wang, N., Liang, H., & Zen, K. (2014). Molecular mechanisms that influence the macrophage m1-m2 polarization balance. *Front Immunol*, *5*, 614. https://doi.org/10.3389/fimmu.2014.00614

Weckx, R., Goossens, C., Derde, S., Pauwels, L., Vander Perre, S., Van den Bergh, G., & Langouche, L. (2021). Identification of the toxic threshold of 3-hydroxybutyrate-sodium supplementation in

septic mice. *BMC Pharmacology and Toxicology*, *22*(1), 50. https://doi.org/10.1186/s40360-021-00517-7

Weis, W. I., & Kobilka, B. K. (2018). The Molecular Basis of G Protein-Coupled Receptor Activation. *Annu Rev Biochem*, *87*, 897-919. https://doi.org/10.1146/annurev-biochem-060614-033910

Wheless, J. W. (2008). History of the ketogenic diet. *Epilepsia*, *49*(s8), 3-5. https://doi.org/https://doi.org/10.1111/j.1528-1167.2008.01821.x

Wiig, H., Schröder, A., Neuhofer, W., Jantsch, J., Kopp, C., Karlsen, T. V., Boschmann, M., Goss, J., Bry, M., Rakova, N., Dahlmann, A., Brenner, S., Tenstad, O., Nurmi, H., Mervaala, E., Wagner, H., Beck, F. X., Müller, D. N., Kerjaschki, D., . . . Titze, J. (2013). Immune cells control skin lymphatic electrolyte homeostasis and blood pressure. *J Clin Invest*, *123*(7), 2803-2815. https://doi.org/10.1172/jci60113

Wolf, A. M., Wolf, D., Rumpold, H., Enrich, B., & Tilg, H. (2004). Adiponectin induces the anti-inflammatory cytokines IL-10 and IL-1RA in human leukocytes. *Biochemical and Biophysical Research Communications*, *323*(2), 630-635. https://doi.org/https://doi.org/10.1016/j.bbrc.2004.08.145

Xiao, G., Harhaj, E. W., & Sun, S. C. (2001). NF-kappaB-inducing kinase regulates the processing of NF-kappaB2 p100. *Mol Cell*, *7*(2), 401-409. https://doi.org/10.1016/s1097-2765(01)00187-3

Xing, D., Oparil, S., Yu, H., Gong, K., Feng, W., Black, J., Chen, Y. F., & Nozell, S. (2012). Estrogen modulates NFκB signaling by enhancing IκBα levels and blocking p65 binding at the promoters of inflammatory genes via estrogen receptor-β. *PLoS One*, *7*(6), e36890. https://doi.org/10.1371/journal.pone.0036890

Yesudhas, D., Gosu, V., Anwar, M. A., & Choi, S. (2014). Multiple roles of toll-like receptor 4 in colorectal cancer. *Front Immunol*, *5*, 334. https://doi.org/10.3389/fimmu.2014.00334

Youm, Y. H., Nguyen, K. Y., Grant, R. W., Goldberg, E. L., Bodogai, M., Kim, D., D'Agostino, D., Planavsky, N., Lupfer, C., Kanneganti, T. D., Kang, S., Horvath, T. L., Fahmy, T. M., Crawford, P. A., Biragyn, A., Alnemri, E., & Dixit, V. D. (2015). The ketone metabolite β-hydroxybutyrate blocks NLRP3 inflammasome-mediated inflammatory disease. *Nature medicine*, *21*(3), 263-269. https://doi.org/10.1038/nm.3804

Yum, M.-S., Ko, T.-S., & Kim, D. W. (2012). Anticonvulsant Effects of β-Hydroxybutyrate in Mice. *Journal of epilepsy research*, *2*(2), 29-32. https://doi.org/10.14581/jer.12008

Yum, M. S., Ko, T. S., & Kim, D. W. (2012). Anticonvulsant Effects of β-Hydroxybutyrate in Mice. *J Epilepsy Res*, *2*(2), 29-32. https://doi.org/10.14581/jer.12008

Zhang, H., & Sun, S. C. (2015). NF-κB in inflammation and renal diseases. *Cell Biosci*, *5*, 63. https://doi.org/10.1186/s13578-015-0056-4

Zhang, J.-M., & An, J. (2007). Cytokines, inflammation, and pain. *International anesthesiology clinics*, *45*(2), 27-37. https://doi.org/10.1097/AIA.0b013e318034194e

Zhang, J. M., & An, J. (2007). Cytokines, inflammation, and pain. *International anesthesiology clinics*, *45*(2), 27-37. https://doi.org/10.1097/AIA.0b013e318034194e

Zhang, M. A., Rego, D., Moshkova, M., Kebir, H., Chruscinski, A., Nguyen, H., Akkermann, R., Stanczyk, F. Z., Prat, A., Steinman, L., & Dunn, S. E. (2012). Peroxisome proliferator-activated receptor (PPAR)α and -γ regulate IFNγ and IL-17A production by human T cells in a sex-specific way. *Proc Natl Acad Sci U S A*, *109*(24), 9505-9510. https://doi.org/10.1073/pnas.1118458109

Zhou, R., Yazdi, A. S., Menu, P., & Tschopp, J. (2011). A role for mitochondria in NLRP3 inflammasome activation. *Nature*, *469*(7329), 221-225. https://doi.org/10.1038/nature09663

Appendix 1 – Materials and instruments

Chemicals and reagents

Chemical name	Obtained from	Catalogue No.
DL-β-hydroxybutyric acid sodium salt	Sigma-Aldrich, Missouri, USA	H6501
Ethylenediamine tetraacetic acid	Sigma-Aldrich, Missouri, USA	03690
Lipopolysaccharide (*Escherichia coli* O55:B5)	Sigma-Aldrich, Missouri, USA	L2880
IsoFlo® Vet. (Isoflurane liquid form)	Zoetis Belgium S.A, Belgium	002185
D-Luciferin Firefly	Biosynth, Switzerland	L-8200
Zoletil Forte	Virbac, Norway	---------
Rompun Vet. (Xylazin)	Bayer Animal Health, Germany	---------
Fentadon Vet. (Fentanyl citrate)	Dechra Veterinary Producs AS, Norway	---------

Kits

Kit name	Obtained from	Catalogue No.
D-3-hydroxybutyric acid assay kit	NeoGen|Megazyme, Ireland	K-HDBA
IL-1 beta Mouse ProcartaPlex™ Simplex Kit	ThermoFischer, Massachusetts, USA	EPX01A-26002-901
IL-6 Mouse ProcartaPlex™ Simplex Kit	ThermoFischer, Massachusetts, USA	EPX01A-20603-901
IL-10 Mouse ProcartaPlex™ Simplex Kit	ThermoFischer, Massachusetts, USA	EPX01A-20614-901
IL-18 Mouse ProcartaPlex™ Simplex Kit	ThermoFischer, Massachusetts, USA	EPX01A-20618-901
INF gamma Mouse ProcartaPlex™ Simplex Kit	ThermoFischer, Massachusetts, USA	EPX01A-20606-901
TNF alpha Mouse ProcartaPlex™ Simplex Kit	ThermoFischer, Massachusetts, USA	EPX01A-20607-901
ProcartaPlex™ Mouse Basic Kit	ThermoFischer, Massachusetts, USA	EPX01A-20440-901

Instruments and software

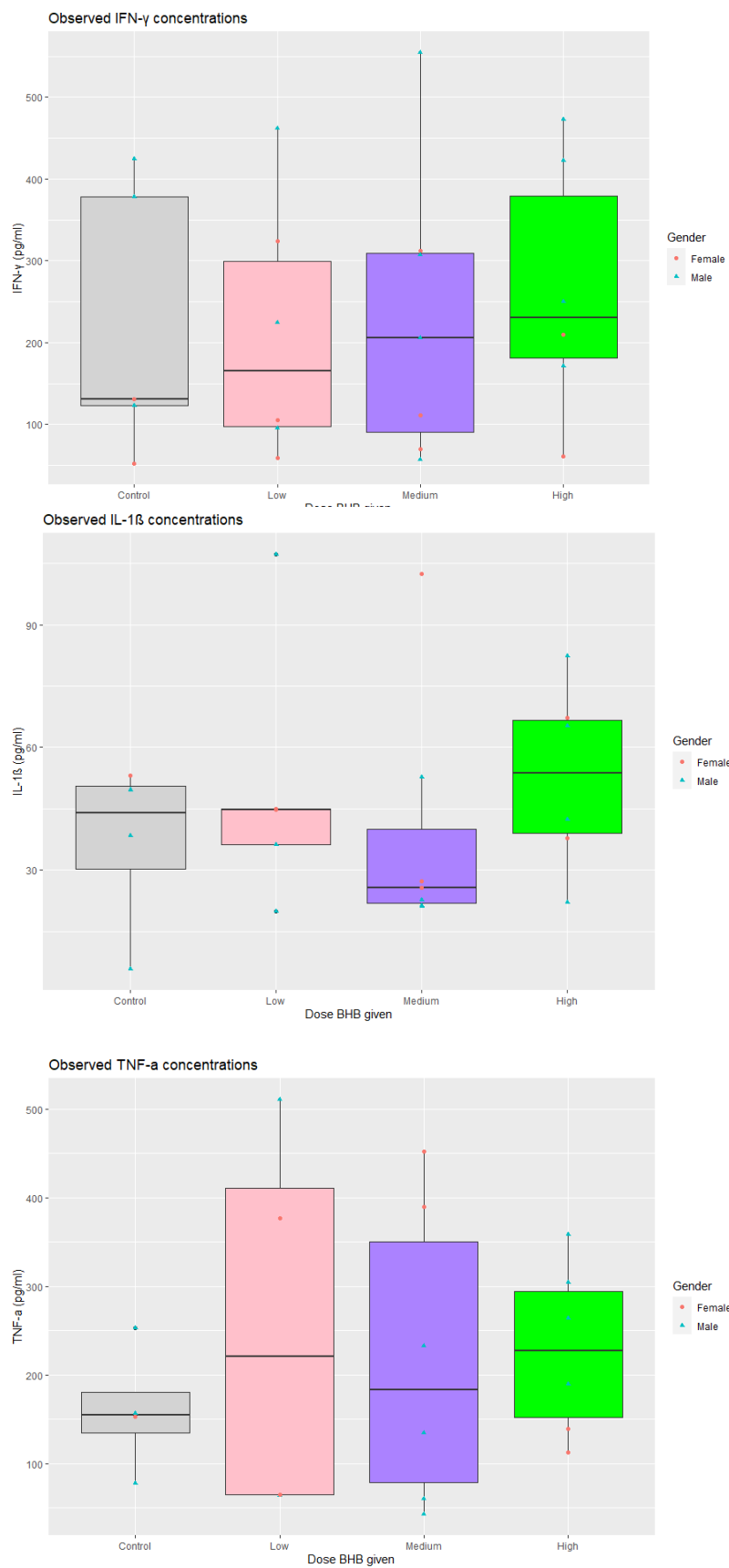| Product	Obtained from	Software
FreeStyle Precision Neo	Abbot Norge AS, Norway	---------
IVIS Lumina II	PerkinElmer, Massachusetts, USA	Living Image®
XGI-8 High-Flow vaporizer	PerkinElmer, Massachusetts, USA	---------
Bio-Plex 200	Bio-Rad, California, USA	Bio-Plex Manager Software 6.1
SpectraMax M2e	Marshall Scientific, Hampton, USA	SoftMax Pro 7.1

Manuals

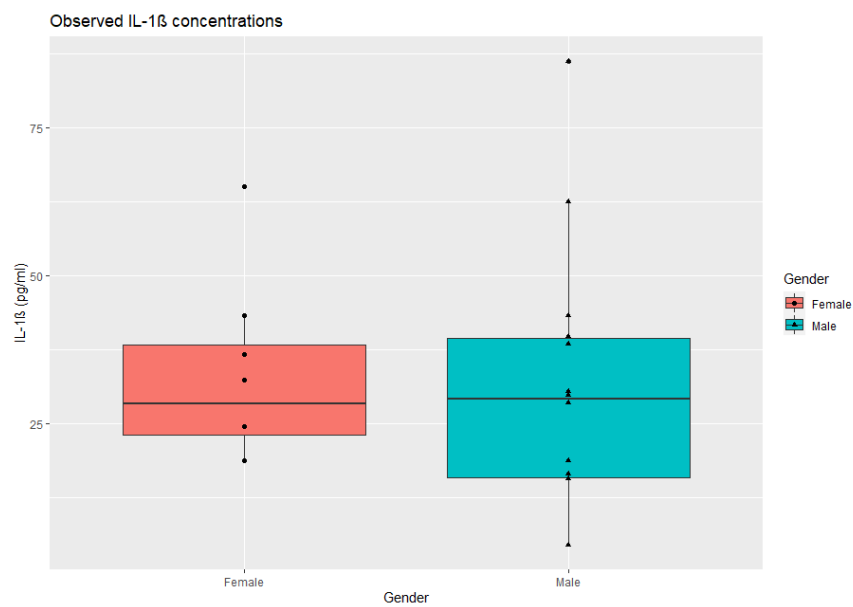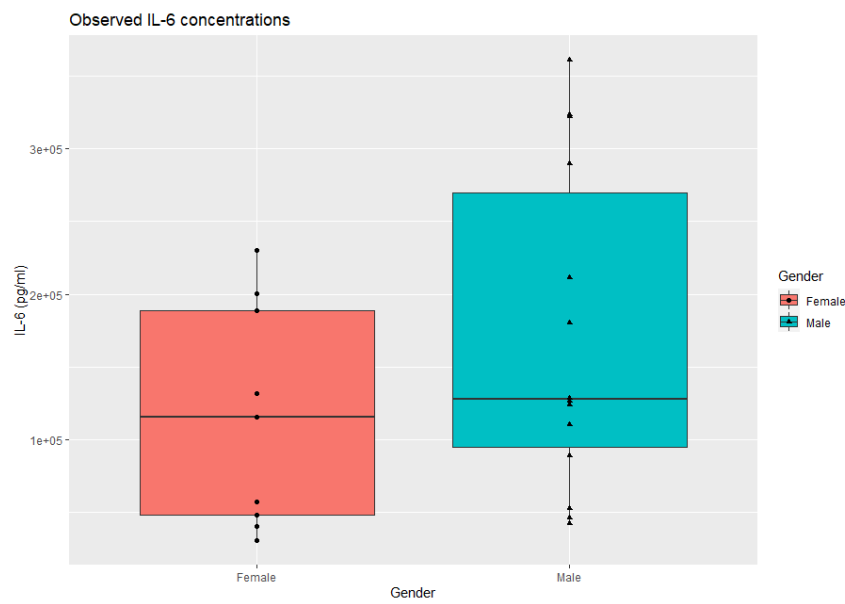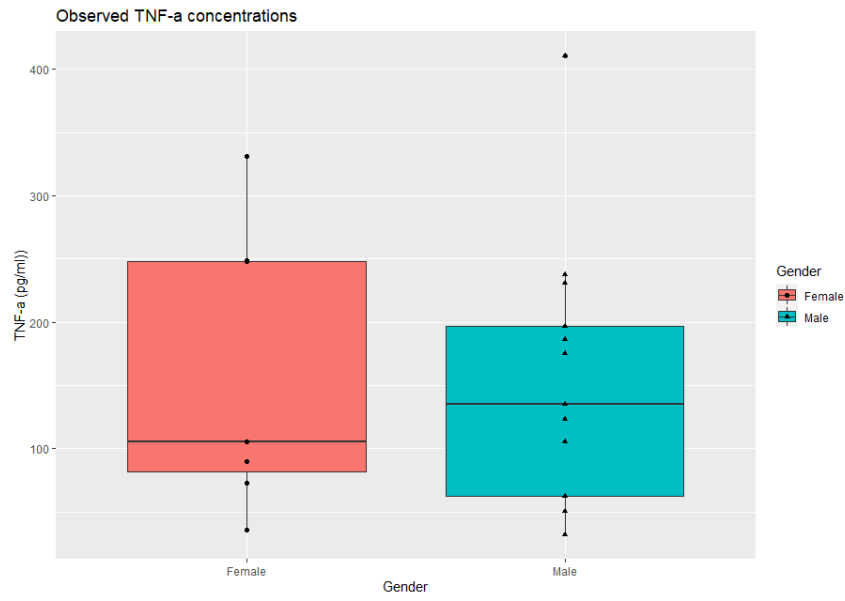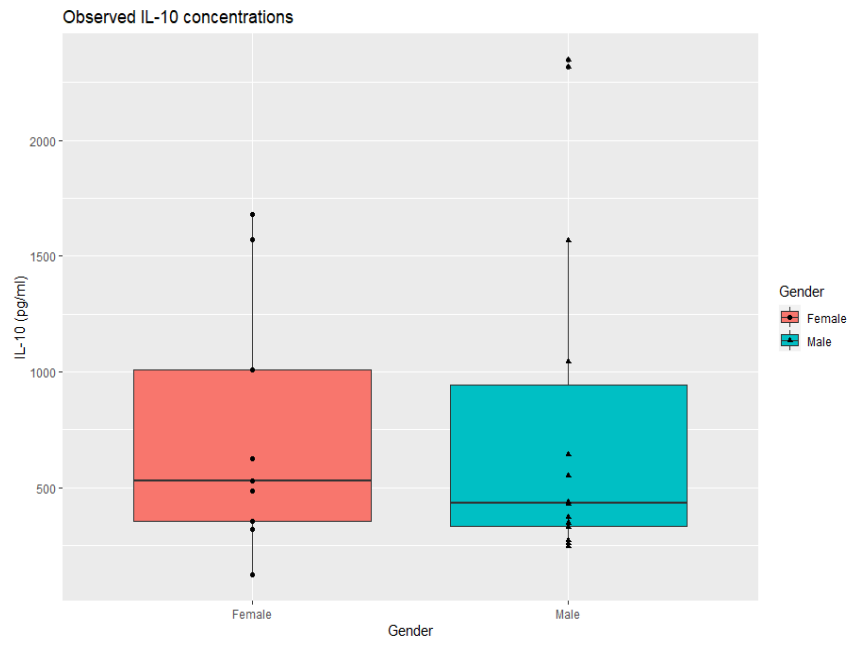| Product	Manual (URL)
Megazyme Assay Protocol	https://www.Megazyme.com/documents/Assay_Protocol/K-HDBA_DATA.pdf
Bio-Plex 200 System Hardware Instruction Manual	https://rai.unam.mx/manuales/umyp_Manual_Bioplex.pdf
Bio-Plex Manager Software 6.2 User Guide	https://www.bio-rad.com/webroot/web/pdf/lsr/literature/10022815.pdf

Appendix 2 Additional data

Raw data from Cytokine profiling

Mouse	Gender	Cage ID	Age (Weeks)	Group	BHB given (milimol/Kg)	IFN gamma	TNF alpha	IL 6	IL 1 beta	IL 10
1	Male	326	17	Control	0	329,84	196,44	126951,77	38,54	328,85
2	Male	326	17	High	15	166,06	237,78	361151,22	43,25	2314,75
3	Male	326	17	Medium	10	41,92	31,57	89431	15,75	1043,74
4	Male	326	17	Low	5	75,1	50,56	42714,62	28,56	370,08
5	Female	325	17	Control	0					
6	Female	325	17	High	15	39,41	72,83	200185,21	24,54	1009,75
7	Female	325	17	Medium	10	77,07		132142,16	18,83	622,83
8	Female	325	17	Low	5	75,94		188600,57	32,41	1571,61
9	Female	325	17	Control	0	34,58		40897,65		317,5
10	Female	325	17	High	15	135,18	89,86	229969,13	43,25	1678,42
11	Male	327	17	Medium	10	418,44	175,33	289457,98	39,74	551,9
12	Male	327	17	Low	5	371,47	410,78	322328,15	86,24	347,66
13	Male	303	21	Control	0	300,63	62,12	46717,26	30,5	429,13
14	Male	303	21	High	15	121,62	135,03	180511,93	15,75	640,44
15	Female	343	21	Medium	10	198,72	247,56	115875,39	65,12	526,87
16	Female	343	21	Low	5	177,46	35,71	30630,16	24,54	121,51
17	Male	309	21	Control	0	96,78	123,12	52992,82	4,5	259,93
18	Male	309	21	High	15	320,35	230,88	323519,14	62,5	2348,08
19	Male	309	21	Medium	10	161,72	105,7	128443,07	16,54	436,45
20	Male	306	21	High	15	332,73	185,97	211520,37	29,86	1564,92
21	Male	306	21	Medium	10	255,29	50,56	124206,35	18,83	271,57
22	Male	306	21	Low	5	178,55		110713,25	15,75	244,31
23	Female	307	21	Control	0	90,44	105,7	57180,54	36,73	355,15
24	Female	307	21	High	15					
25	Female	307	21	Medium	10	51,38	330,89		18,83	483,69
26	Female	307	21	Low	5	39,09	248,53	48373,42		

Cytokine profiling: Additional figures

Observed IFN-γ concentrations

Observed IL-1ß concentrations

Observed TNF-a concentrations

Observed TNF-a concentrations

Observed IL-6 concentrations

Observed IL-1ß concentrations
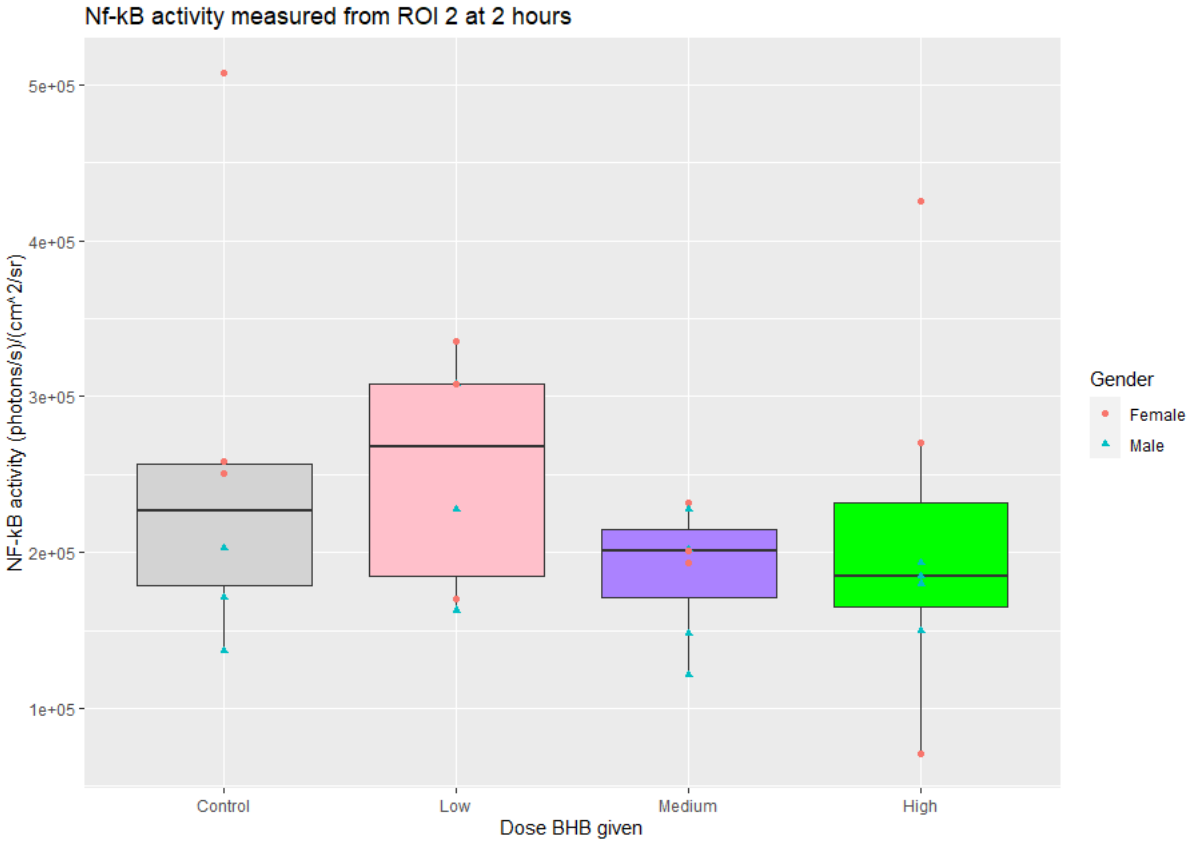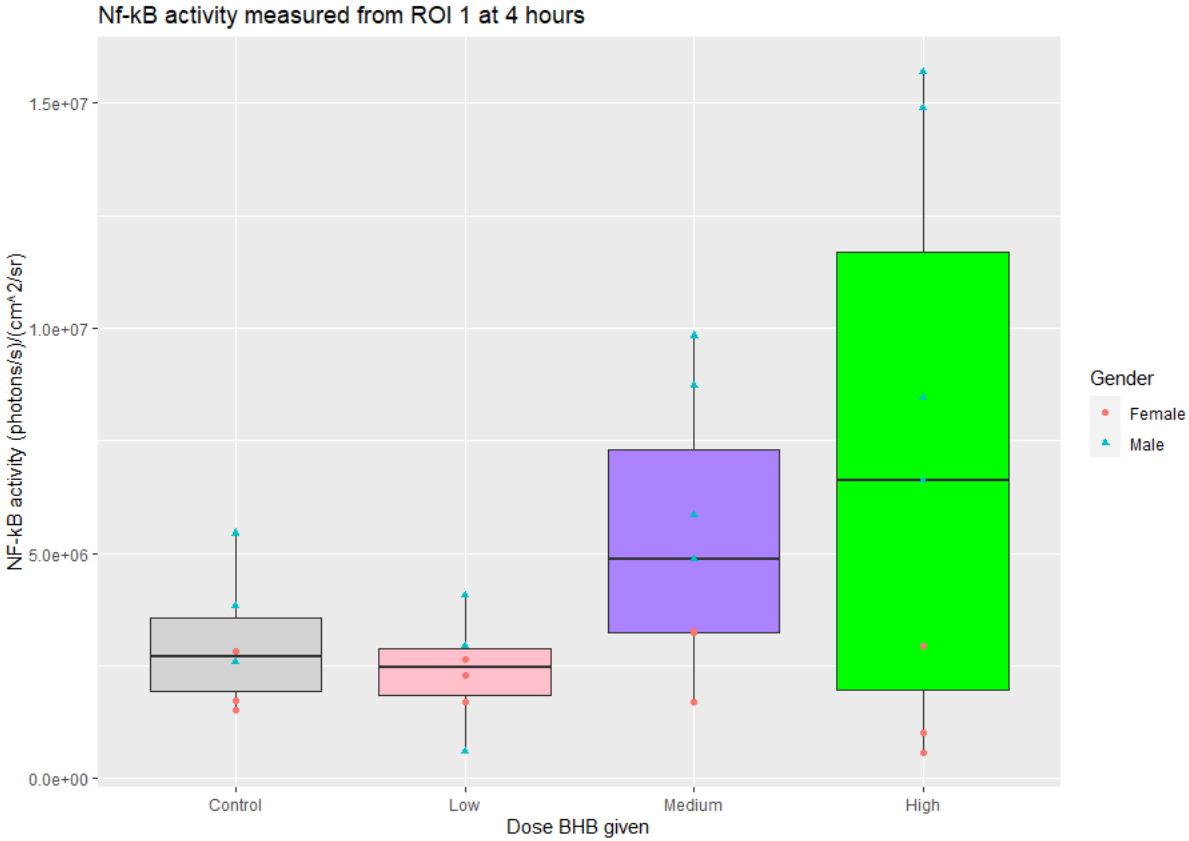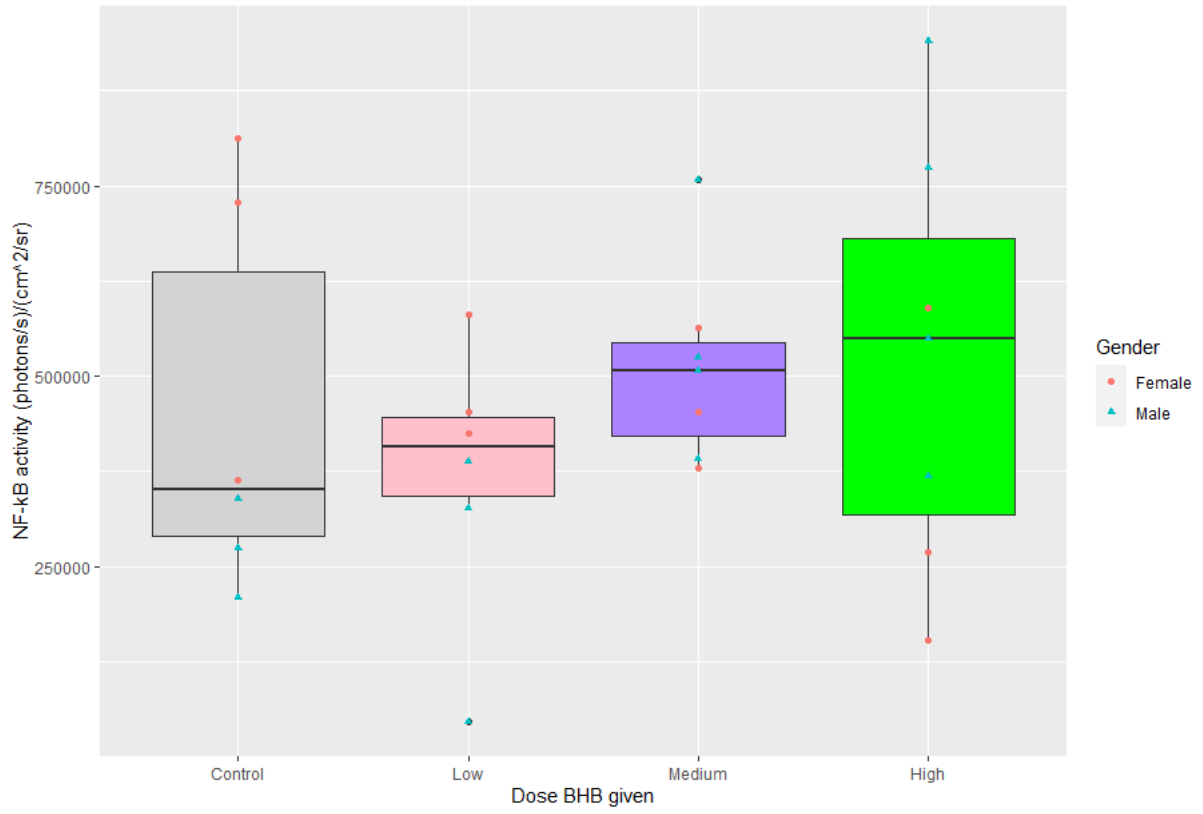
Observed IL-10 concentrations

Raw data from *In vivo* measuring of NF-κB activity

Mouse	Gender	Cage ID	Age (Weeks)	Group	BHB given (milimol/Kg)	Avg radiance Liver 2H	Avg radiance Liver 4H	Avg radiance Abdomen 2H	Avg radiance Abdomen 4H
1	Male	326	17	Control	0	1,88E+06	5,45E+06	2,03E+05	2,74E+05
2	Male	326	17	High	15	1,56E+06	1,57E+07	1,93E+05	9,41E+05
3	Male	326	17	Medium	10	6,88E+05	5,84E+06	1,48E+05	5,08E+05
4	Male	326	17	Low	5	3,03E+06	6,00E+05	2,28E+05	4,52E+04
5	Female	325	17	Control	0	6,66E+05	1,73E+06	2,59E+05	3,64E+05
6	Female	325	17	High	15	2,15E+05	2,93E+06	7,05E+04	5,89E+05
7	Female	325	17	Medium	10	8,51E+05	3,26E+06	2,31E+05	5,64E+05
8	Female	325	17	Low	5	5,41E+05	1,69E+06	1,70E+05	4,25E+05
9	Female	325	17	Control	0	6,85E+05	1,51E+06	2,51E+05	7,29E+05
10	Female	325	17	High	15	6,23E+05	5,57E+05	4,26E+05	2,69E+05
11	Male	327	17	Medium	10	8,26E+05	8,73E+06	1,21E+05	7,58E+05
12	Male	327	17	Low	5	8,30E+05	2,95E+06	1,63E+05	3,27E+05
13	Male	303	21	Control	0	1,17E+06	2,58E+06	1,71E+05	3,39E+05
14	Male	303	21	High	15	1,25E+06	6,61E+06	1,80E+05	7,74E+05
15	Female	343	21	Medium	10	5,17E+05	1,68E+06	1,94E+05	4,53E+05
16	Female	343	21	Low	5	9,39E+05	2,28E+06	3,36E+05	5,80E+05
17	Male	309	21	Control	0	1,53E+06	3,82E+06	1,37E+05	2,10E+05
18	Male	309	21	High	15	1,90E+06	8,46E+06	1,85E+05	3,68E+05
19	Male	309	21	Medium	10	1,96E+06	9,84E+06	2,02E+05	3,91E+05
20	Male	306	21	High	15	2,61E+06	1,49E+07	1,50E+05	5,49E+05
21	Male	306	21	Medium	10	9,98E+05	4,87E+06	2,27E+05	5,25E+05
22	Male	306	21	Low	5	1,62E+06	4,07E+06	3,08E+05	3,88E+05
23	Female	307	21	Control	0	1,26E+06	2,81E+06	5,08E+05	8,12E+05
24	Female	307	21	High	15	1,13E+06	1,01E+06	2,70E+05	1,53E+05
25	Female	307	21	Medium	10	1,12E+06	3,23E+06	2,01E+05	3,79E+05
26	Female	307	21	Low	5	1,15E+06	2,65E+06	3,08E+05	4,54E+05

In vivo measuring of NF-κB activity: Additional figures

Nf-kB activity measured from ROI 1 at 4 hours

Nf-kB activity measured from ROI 2 at 2 hours

Nf-kB activity measured from ROI 2 at 4 hours